学位（博士）論文

ポリ（４－ブチルトリフェニルアミン）とポリ（メタクリル酸メチル）からなるポリマーブレンド粒子の構造制御

Morphology Control of Polymer Blend Particles Consisting of Poly(4-butyltriphenylamine) and Poly(methyl methacrylate)

2019.3

東京農工大学大学院

生物システム応用科学府

生物機能システム科学専攻

菊池　秀

指導教員：荻野　賢司

CONTENT

Chapter 1

Introduction

1-1. Application of polymer composite particles

Polymer composite particles consisting of different polymers provide a broader spectrum of physical properties than particles with uniform composition as shown in Figure 1-1. For instance, core-shell structured particles with soft core surrounded by hard shell dispersed into resin improve the impact resistance (Figure 1-1b).[1,2,3] The flexible core relieves the stress, and prevents the cracks from widening by deformation. The shell layer which is compatible with the matrix provides homogeneous dispersion of the particles. For example it was reported that polycarbonate is toughened by the particles consisting of natural rubber coated with the PMMA shell.[4] Core-shell particles work as a pressure responsive adhesive by covering adhesive polymer with hard polymeric shell as well. The career for drug delivery system, in which the core enclose medicine and shell control the release of the components and protect them from the external stimuli, is also one of the applications of core-shell particles (Figure 1-1c).[5,6] The asymmetric structure of the Janus particle, which has two surfaces with different physical or chemical properties, gives many applications. The Janus particles used in electronic paper rotate in response to electric field due to the opposite electric charge on each surface (Figure 1-1e).[7] The Janus particles with hydrophilic and hydrophobic surface work as a surfactant in Pickering emulsion (Figure 1-1f).[8,9] The self assembly of the Janus particles is currently paid a lot of attention as a building block for microscopic architecture.[10] The particles having periodic structure about the same size as wavelength of light are expected to possess unique optical characteristics. Periodic modulation of the dielectric constant inhibits the propagation of electromagnetic waves based on the Bragg reflection. Blocked waves are confined in the modulation and emitted through the defect points. These confinements of electromagnetic waves can be applied for optical devices such as a laser oscillator. Sipe et al. have proposed the idea of the spherical dielectric resonator using multilayered particles. The periodic modulation confines the lights produced

from the fluorescent dyes embedded in the particles (Figure 1-1g, h).[11,12] Spherical resonator can be used for photonic devices such as optical switches and limiters. The studies of onion-like particle with alternating layer composed of different polymers have been conducted with the aim of producing spherical resonator.[13,14]

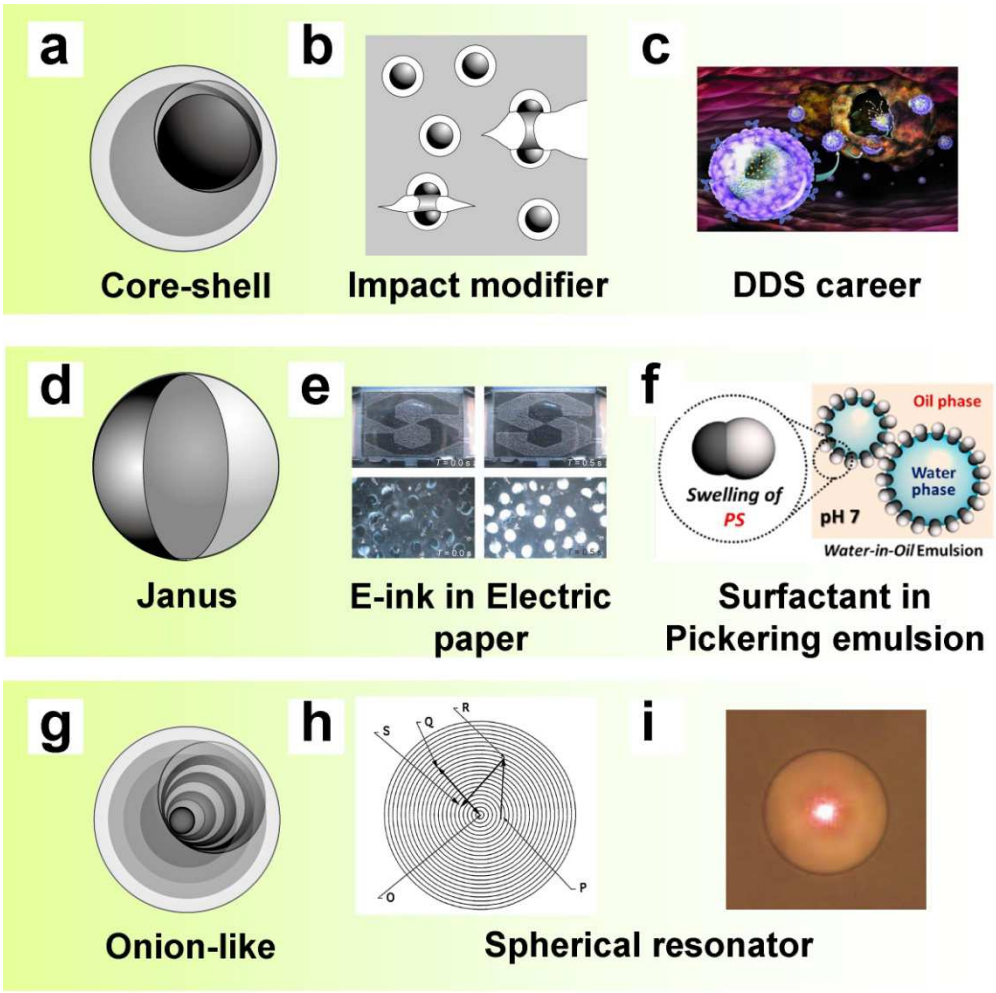

Figure 1-1. (a, d, g) Morphologies and (b, c, e, f, h, i) applications of polymer composite particles: Schematic images of (a) Core-shell-, (d) Janus- and (g) onion-like particles. (b) Schematic image of the core-shell typed impact modifiers dispersed in the resin. Soft cores prevent the cracking from growing. (c) Careers for drug delivery system (DDS).[5] (e) Color switching test for electric paper using Janus particles.[7] (f) pH-responsive surfactants using Janus particles in Pickering emulsion.[8] (h) Prohibition of propagation in a radially symmetric modulation.[11] (i) Spherical resonator using cholesteric liquid-crystal confined in glycerol droplets. Lasing becomes very intense at the center of the droplet.[12]

1-2. Fabrication of polymer particles

Polymer particles are generally fabricated by suspension polymerization, emulsion polymerization, and dispersion polymerization.[15] In these methods, the particles are formed by addition polymerization of vinyl monomers in aqueous medium. For suspension polymerization, the monomers are suspended as droplets in the water by means of a stirrer and a stabilizer. The initiators, which are soluble in the monomers, initiate the polymerization in the droplets. The monomer droplets are directly converted into the polymer particles of approximately the same size of the droplets. The size of the particles is usually in the range of 20 μm- 2 mm, and polydisperse particles are obtained. For emulsion polymerization, the polymerization starts with an emulsion incorporating water, monomer, and surfactant. Unlike the suspension polymerization, the initiators are soluble in the water. Therefore, the polymerization starts in the water phase to form oligomers possessing radicals. The oligoradicals formed in the aqueous medium are surrounded by the surfactants, and form stabilized nuclei. These nuclei absorb the further oligoradicals and monomers from monomer droplets. In this way, the nuclei grow to the particles as polymerization proceeds until the monomer is completely consumed. The size of the particles is usually in the range of 50-300 nm. Monodisperse particles can be obtained from emulsion polymerization by suppressing the further formation of the nuclei during growing step. Dispersion polymerization is a series of the precipitation polymerization. The reaction medium is a good solvent for the monomer and the initiator, but is a non-solvent for the resulting polymer. As the polymerization reaction proceeds, the polymers precipitate forming particles. After the nucleation, the particles grow via the polymerization of monomers absorbed in the individual particles. The size of the particles is usually in the range of 0.1-10 μm, and monodisperse particles are obtained.

Seeded polymerization is common method to produce polymer composite particles among synthetic approaches. In this method, the monomers diffused in seed particles cause polymerization at the inside of the particles and swell them.[16,17] Composite particles are obtained by diffusing second monomers which is different from the polymers consisting the particles. The morphologies of the particles depend on the location where the polymerization of the second monomers in the seed particles. The absorbed monomers penetrate to the center of the seed particles and cause polymerization to form "core-shell" particles under the thermodynamic equilibrium. However, kinetic effects such as high viscosity inside the seed particles delays the penetration and localizes the monomers at the fringe of the sphere to form "inversed core-shell".[18,19] Furthermore, the suitable choice of the combination of seed polymer and second monomer, and controlled polymerization rate can produce "snowman-like" and "confetti like" structures.[20,21,22,] These synthetic approach has advantage for mass production of monodispersed particles. However, seeded polymerization needs at least two steps to develop composite particles. In addition, the kinds of polymer are limited due to the reactivity of the monomers in aqueous medium.

1-3. Solvent evaporation method

"Solvent evaporation method", in which polymer particles are obtained by solvent evaporation from polymer solution droplets dispersed in aqueous medium (Figure 1-2), has advantageous to prepare polymer composite particles. This method can produce composite particles in a single step from polymer blend solution droplets. In this method, a polymer solution is dispersed into an aqueous phase. The liquid-liquid phase separation occurs at the critical concentration, when the evaporation of the solvent from the solution droplets proceeds. Other advantage of this method is available for any polymers which can dissolve into organic solvent. Moreover, the technology to produce monodispersed solution droplet

such as membrane emulsification[23,24,25] and microfluidic fabrication[26,27,28] has achieved to produce monodispersed particles from solvent evaporation method.

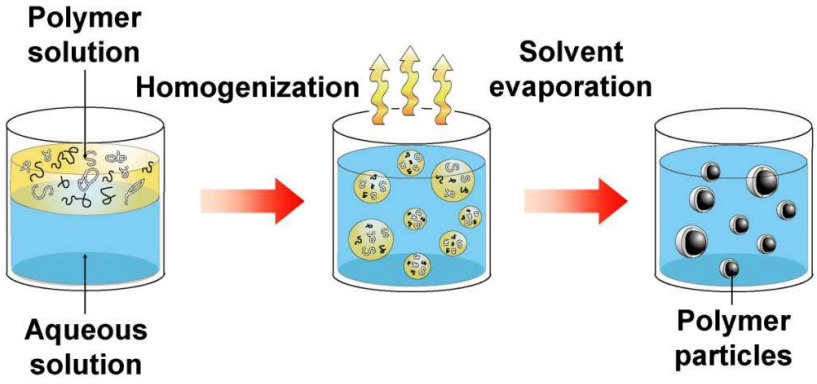

Figure 1-2. Solvent evaporation method.

As similar to the seeded polymerization, thermodynamic and kinetic factor decide the structure of the particles obtained from a solvent evaporation method.[29] For instance, three interfaces including polymer-A/polymer-B, polymer-A/water, and polymer-B/water are formed in the phase separated polymer blend solution droplets dispersed in aqueous medium. When the interfacial tension of polymer-A/water is higher than that of polymer-B/water, the particles form core-shell structure with polymer-A core covered by polymer-B shell to avoid contact between polymer-A and water. When the interfacial tension of polymer-A/water is close to that of the polymer-B/water, the particles become Janus structure. When the interfacial tension of polymer-A/polymer-B is higher than that of polymer/water interface, the particles form "dumbbell-like" structure to decrease the contact area between polymer-A and polymer-B (Figure 1-3). While the phase separated structures move to the most thermodynamically stable morphology as the solvent evaporates from the solution droplets, kinetic effects such as high viscosity suppress the morphological transition. For instance, the phase separated structure of poly(styrene) (PS)/poly(methyl methacrylate) (PMMA) blend in toluene solution droplet is Janus at the beginning of the phase separation because the interfacial tensions of polymer/water interface are nearly equal between PS and PMMA for

the low concentration of polymer. The morphology changes from Janus to core-shell structure with PS core and PMMA shell as the solvent evaporate from the droplets since PMMA is more hydrophilic than PS. However the shape of the particles composed of the polymer with high molecular weight remained as Janus due to the high viscosity. The effects of the types of the solvent[30] and the surfactants[31, 32], and molecular weight of polymers[33] on the PS/PMMA composite particles fabricated from solvent evaporation method have been extensively studied. These studies have reported polymer composite particles with various morphologies including core-shell, Janus, dumbbell-like structure.

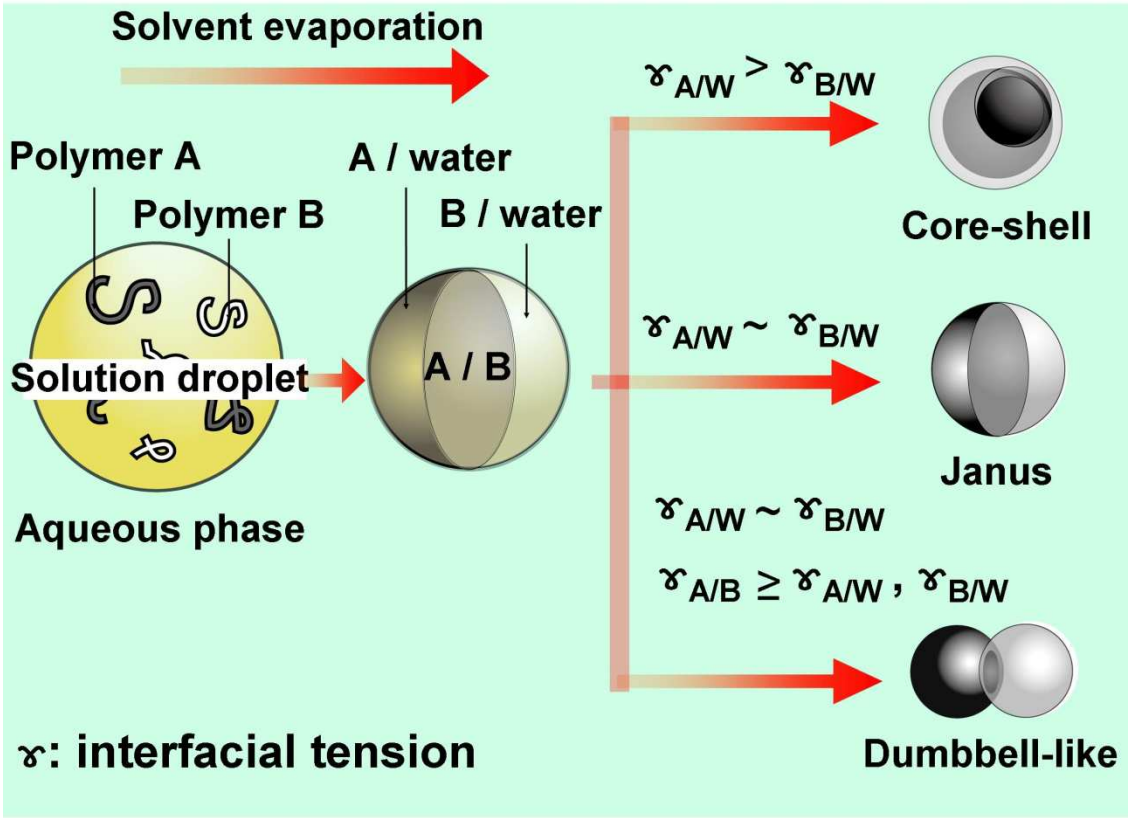

Figure 1-3. Mechanism of the formation of phase separated structure in the solvent evaporation method.

1-4. Effect of block copolymer on the morphology

Block copolymer causes phase separation in nano scale. Phase separated structures has been seen in film or bulk sample solidified from melted polymer or polymer solution. The

phase separated structure forms various periodic structures including “lamella”, “cylinder”, and “microsphere” depending on the volume ratio of segments and molecular weight (Figure 1-4).[34] The periodic length increases as the molecular weight increases, whereas addition of homopolymer into block copolymer swells the spacing of corresponding polymer domain as well.[35] The rate of the expansion becomes high as the molecular weight of homopolymer increases.

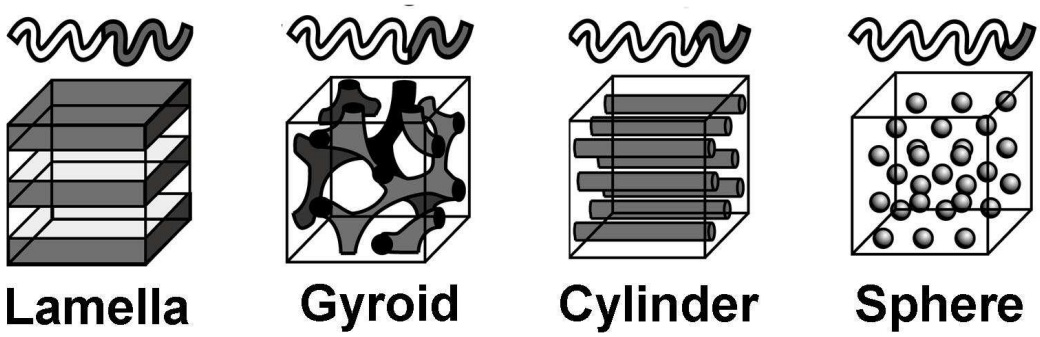

Figure 1-4. The microphase separated structures of block copolymer.

There are few studies to prepare the particles consisting of block copolymers via synthetic approaches. For emulsion polymerization, using macroinitiators with water soluble polymeric chains as the surfactant for the emulsion polymerization provides the particles consisting of the amphiphilic block copolymer.[36] Using seed particles consisting of the macroinitiators in seeded polymerization give block copolymer particles as well.[37, 38] To synthesize the particles consisting of block copolymers requires multiple steps, and controlling the structure of microphase separation in synthetic process is technically difficult.

These periodic structures can be seen in the block copolymer particles fabricated by a solvent evaporation method (Figure 1-5). [39,40,41] Okubo et al. unexpectedly found that graft copolymer of PMMA and PS (PMMA-*g*-PS) in PMMS/PS blend causes the formation of onion-like multi layered particles in solvent evaporation method.[42,43,44] Afterwards, they have reported that block copolymer (PMMA-*b*-PS) also form multi layered particle,[45] and the periodic length of lamella is controllable by adding PMMA and PS homopolymers.[46] Hawker

et al. have also reported the multi layered particle consisting of PS-*b*-poly(2-vinylpyridine) (P2VP). They found that the surfactant in aqueous medium changes the morphology from onion-like to striped particle, in which lamellas are stacked in one direction.[47,48] This is the analogy with the selective wetting and associated self-assembly of block copolymer in thin films on the substrate.[49,50] The polymer composition at the surface of the particle is determined by the affinity between polymer and the inner surface of the droplet. Since the surfactants locate at the surface of the solution droplet with directing hydrophobic section to the inside of the droplets, the affinity of the inner surface can be controled by modifying the hydrophobic part of the surfactants.

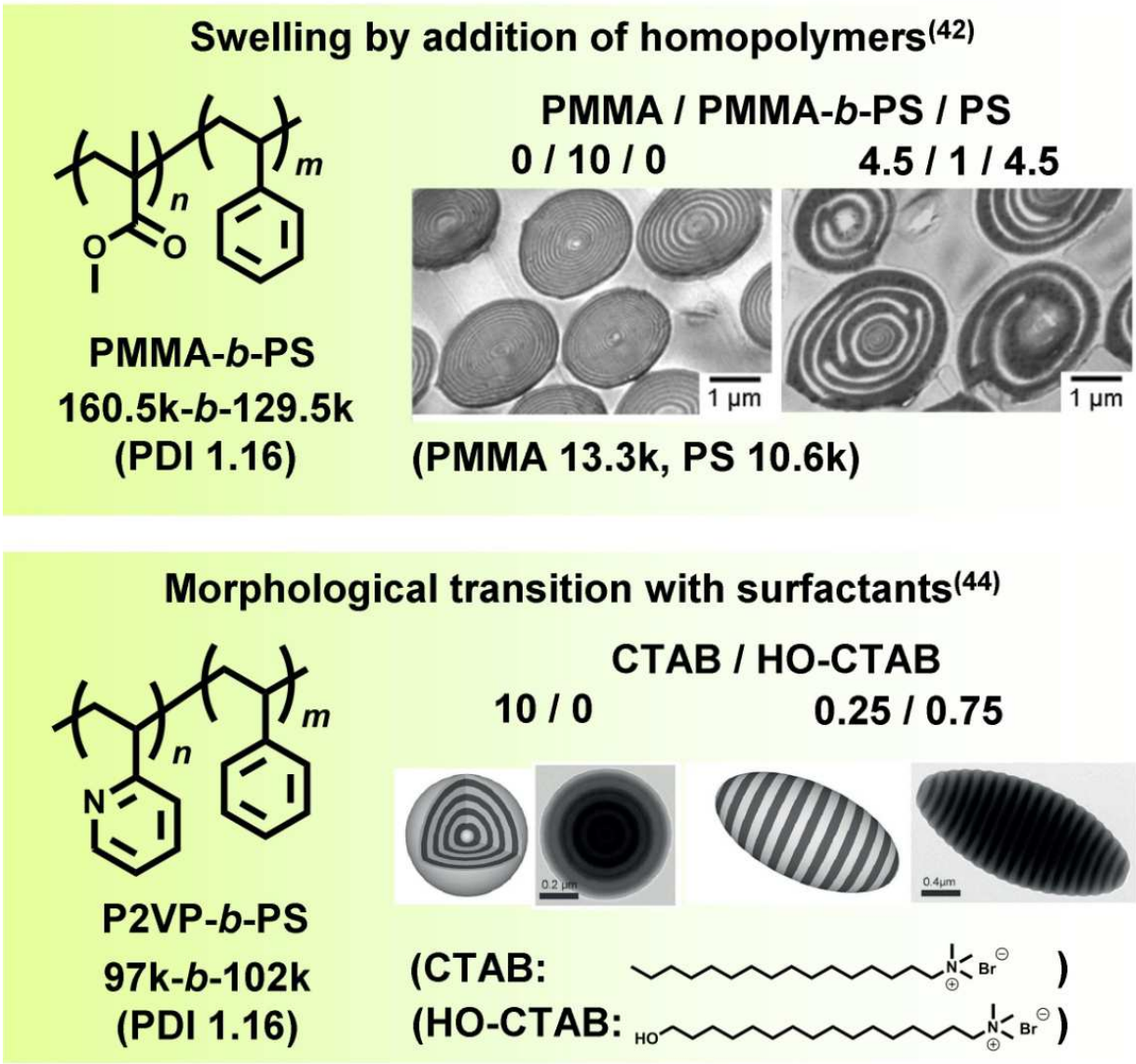

Figure 1-5. Block copolymer particles with ordered structures.[46, 48]

1-4. Aim of this thesis

The aim of this thesis is to control the morphology of the polymer composite particles consisting of poly(4-butyl triphenylamine) (PBTPA) and PMMA via solvent evaporation method. The section 1-1 has shown various applications of polymer composite particles originated from the synergy between chemical properties of polymers and the morphologies of particles. Among the many approaches, solvent evaporation method is the optimal technique, which can provide polymer composite particles in a single step. The particles with

various structures from core-shell to onion-like have been fabricated via a solvent evaporation method. However, the materials of particles have been limited to the certain polymers such as PS, P2VP and PMMA. Whereas, using conjugated polymers which have excellent thermal and electronic properties as the materials for polymer particles can provide novel applications to composite particles. In particular, the author focused on the PBTPA as the material (Figure 1-6). PBTPA is a promising material in photovoltaic, [51] and photorefractive [52] applications due to high hole-transporting properties. PBTPA also has excellent properties as optical material. High refractive index of PBTPA, n = 1.71 at 633 nm, allows us to easily generate high contrast of refractive index by combining PBTPA with other polymers. Polymer blend particles containing PBTPA with well-defined phase separated structure can be utilized in optical applications. Therefore it is important to control the internal structure of the particles. For example, when light enter a interface between polymer-1 and -2, some of the light is reflected, depending on the angle of incidence and the refractive indexes of the polymers. In case the angle of incidence is perpendicular to the interface, the fraction of reflected light is given by the reflection coefficient R:

$$R = (n_2-n_1)^2/(n_2+n_1)^2 \quad (1\text{-}1)$$

where n_1 and n_2 are the refractive indexes of polymer-1 and -2, respectively. Equation 1-1 means that the refraction rate becomes higher as the increase of the contrast of refractive index. If spherical resonators or photonic crystals composed of PBTPA can be prepare a, high contrast of the refractive index can increase the efficiency of the devices. In this thesis, PMMA was used as the counter polymer to PBTPA, because PMMA has high transparency which is suitable for the material of an optical device. Furthermore, the molecular weight and distribution of PMMA are controllable via living polymerization.

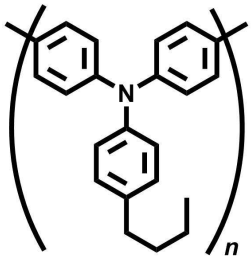

Poly(4-butyltriphenylamine)
(PBTPA)

Figure 1-6. Chemical structure of PBTPA

1-5. Content

This thesis consists of six chapters. Chapter 2 and 3 are focusing on the PBTPA/PMMA blend particles fabricated from solvent evaporation method. The author proved that the morphologies can be controlled by choosing preparation conditions through the microscopic observation and thermodynamic analysis with measurements of interfacial tensions. Based on the knowledge obtained in chapter 2 and 3, the morphology of PBTPA/PBTPA-*b*-PMMA/PMMA blend particles are discussed in chapter 4. Nano-sized structure originated from PBTPA-*b*-PMMA was introduced to the particles. In chapter 5, the author reports the morphological transition in polymer blend solution induced by UV light as novel method for structure control. The outline of the thesis is shown in Figure 1-7.

In chapter 2, the effects of the surfactant on the morphology of PBTPA/PMMA blend particle are presented.

In chapter 3, the effects of the solvent, molecular weight and composition of polymers, and evaporation speed are presented.

In chapter 4, the effects of the molecular weight and segment ratio of PBTPA-*b*-PMMA on the morphology of PBTPA/PBTPA-*b*-PMMA/PMMA blend particle are presented.

In chapter 5, the effects of the UV light irradiation on the morphology of phase separated PBTPA/PMMA solution droplets are presented.

In chapter 6, the author presents the general conclusion.

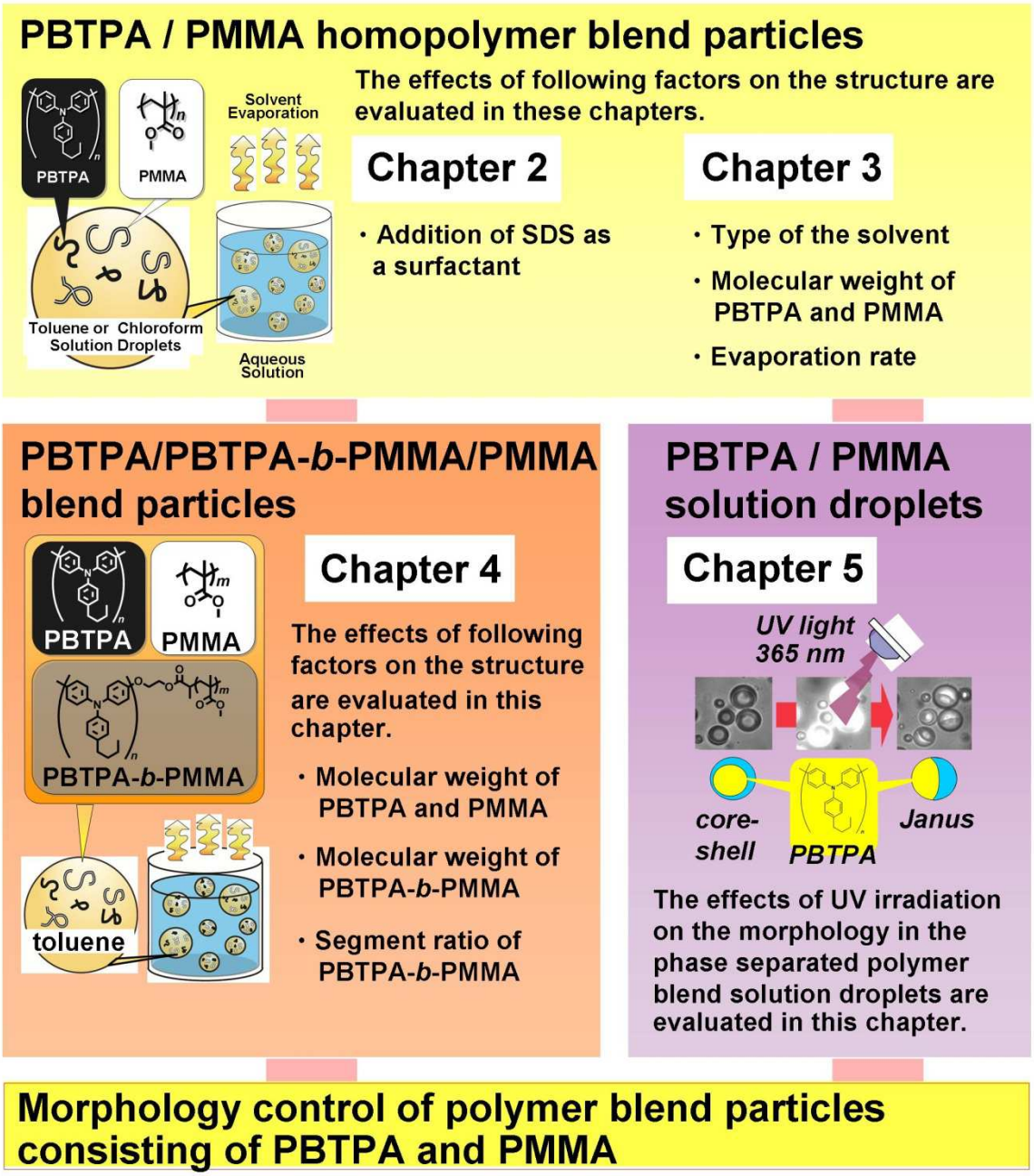

Figure 1-7. Structure of the thesis.

1-6. References

(1) Becu, L.; Maazouz, A.; Sautereau, H.; Gerard, J. F. Fracture behavior of epoxy polymers modified with core-shell rubber particles. *J. Appl. Polym. Sci.* **1997**, *65*, 2419–2431.

(2) Dong, L.; Tong, Y.; An, Y.; Tang, H.; Zhuang, Y.; Feng, Z.; Study of The Blends Containing Core-Shell Latex Polymer. *Eur. Polym. J.* **1997**, *33*, 501–503.

(3) Maestrini, C.; Monti, L.; Kausch, H. H. Influence of particle-craze interactions on the sub-critical fracture of core-shell HIPS. *Polymer*, **1996**, *37*, 1607–1619.

(4) Schneider, M.; Pith, T.; Lambla, M. The role of the morphology of natural rubber and polybutylacrylate-based composite latex particles on the toughness of polycarbonate/brittle polymer blends. *Polym. Adv. Technol.* **1996**, *7*, 425–436.

(5) Manish, G.; Vimukta, S. Targeted drug delivery system: A review. *Res. J. Chem. Sci.* **2011**, *1*, 135−138.

(6) Mora-Huertas, C.E.; Fessi, H.; Elaissari, A.; Polymer-based nanocapsules for drug delivery. *Int. J. Pharm.* **2010**, *385*, 113-142.

(7) Nisisako, T.; Torii, T.; Takahashi, T.; Takizawa Y. Synthesis of monodisperse bicolored Janus particles with electrical anisotropy using a microfluidic co-flow system. *Adv. Mater.* **2006**, *18*, 1152−1156.

(8) Ku, K. H.; Lee, Y. J.; Yi, G.; Jang, S. G.; Schmidt, B. V. K. J.; Liao, K.; Klinger, D.; Hawker, C. J.; Kim, B. J. Shape-tunable biphasic Janus particles as pH-responsive switchable surfactants. *Macromolecules*, **2017**, *50*, 9276−9285.

(9) Tu, F.; Lee, D. Shape-changing and amphiphilicity-reversing Janus particles with pH-responsive surfactant properties. *J. Am. Chem. Soc.* **2014**, *136*, 9999−10006.

(10) Zhang, J.; Grzybowski, B. A.; Granick, S. Janus Particle Synthesis, Assembly, and Application. *Langmuir*, **2017**, *33*, 6964−6977.

(11) Brady, D.; Papen, G.; Sipe, J. E. Spherical distributed dielectric resonators. *J. Opt. Soc. Am. B* **1993**, *10*, 644−657.

(12) Humar, M.; Muševič, I. 3D microlasers from self-assembled cholesteric liquid-crystal microdroplets. *Optics Express* **2010**, *18*, 26995–27003.

(13) Gourevich, I.; Field, L. M.; Wei, Z.; Paquet, C.; Petukhova, A.; Alteheld, A.; Kumacheva E. polymer multilayer particles: A route to spherical dielectric resonators. *Macromolecules*, **2006**, *39*, 1449–1454.

(14) Petukhova, A.; Paton, A. S.; Wei, Z.; Gourevich, I.; Nair, S. V.; Ruda, H. E.; Shik, A.; Kumacheva E. Polymer multilayer microspheres loaded with semiconductor quantum dots. *Adv. Funct. Mater.* **2008**, *18*, 1961–1968.

(15) Arshady, R. Suspension, emulsion, and dispersion polymerization: A methodological survey. *Colloid Polym. Sci.* **1992**, *270*, 717–732.

(16) Wang, D.; Dimonie, V. L.; Sudol, E. D.; El-Aasser, M. S. Seeded dispersion polymerization. J. Appl. Polym. Sci. 2002, 84, 2710–2720.

(17) Cunningham, M. F.; Mahabadi, H. K.; Wright, H. M. Supermicron Polymer Particles with Core-Shell Type Morphologies. *J. Polym. Sci., Part A: Polym. Chem.* **2000**, *38*, 345–351.

(18) Stubbs, J.; Karlsson, O.; Jönsson, J. E.; Sundberg, E.; Durant,Y.; Sundberg, D. Non-equilibrium particle morphology development in seeded emulsion polymerization. 1: penetration of monomer and radicals as a function of monomer feed rate during second stage polymerization. *Colloids Surf. A* **1999**, *153*, 255–270.

(19) Karlsson, L. E.; Karlsson, O. J.; Sundberg, D. C. Nonequilibrium particle morphology development in seeded emulsion polymerization. II. Influence of seed polymer T_g. *J. Appl. Polym. Sci.* **2003**, *90*, 905–915.

(20) Ostovar, M.; Eslami, H. Synthesis of nanostructured confetti-like and mace-like particles via dispersion polymerization of alkyl methacrylates on polystyrene seeds. Colloid Polym. Sci. **2016**, *294*, 1633–1642.

(21) Chen, M. Q.; Kaneko, T.; Chen, C. H.; Akashi, M. Preparation of "Confetti" Particles by Dispersion Copolymerization of Acrylonitrile/Styrene with Poly(ethylene glycol) Macromonomer. *Chem. Lett.* **2001**, *30*, 1306–1307.

(22) Okubo, M.; Miya, T.; Minami, H.; Takekoh, R. Morphology of micron-sized, monodisperse, nonspherical polystyrene/poly(*n*-butyl methacrylate) composite particles produced by seeded dispersion polymerization. *J. Appl. Polym. Sci.* **2002**, *83*, 2013–2021.

(23) Ma, G. H.; Nagai, M.; Omi, S. Preparation of uniform poly(lactide) microspheres by employing the Shirasu Porous Glass (SPG) emulsification technique. *Colloid. Surf. A: Physicochem. Eng. Aspects,* **1999**, *153*, 383–394.

(24) Liu, R.; Ma, G. H.; Meng, F. T.; Su, Z. G. Preparation of uniform-sized PLA microcapsules by combining Shirasu porous glass membrane emulsification technique and multiple emulsion-solvent evaporation method. *J. Control. Release* **2005**, *103*, 31–43.

(25) Ma, G. H.; Nagai, M.; Omi, S. Effect of lauryl alcohol on morphology of uniform polystyrene-poly (methyl methacrylate) composite microspheres fabricated by porous glass membrane emulsification technique. *J. Colloid Interface Sci.* **1999**, *219*, 110–128.

(26) Nisisako, T.; Torii, T.; Higuchi, T. Novel microreactors for functional polymer beads. *Chem. Eng. J.* **2004**, *101*, 23–29.

(27) Wang, J. T.; Wang, J.; Han, J. J. Fabrication of Advanced Particles and Particle-Based Materials Assisted by Droplet-Based Microfluidics. *Small* **2011**, *7*, 1728–1754.

(28) Xu, S.; Nie, Z.; Seo, M.; Lewis, P.; Kumacheva, E.; Stone, H. A.; Garstecki, P.; Weibel, D. B.; Gitlin, I.; Whitesides, G. M. Generation of Monodisperse Particles by Using Microfluidics: Control over Size, Shape, and Composition. *Angew. Chem., Int. Ed.* **2005** , *44* , 724 – 728 .

(29) Torza, S.; Mason, S. Three-phase interactions in shear and electrical fields. *J. Colloid Interface Sci.* **1970**, *33*, 67–83.

(30) Okubo, M.; Saito, N.; Fujibayashi, T. Preparation of polystyrene/poly(methyl methacrylate) composite particles having a dent. *J. Appl. Colloid Polym Sci*, **2005**, *283*, 691–698.

(31) Saito, N.; Kagari, Y.; Okubo, M. effect of colloidal stabilizer on the shape of polystyrene/poly(methyl methacrylate) composite particles prepared in aqueous medium by the solvent evaporation method. *Langmuir* **2006**, *22*, 9397–9402.

(32) Ge, X.; Wang, M.; Ji, X.; Ge, X.; Liu, H. Effects of concentration of nonionic surfactant and molecular weight of polymers on the morphology of anisotropic

polystyrene/poly(methyl methacrylate) composite particles prepared by solvent evaporation method. *Colloid Polym. Sci.* **2009**, *287*, 819–827.

(33) Tanaka, T.; Nakatsuru, R.; Kagari, Y.; Saito, N.; Okubo, M. Effect of molecular weight on the morphology of polystyrene/poly(methyl methacrylate) composite particles prepared by the solvent evaporation method. *Langmuir* **2008**, *24*, 12267–12271.

(34) Bates, F. S.; Fredrickson, G. H. Block copolymers-designer soft materials. *Phys. Today*, **1999**, *52*, 32–38.

(35) Winey, K. I.; Thomas, E. L.; Fetters, L. J. Swelling of lamellar diblock copolymer by homopolymer: influences of homopolymer concentration and molecular weight. *Macromolecules*, **1991**, *24*, 6182–6188.

(36) Tauer, K.; Antonietti, M.; Rosengarten, L.; Müller, H. Initiators based on poly(ethylene glycol) for starting heterophase polymerizations: generation of block copolymers and new particle morphologies. *Macromol. Chem. Phys.* **1998**, *199*, 897–908.

(37) Herrera, V.; Pirri, R.; Leiza, J. R.; Asua, J. M. Effect of in-Situ-Produced Block Copolymer on Latex Particle Morphology. *Macromolecules*, **2006**, *39*, 6969–6974.

(38) Kitayama, Y.; Kagawa, Y.; Minami, H.; Okubo, M. Preparation of Micrometer-Sized, Onionlike Multilayered Block Copolymer Particles by Two-Step AGET ATRP in Aqueous Dispersed Systems: Effect of the Second-Step Polymerization Temperature. *Langmuir* **2010**, *26*, 7029–7034.

(39) Ku, K. H.; Shin, J. M.; Yun, H.; Yi, G. R.; Jang, S. G.; Kim, B. J. Multidimensional Design of Anisotropic Polymer Particles from Solvent-Evaporative Emulsion. *Adv. Funct. Mater.* **2018**, *28*, 1802961.

(40) Shin, J. M.; Kim, Y. J.; Yun, H.; Yi, G. R.; Kim, B. J. Morphological Evolution of Block Copolymer Particles: Effect of Solvent Evaporation Rate on Particle Shape and Morphology. *ACS Nano*, **2017**, *11*, 2133–2142.

(41) Deng, R.; Liang, F.; Li, W.; Yang, Z.; Zhu, J. Reversible Transformation of Nanostructured Polymer Particles. *Macromolecules*, **2013**, *46*, 7012–7017.

(42) Okubo, M.; Takekoh, R.; Saito, N. Effect of graft polymer on the formation of micron-sized, monodisperse, ‘‘onion-like’’alternately multilayered poly(methyl methacrylate)/polystyrene composite particles by reconstruction of morphology with the solvent-absorbing/releasing method. *Colloid. Polym. Sci.* **2003**, *281*, 945–950.

(43) Okubo, M.; Takekoh, R.; Saito, N. Formation mechanism of an ‘‘onionlike’’ multilayered structure by reconstruction of the morphology of micron-sized, monodisperse poly(methyl methacrylate)/polystyrene composite particles with the solvent-absorbing/solvent-releasing method. *Colloid. Polym. Sci.* **2004**, *282*, 1192–1197.

(44) Okubo, M.; Takekoh, R.; Izumi, J. Preparation of micron-sized, monodispersed, “onion-like” multilayered poly(methyl methacrylate)/polysterene composite particles by reconstruction of morphology with the solvent-absorbing/releasing method. *Colloid. Polym. Sci.* **2001**, *279*, 513–518.

(45) Okubo, M.; Saito, N.; Takekoh, R.; Kobayashi, H. Morphology of polystyrene/polystyrene-block-poly(methyl methacrylate)/poly(methyl methacrylate) composite particles. *Polymer* **2005**, *46*, 1151–1156.

(46) Tanaka, T.; Saito, N.; Okubo, M. Control of layer thickness of onionlike multilayered composite polymer particles prepared by the solvent evaporation method. *Macromolecules*, **2009**, *42*, 7423–7429.

(47) Jang, S. G.; Audus, D. J.; Klinger, D; Krogstad, D. V.; Kim, B. J., Cameron, A.; Kim, S.; Delaney, K. T.; Hur, S.; Killops, K. L.; Fredrickson, G. H.; Kramer, E. J.; Hawker, C. J. Striped, ellipsoidal particles by controlled assembly of diblock copolymers. *J. Am. Chem. Soc.*, **2013**, *135*, 6649–6657.

(48) Klinger, D.; Wang, C. X.; Connal, L. A.; Audus, D. J.; Jang, S. G.; Kraemer, S.; Killops, K. L.; Fredrickson, G. H.; Kramer, E. J.; Hawker, C. J. A facile synthesis of dynamic, shape-changing polymer particles. *Angew. Chem. Int. Ed.* **2014**, *53*, 7018–7022.

(49)Mansky, P.; Liu, Y.; Huang, E.; T. Russell, P.; Hawker, C. Controlling Polymer-Surface Interactions with Random Copolymer Brushes. *Science* **1997**, *275*, 1458–1460.

(50) Ryu, D. Y.; Ham, S.; Kim, E.; Jeong, U.; Hawker, C. J.; Russell, T. P. Cylindrical Microdomain Orientation of PS-*b*-PMMA on the Balanced Interfacial Interactions: Composition Effect of Block Copolymers. *Macromolecules*, **2009**, *42*, 4902–4906.

(51) Tsuchiya, K.; Kikuchi, T.; Songeun, M.; Shimomura, T.; Ogino, K. synthesis of diblock copolymer consisting of poly(4-butyltriphenylamine) and morphological control in photovoltaic application. *Polymers* **2011**, *3*, 1051-1064.

(52) Cao, Z.; Abe, Y.; Nagahama, T.; Tsuchiya, K.; Ogino, K.; Synthesis and characterization of polytriphenylamine based graft polymers for photorefractive application. *Polymer* **2013**, *54*, 269-276.

Chapter 2

Fabrication of core-shell structured microspheres of blends of poly(4-butyltriphenylamine) and poly(methyl methacrylate)

2-1. Introduction

The aim of this chapter is to investigate the effects of an additional surfactant on the morphology of the particles consisting of poly(methyl methacrylate) (PMMA) and poly(4-butyltriphenylamine) (PBTPA) homopolymers. Suspension stabilizers and surfactants not only form stable dispersion of the droplets of a polymer solution, but also have great effect on the morphology of the particles. For example, for the combination of poly(styrene) (PS) and PMMA, using poly(vinyl alcohol) (PVA) as a stabilizer gives core-shell structure in which more hydrophilic PMMA-shell surrounds PS-core, while using SDS as a surfactant gives Janus type structure.[1,2] This is because surfactants such as SDS are strongly absorbed to the interface between polymer solution and aqueous phase and reduces the gap of the hydrophilicity between PMMA and PS phase. Furthermore, Ge et al. have reported the formation of "snowman-like" particles by addition of nonionic surfactant, OP-10.[3] The interfacial tension of polymer/polymer interface is generally small enough to be ignorable compared with that of polymer/water interface. However, when the interfacial tension of polymer/water interface is lowered to the comparable value to that of polymer/polymer interface by the addition of surfactants, the interfacial area between polymers shrinks to keep the thermodynamic equilibrium and cause the formation of snowman-like particles.

In the case of the combination of PBTPA and PMMA, the addition of SDS to PVA aqueous solution caused dramatic transition from Janus type structure to "inverse core-shell" one in which the PMMA core was surrounded by the PBTPA shell. Furthermore, the inverse core-shell particles exhibited symmetric structure with uniformed thickness of the PBTPA shell. Symmetric core-shell particles have attracted special interest for the component of photonic crystal. Close-packed submicron particles reflect the light in specific wavelength following Bragg's formula.[4] When the wavelength is within the range of visible light, the crystal shows structural color.[5] These colorized materials can be the substitutes of toxic dyes. In particular,

it has been reported that the existence of shell not only adjust the position of the core, but also high refractive index contrast between core and shell make refractance at Bragg angle stronger and improve transmitted color purity.[6,7,8,9,10,11] Commonly, synthetic approaches including seeded and emulsion polymerization have been used for the fabrication of core-shell particles.[12,13] While polymerization methods are considered advantageous in the mass production of mono-sized microspheres, monomers available for the reactions are limited, and multiple steps are needed to obtain composite particles.

This chapter reports the facile fabrication of symmetric core-shell particles. In particular, the effects of the polymer compositions, the concentration of SDS and the molecular weight on the morphology were investigated. Furthermore, the measurements of the interfacial tensions between the polymer and the aqueous solution via a pendant drop method revealed that the addition of SDS induced the preferential formation of the PBTPA-shell by allowing the interface between the organic and the aqueous solution to have high affinity to PBTPA.

2-2. Experimental section

2-2-1. Synthesis of PBTPA monomer.

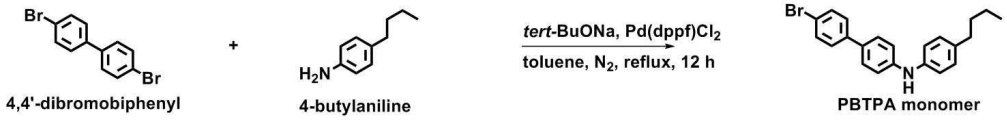

<Materials>

4-butylaniline: TCI, Tokyo, Japan

4,4`-dibromobiphenyl: Wako, Tokyo, Japan

Sodium *tert*-butoxide (*tert*-BuONa): TCI, Tokyo, Japan

[1,1`-*bis*-(diphenylphosphino)ferrocene]dichloropalladium(II) ($Pd(dppf)Cl_2$): Wako, Tokyo, Japan

Toluene, deoxidized: Wako, Tokyo, Japan; for Organic Synthesis

<Operations>

To a 200-mL flask equipped with a magnetic stirrer bar and a condenser were added 4,4`-dibromobiphenyl (15.6 g, 50 mmol), *tert*-BuONa (6.8 g, 70 mmol) and ($Pd(dppf)Cl_2$) (0.41 g, 0.5 mmol). Toluene (100 mL) and 4-butylaniline (7.4 g, 50 mmol) were added via a syringe. The mixture was stirred at 120 °C for 12 h under a nitrogen atmosphere. After cooling down to ambient temperature, the reaction mixture was filtered through a silica pad and concentrated by evaporation. The product was purified by column chromatography on silica gel (eluent: hexane/toluene = 1/1, v/v) and recrystallized in cyclohexane. The white solid of PBTPA monomer (4.8 g, 26%) was obtained. ^{1}H NMR [300 MHz, $CDCl_3$, δ (ppm)] δ7.52 (*d*, 2H), 7.44 (*d*, 2H), 7.41 (*d*, 2H), 7.12 (*d*, 2H), 7.07 (*s*, 4H), 5.76 (*s*, 1H), 2.57 (*s*, 2H), 1.59 (*tt*, 2H), 1.38 (*tqua*, 2H), 0.94 (*t*, 3H)

2-2-2. Synthesis of PBTPA homopolymer.

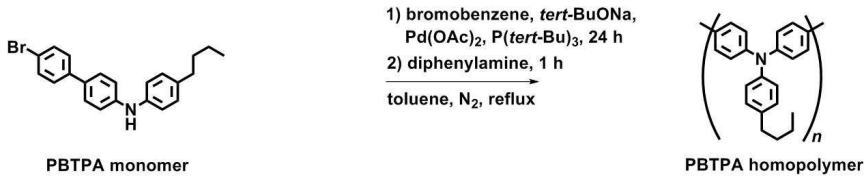

PBTPA monomer PBTPA homopolymer

<Materials>

Bromobenzene: Kanto Chemical Co.,Inc., Tokyo, Japan; Cica 1st Grade

Palladium acetate(II) ($Pd(OAc)_2$): Wako, Tokyo, Japan

Sodium *tert*-butoxide (*tert*-BuONa): TCI, Tokyo, Japan

Tri-*tert*-butylphosphine (P(*tert*-$Bu)_3$): Wako, Tokyo, Japan

Diphenylamine: TCI, Tokyo, Japan

Toluene, deoxidized: Wako, Tokyo, Japan; for Organic Synthesis

<Operations>

To a 20-mL glass vial equipped with a magnetic stirrer bar and a nitrogen inlet was added $Pd(OAc)_2$ (30 mg, 0.13 mmol). Toluene (1 mL), bromobenzene (0.2 g, 1.3 mmol) and 0.5 M P(*tert*-$Bu)_3$ solution in toluene (1 mL, 0.53 mmol) were added via a syringe. The mixture was stirred at room temperature for 1 h under a nitrogen atmosphere. Separately, to a 50-mL flask equipped with a magnetic stirrer bar and a condenser were added PBTPA monomer (2.5 g, 6.6 mmol) and *tert*-BuONa (0.70 g, 7.2 mmol). Toluene (23 mL) and the solution of initiator were added via a syringe. The mixture was stirred at 120 °C for 24 h under a nitrogen atmosphere followed by the addition of toluene solution of diphenylamine (0.44 g, 2.6 mmol) and additional stirring at 120 °C for 1 h. After cooling down to ambient temperature, the reaction mixture was filtered and poured into methanol. The precipitation was purified by a Soxhlet extraction using 2-butanone for 2 days. Finally, the product was reprecipitated from acetone. The pale yellow solid of PBTPA homopolymer (1.3 g, 65%) was obtained. ^{1}H NMR

[300 MHz, $CDCl_3$, δ(ppm)] δ 7.44 (*d*), 7.20-6.80 (*s*), 2.58 (*s*), 1.60 (*tt*), 1.38 (*tqua*), 0.94(*t*); GPC: M_n=4100, PDI=1.6

2-2-3. Synthesis of PMMA homopolymer.

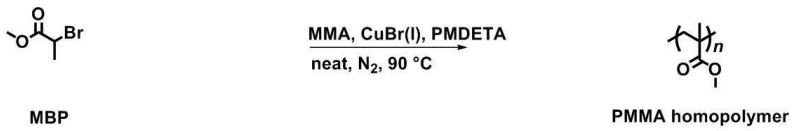

MBP PMMA homopolymer

<Materials>

Methyl methacrylate (MMA): Wako, Tokyo, Japan; distilled over CaH_2 under reduced pressure before use

Methyl 2-bromopropionate (MBP): TCI, Tokyo, Japan

Copper(I) bromide (CuBr(I)): TCI, Tokyo, Japan; washed with acetic acid and dried in vacuo before use

N, N, N', N', N"-pentamethyldiethylenetriamine (PMDETA): Wako, Tokyo, Japan; Wako 1st Grade

<Operations>

To a 20-mL flask equipped with a magnetic stirrer bar were added CuBr(I) (29 mg, 0.20 mmol), MMA (14.0 g, 140 mmol), MBP (17 mg, 0.1 mmol), and PMDETA (69 mg, 0.4 mmol). After three freeze-pump-thaw cycles, the mixture was stirred at 90 °C for 24 h under nitrogen atmosphere. After cooling down to ambient temperature, THF (14 mL) was added to the reaction mixture. The THF solution of reaction mixture was filtered through alumina chromatographic column and concentrated by evaporation. The reaction mixture was poured into methanol. The white solid of PMMA (6.9 g, 49%) was obtained; GPC: M_n=40,000, PDI=2.7.

2-2-4. Characterization

^{1}H-NMR spectra were recorded at 25 °C on a JEOL ECX300 instrument at 300 MHz. Deutrated chloroform was used as a solvent with tetramethylsilane as an internal standard. Number- and weight-average molecular weights (M_n and M_w) were determined by gel permeation chromatography (GPC) analysis with a JASCO RI-2031 detector eluted with chloroform at a flow rate of 1.0 mL min^{-1} and calibrated by standard polystyrene samples. The density (ρ) of polymers (PBTPA; ρ = 1.09 g cm^{-1}, PMMA; ρ = 1.20 g mL^{-1}) was evaluated by using an electronic balance AUX220 (Shimadzu Co., Kyoto, Japan).

2-2-5. Contact angle and interfacial tension

The contact angles of liquid on polymer films was measured by a contact angle gauge (DM-501, Kyowa Interface Science Co., Ltd., Japan). Polymer thin films were fabricated on glass slides by spin-coating of 10 g L^{-1} of the polymer solution in toluene at 3,000 rpm for 60 s. Interfacial tension between the polymer and aqueous solutions was calculated from the Young equation[14], Equation (2-1):

$$\gamma_{sl} = \gamma_l \cos\theta - \gamma_s \tag{2-1}$$

where γ_{sl} is the interfacial tension corresponding to polymer and liquid interface, θ is contact angle. γ_l and γ_s are the surface tension corresponding to liquid and solid (polymer), respectively. The surface tensions of distilled water and the aqueous solution containing 0.6 wt% of PVA with or without 0.3 wt% SDS measured by the Whilhemy plate method with a surface tensiometer (DY-700, Kyowa Interface Science Co., Ltd., Japan) were 72.86, 44.00 and 46.10 mN m^{-1}, respectively. The surface tension of the polymer film was calculated from the following Equation (2) expressed by Owens and Wendt[15]:

$$(1 + \cos\theta_i)\,\gamma_l = 2\,\{(\gamma_l^d\,\gamma_s^d)^{1/2} + (\gamma_l^p\,\gamma_s^p)^{1/2}\} \tag{2-2}$$

where “d” means dispersion and “p” polar component. γ_l^d and γ_l^p can be obtained by considering known data for two liquids (distilled water; γ_d^d = 21.8 mN m^{-1} and γ_s^p = 51.0 mN m^{-1}, diiodomethane; γ_d^d = 48.5 mN m^{-1} and γ_s^p = 2.3 mN m^{-1})[16].

Interfacial tension between polymer- and aqueous solutions was measured by a pendant drop method with a contact angle gauge (DM-501, Kyowa Interface Science Co., Ltd., Japan) at room temperature (ca. 20 °C). A drop of the polymer solution in toluene (10 wt%) with a volume of 15-30 μL was formed at the tip of the stainless steel needle in a glass cell filled with the aqueous solution containing 0.6 wt% of PVA with or without SDS (0.006-0.3 wt%), and allowed to stand for 30 minutes to stabilize.

2-2-6. Fabrication of Polymer Blend Particles with PBTPA and PMMA

Polymer blend particles were fabricated as follows. The mixture of PBTPA and PMMA at weight ratio of 3:7, 5:5 and 7:3 (totally 0.1 g) (3.2:6.8, 5.2:4.8 and 7.2:2.8 in volume ratio) was dissolved into 0.9 g of toluene. The homogeneous solution (1.0 g) was dispersed into 6.7 mL of the aqueous solution containing 0.6 wt% of PVA with or without SDS (0.006-0.3 wt%) using a homogenizer (X520 CAT, As One Co., Japan) at 25,000 rpm for 1 s in a test-tube (115-mL. i.d.= 2.7 cm). The obtained dispersion was stirred with a mechanical stirrer (Shinto Scientific Co., Ltd., Japan) at 100 rpm to evaporate the solvent at room temperature. The particles were collected by centrifugation, and washed with distilled water three times.

2-2-7. Observation of polymer blend particles.

Blend particles were observed by optical microscope (OM), scanning electron microscope (SEM) (JSM-6510, JEOL Ltd., Japan) and transmission electron microscope (TEM) (JEM-2100, JEOL Ltd., Japan). Samples for SEM measurements were prepared by putting one drop of the dispersion of particles in distilled water on a sample stage and then drying in air. The samples were coated by gold (Au) with an ion coater (IB-3, EIKO Engineering Co., Ltd., Japan) to avoid the charging. Specimens for TEM observations were prepared as follows;

dried particles were dispersed to an epoxy resin, cured at 60 °C for three days, and microtomed (UC7, Leica, Germany). The ultrathin cross sections were put on the copper grid and stained with ruthenium tetraoxide (RuO_4) vapor at room temperature for 5 min in the capped vial with the presence of 1% RuO_4 aqueous solution.

Table 2-1. Molecular weight of PBTPA and PMMA used for preparing polymer blend particles.

Polymer	M_n (g mol^{-1})	M_w (g mol^{-1})	PDI
PBTPA-1	5,500	10,800	2.0
PBTPA-2	4,800	8,200	1.7
PBTPA-3	9,500	13,600	1.4
PMMA-1	13,200	20,900	1.6
PMMA-2	9,200	12,800	1.4
PMMA-3	33,900	35,200	1.04

2-3. Results and discussion

2-3-1. Interfacial tension of PBTPA and PMMA

Table 2-2 shows the contact angles θ of water, diiodomethane (CH_2I_2), aqueous solution of PVA with and without SDS, and surface tension γ_s of the thin films of PBTPA and PMMA. Fowkes has suggested that total free energy at a surface is the sum of contributions from the different intermolecular forces at the surface.[17] Owens and Wendt attributed the contributions to γ_s^d and γ_s^p: "d" and "p" represent dispersion and polar component, respectively.[15] The total surface tensions of PBTPA and PMMA are close to each other. However, the polar component of PMMA is higher than that of PBTPA. This higher polar component makes PMMA more hydrophilic than PBTPA. Interfacial tensions of polymers calculated from the surface tension and the contact angle are shown in Table 2-3. Smaller interfacial tension demonstrates that PMMA has more affinity to the water phase than PBTPA.

Table 2-2. Contact angles and surface tensions of polymer thin films

Polymer	Contact angle θ (°)				surface tension (mN m^{-1})[b]		
	Water	CH_2I_2	0.6 wt% PVA aq	0.6 wt% PVA + 0.3 wt% SDS[a] aq	γ_s^d	γ_s^h	γ_s
PMMA	79.1	35.4	75.7	62.3	38.8	3.9	42.7
PBTPA	96.5	34.8	83.4	69.4	42.7	0.1	42.8

[a] SDS: sodium dodecyl sulfate, [b] γ_s^d and γ_s^h mean dispersion and polar component of surface tension. $\gamma_s^d + \gamma_s^h = \gamma_s$.

Table 2-3. Interfacial tensions between polymer thin films and the aqueous solution containing 0.6 wt% of PVA with or without 0.3 wt% SDS.

Polymer	Interfacial tension γ_{sl} (mN m^{-1})	
	0.6 wt% PVA aq	0.6 wt% PVA + 0.3 wt% SDS aq
PMMA	30.9	21.8
PBTPA	38.2	28.0

2-3-2. Effect of the composition

Figure 2-1 shows OM and SEM images of polymer blend particles fabricated from toluene solution droplets. OM images demonstrated that all particles showed core-shell like structure regardless of weight ratio of PBTPA and PMMA (Figures 2-1a, 2-1d and 2-1g). The surfaces of composite particles were smooth as shown in SEM images (Figures 2-1b, 2-1e and 2-1h). The shape of the PBTPA phase can be identified by soaking particles in acetone since acetone can only dissolve PMMA. Spherical particles remained after soaking process at all the compositions (Figures 2-1c, 2-1f and 2-1i), which means that the core is PBTPA. However, the PBTPA domain had two surfaces with different curvature. Each of the surfaces is originated from the interface between PBTPA/PMMA or PBTPA/aqueous phase, respectively. This indicates that the PBTPA domain was not completely engulfed by the

PMMA domain, and protrudes to the surface of the particles. From this asymmetric morphology, the composite particles are classified as the Janus type. TEM observation in which RuO_4 can only stain the PBTPA also proved the identification of the inner morphology. As shown in Figure 2-2, the PBTPA core appeared as dark region surrounded by bright region of PMMA shell. The morphology of particles from toluene can be thermodynamically explained. As shown in Table 2-3, since the interfacial tension between PBTPA and PVA aqueous solution is higher than that of PMMA, it is reasonable that the PMMA domain tend to cover the PBTPA domain.

Figure 2-3 shows OM and SEM images of polymer blend particles fabricated from toluene solution droplets dispersed in the PVA aqueous solution containing SDS as an additional surfactant. When the weight ratio of PBTPA:PMMA was 3:7, all particles exhibited Janus typed phase separation as shown in OM and SEM images (Figures 2-3a and 2-3b). Hemispherical residues remained after soaking in acetone (Figure 2-3c). When the weight ratio of PBTPA:PMMA was 5:5, OM did not capture the phase separation inside the particles (Figure 2-3d). As shown in SEM images, the residual PBTPA domain after soaking in acetone was spherical. From the images of cracked particles, a cavity existed inside the sphere (Figure 2-3f). The existence of the hollow suggests that the PMMA core was surrounded by the PBTPA shell. For the particles with 30 wt% of PMMA, hollow particles

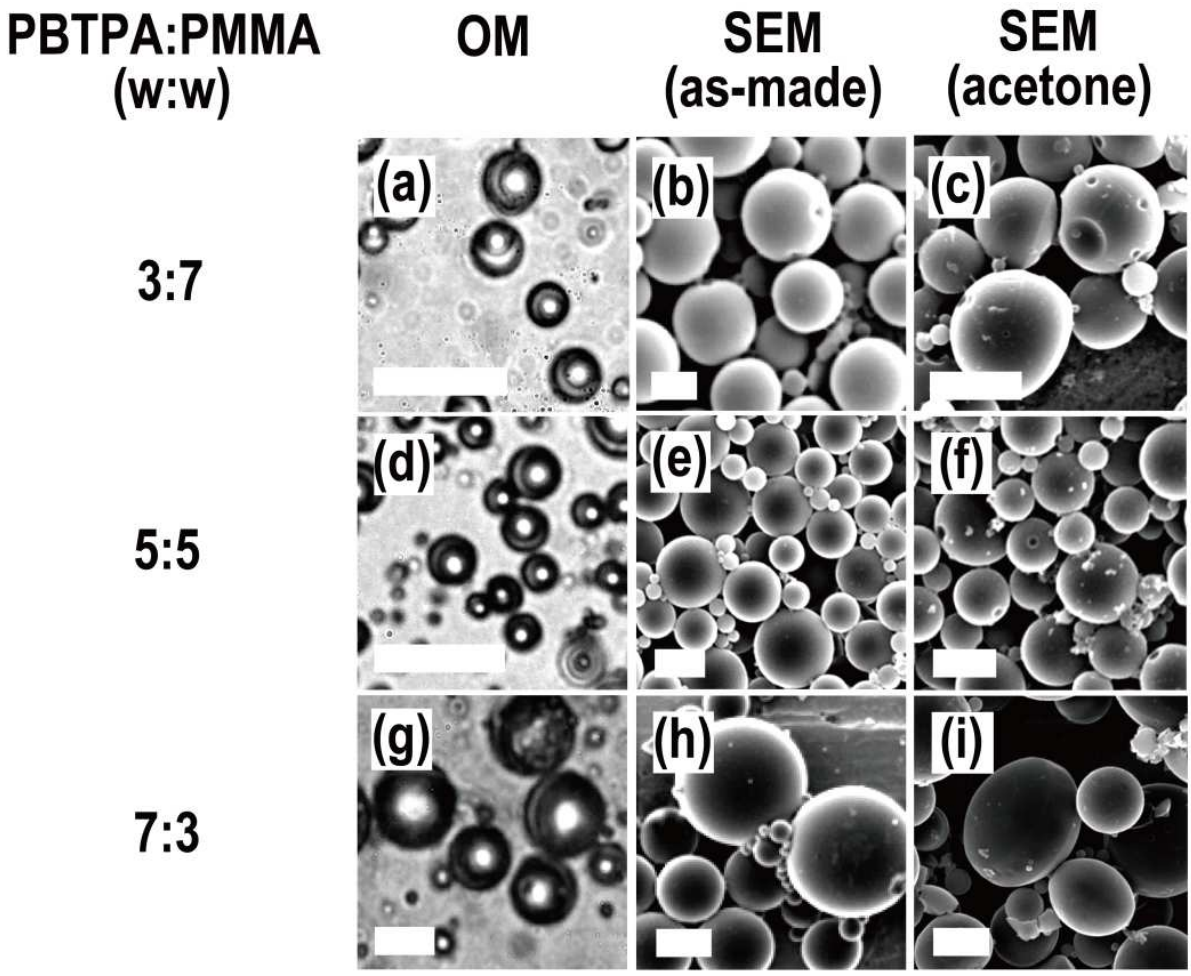

Figure 2-1. OM (**a**, **d**, **g**) and SEM (**b**, **c**, **e**, **f**, **h**, **i**) images of polymer blend particles fabricated from toluene solution droplets of polymers (10 wt%) dispersed in 0.6 wt% PVA aqueous solution. The weight ratios of PBTPA:PMMA were 3:7 (**a-c**), 5:5 (**d-f**), 7:3 (**g-i**), respectively. As-made particles (**a**, **b**, **d**, **e**, **g**, **h**) and those after soaking in acetone (**c**, **f**, **i**) were presented. M_n values (g mol^{-1}) of PBTPA and PMMA were 5,500 (PDI = 2.0), and 13,200 (PDI = 1.6), respectively. All scale bars represent 10 μm.

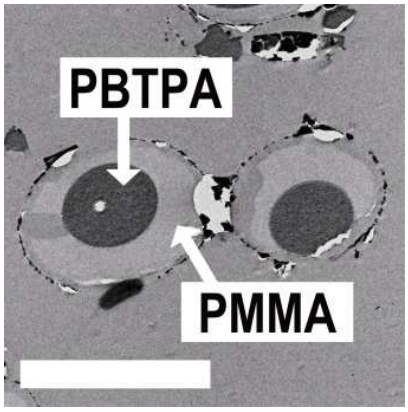

Figure 2-2. TEM image of polymer blend particle (PBTPA:PMMA was 5:5) corresponding to (**d-f**) in Figure 2-1. Dark and bright regions represent PBTPA and PMMA phase, respectively. Scale bar represents 10 μm.

were also obtained after soaking in acetone (Figure 2-3i). The PBTPA shell became thicker than that of the particles with 50 wt% of PMMA. These dependences of the polymer composition on the resulting morphologies were also confirmed by TEM observation as shown in Figure 2-4. The TEM image of the particles with 70 wt% of PMMA showed Janus typed morphology with the hemispherical PBTPA domain (Figure 2-4a). The TEM image of the particles with 50 wt% of PMMA showed coexistence of the Janus and inverse core-shell particles with PMMA core and PBTPA shell (Figure 2-4d). The feature of the inversed particles is that the thickness of the PBTPA layer was uniformed. For the particles with 30 wt% of PMMA, most of the particles showed inverse core-shell morphology, and PBTPA shell became thicker than that of the particles with 50 wt% of PMMA (Figure 2-4g).

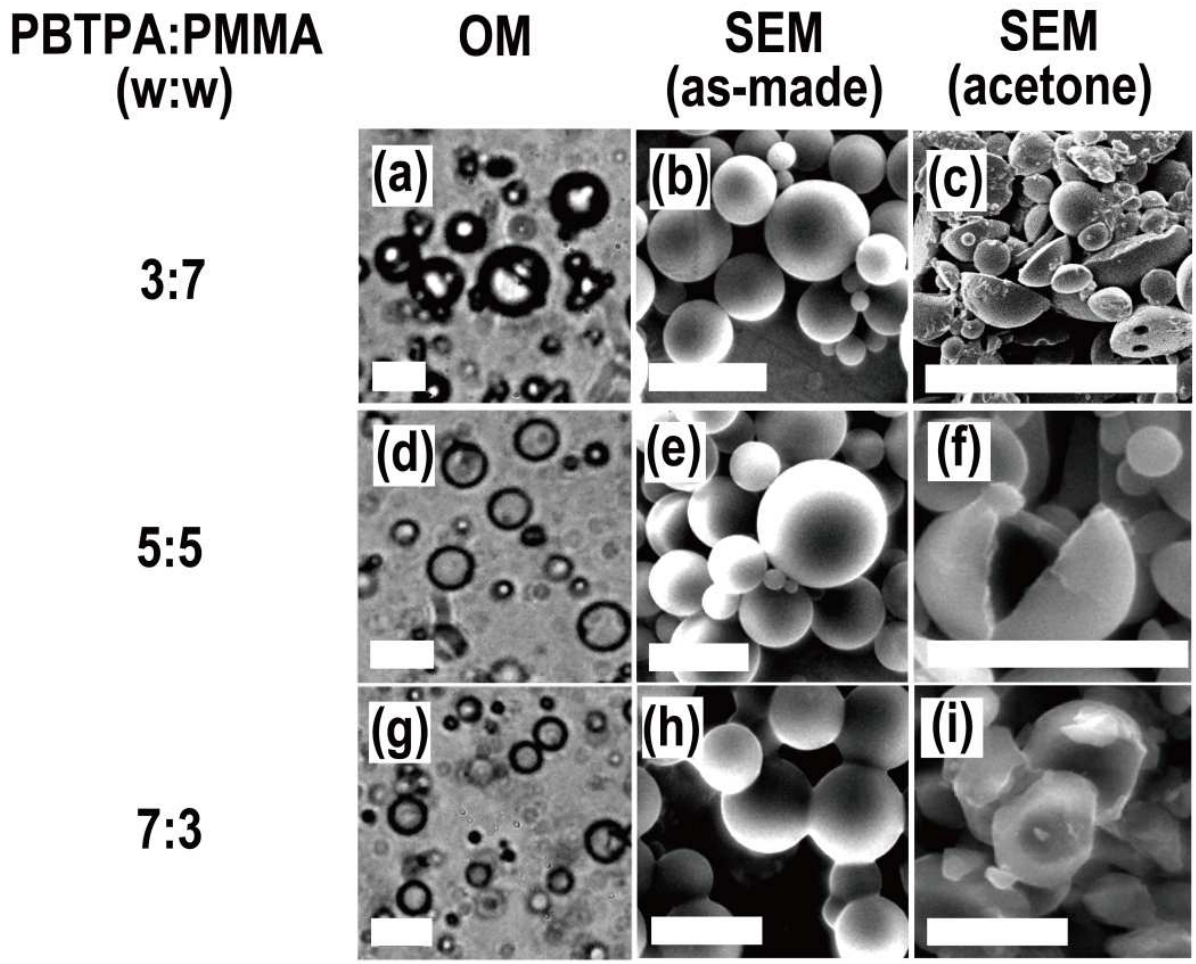

Figure 2-3. OM (**a**, **d**, **g**) and SEM (**b**, **c**, **e**, **f**, **h**, **i**) images of polymer blend particles fabricated from toluene solution droplets of polymers (10 wt%) dispersed in 0.6 wt% PVA aqueous solution with 0.3 wt% SDS. The weight ratios of PBTPA:PMMA were 3:7 (**a**-**c**), 5:5 (**d**-**f**), 7:3 (**g**-**i**), respectively. As-made particles (**a**, **b**, **d**, **e**, **g**, **h**) and those after soaking in acetone (c, **f**, **i**) were shown. PBTPA and PMMA were the same as those in Figure 2-1. All scale bars represent 10 μm.

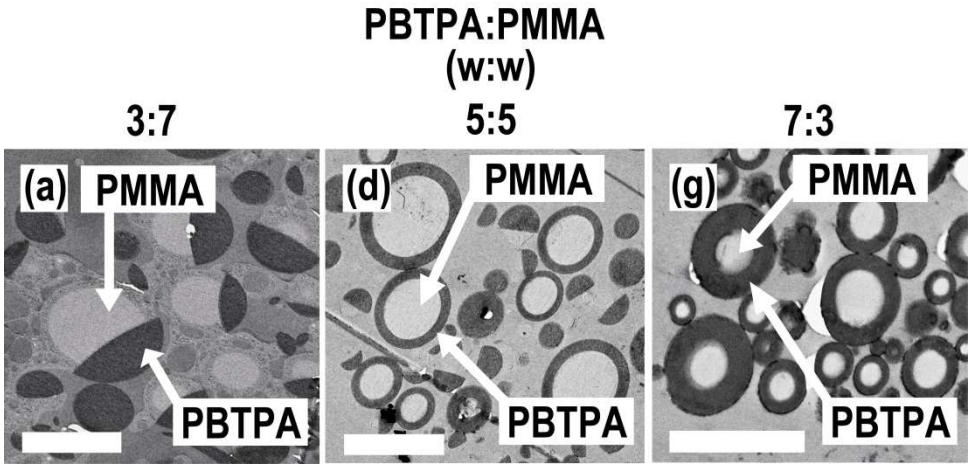

Figure 2-4. TEM images of polymer blend particles (**a**, **d**, **g**) designated in Figure 2-3. All scale bars represent 10 μm.

To clarify the size and composition dependence on the morphology, the size distribution of the residual particles was investigated after the soaking process. Hemispherical- and spherical particles were considered to be originated from Janus and inverse core-shell particles, respectively. The number of particles and the diameter of each particle was manually measured by analysing SEM images. The ratio of inverse core-shell particles to Janus ones was calculated by dividing the number of the spherical particles by the total number of hemispherical- and spherical particles. Figures 2-5a-b shows the distribution of the diameter of hemispherical and spherical particles after soaking in acetone of ca. 200 particles. For the particles with 70 wt% of PMMA, most of the particles were hemispherical originated from Janus type structure. When the weight percent of PMMA was 50 wt%, the both hemispherical- and spherical particles were observed. The most frequent diameters were 1 and 3 μm for hemispherical- and spherical particles, respectively. This result demonstrated that the smaller particles tend to be Janus. For the particles with 30 wt% of PMMA, most of the particles were spherical originated from inverse core-shell particles. The composition dependence on the morphology is shown in Figure 2-5d. The ratio of inverse core-shell particles to Janus ones increased as the percentage of the weight content of PMMA decreased.

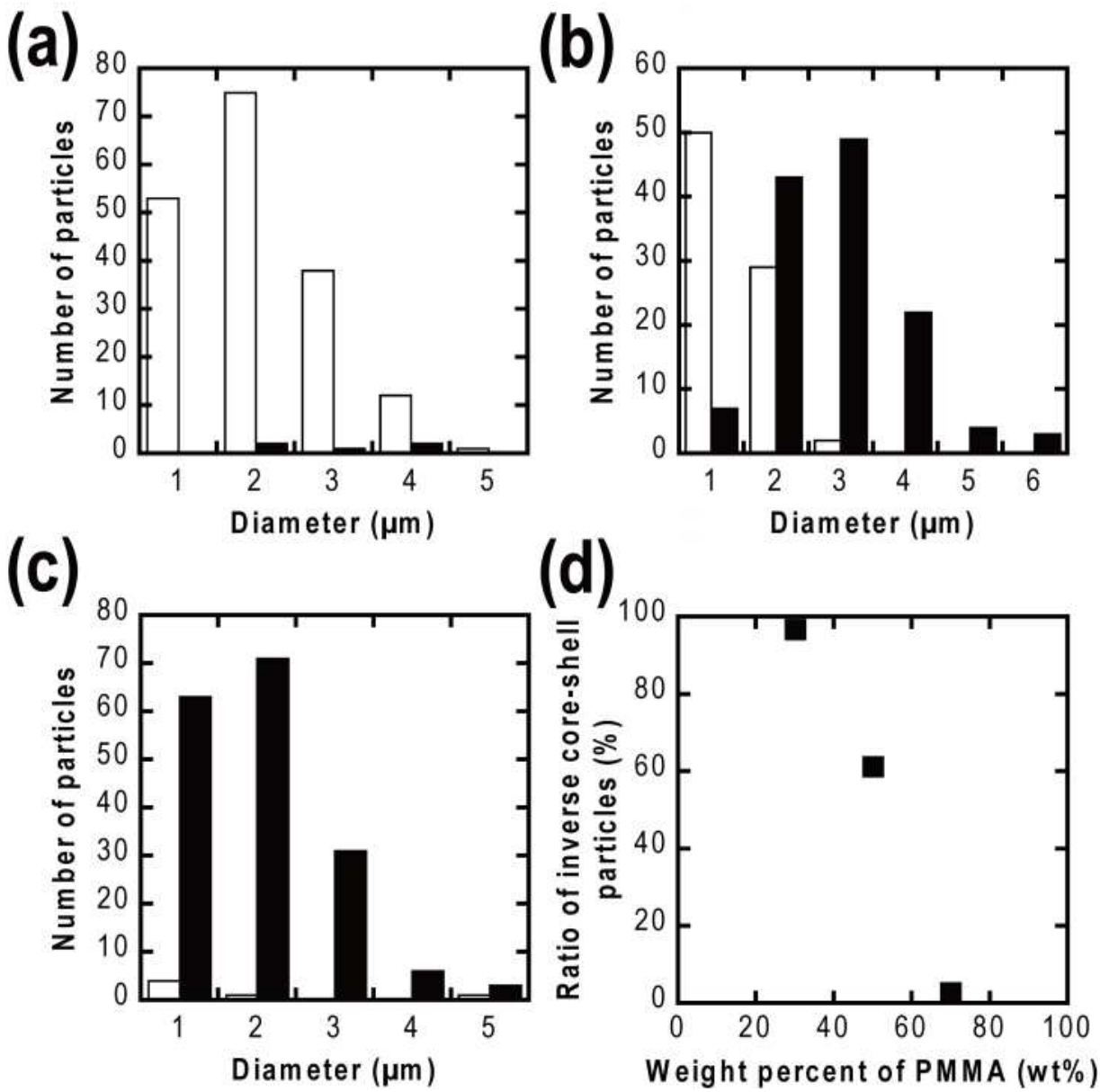

Figure 2-5. Size distributions of spherical (filled bar) - and hemispherical (open bar) particles obtained after soaking in acetone. (**a**); 70 wt%, (**b**); 50 wt% and (**c**); 30 wt% of PMMA. The other fabrication conditions are the same as those described in Figure 2-3. (**d**); relationship between the composition and the ratio of inversed core-shell particles to Janus ones.

2-3-3. Effect of the concentration of SDS

The concentration of SDS has an effect on the morphology as well. Fig. 2-6 shows the OM and SEM images of polymer blend particles fabricated from toluene solution droplets dispersed in the PVA aqueous solution with various concentrations of SDS. When the

concentration of SDS was 0.006 wt%, only Janus particles consisting of hemispherical PBTPA- and PMMA domains were obtained (Figures 2-6a-c). At 0.03 wt % of SDS, the inverse core-shell typed particles appeared as well as Janus typed ones. Some of the Janus particles had multiple PBTPA domains in a sphere (Figures 2-6d-f). When the concentration of SDS was 0.06 wt%, particles larger than 1 μm in a diameter tended to be inversed core-shell typed, whereas relatively smaller particles became Janus (Figures 2-6g-i). When the concentration of SDS was 0.15 and 0.3 wt%, most of the particles were inversed core-shell type. Only a few particles had Janus typed morphology with the PBTPA domain partially engulfing PMMA domain (Figures 2-6j-o).

Figure 2-7 shows the size distribution of hemispherical and spherical particles after soaking in acetone. At first, the distribution peak of particles shifted to the small diameter side with the increase of the SDS concentration. This is because SDS stabilizes small oil droplets and prevents the coalescence. Relatively larger particles exhibited the inverse core-shell morphology. The diameter dependency was clearly observed especially at the SDS concentration of 0.06 wt%. The most frequent diameters were 2 and 1 μm for spherical- and hemispherical particles, respectively (Figure 2-7b). This result is consistent with the size dependence observed in Figure 2-6.

In Figure 2-8, the ratios of inverse core-shell particles of ca. 200 particles (filled squares) are plotted against the concentration of SDS. As the SDS concentration increased, the ratio of the inverse core-shell particles increased up to 90% at SDS 0.15 wt% lower than the critical micelle concentration of SDS (0.24 wt%). The structure of the particles is interpreted by the balance of the interfacial tensions. In Figure 2-8, the interfacial tensions between aqueous solution and 10 wt% toluene solutions of PMMA and PBTPA are also presented by open triangles and circles, respectively. For 0.6 wt% PVA aqueous solution without SDS, PBTPA exhibited higher interfacial tension (8.8 mN m^{-1}) than PMMA (7.9 mN m^{-1}). This relationship

resulted in the formation of the incomplete core-shell structure in which the PMMA domain has larger contact area to the aqueous solution engulfing the PBTPA domain. Addition of 0.006 wt% SDS lowered the tensions of both of the polymer solutions; PBTPA: 7.2 mN m^{-1}; PMMA: 6.9 mN m^{-1}.At this point, most of the particles formed Janus structure consisting with the hemispherical PBTPA- and PMMA domains due to the smaller difference of the interfacial tensions. When the SDS concentration was 0.06 wt%, the interfacial tension of PBTPA solution (6.9 mN m^{-1}) became lower than that of PMMA solution (7.7 mN m^{-1}). This result indicates that the inverse core-shell structure in which PBTPA domain contacts to the aqueous phase is thermodynamically favored. Indeed, the ratio of the inverse core-shell particles reached to 50% at this concentration. PBTPA solution showed lower tension at 0.15 and 0.3 wt% SDS as well, and the ratio reached to around 90%.

2-3-4. Effect of the molecular weight

The effects of the molecular weight on the morphology were investigated as well. Figure 2-9 shows the SEM images of the particles fabricated from various molecular weights of polymers. When the molecular weight of PBTPA was relatively high (M_n = 9,500), composite particles exhibited Janus structure (Figures 2-9a and 2-9b). When the higher molecular weight of PMMA (M_n = 33,900) was utilized, multiple dents were observed on the surface of as-made particles (Figure 2-9c). The shape of the residual particles was spherical. However, a large hole on the surface indicated that PBTPA domain was not completely engulfed by PMMA domains, and protruded to the surface of the particles (Figure 2-9d). These results demonstrate that the formation of inverse core-shell structure was suppressed when higher molecular weight of polymers were utilized.

Hawker et al. reported that the polymer composition at the surface of the polymer particles fabricated by a solvent evaporation method is controllable by suitable choice of the surfactant.

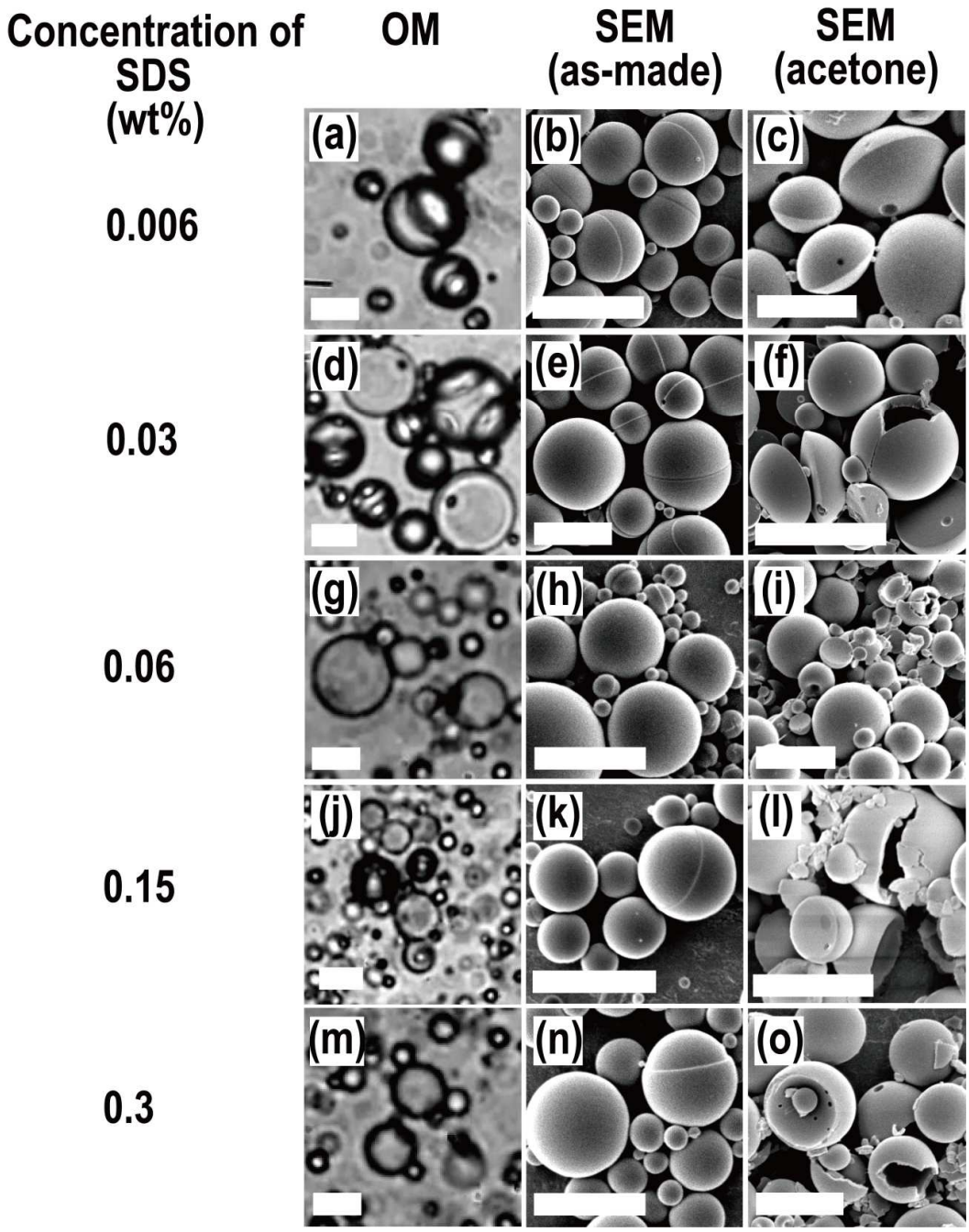

Figure 2-6. OM (**a**, **d**, **g**, **j**, **m**) and SEM (**b**, **c**, **e**, **f**, **h**, **i**, **k**, **l**, **n**, **o**) images of polymer blend particles fabricated from toluene solution droplets of polymers (10 wt%) dispersed in 0.6 wt% PVA aqueous solution with (**a**-**c**) 0.006, (**d**-**f**) 0.03, (**g**-**i**) 0.06 and (**j**-**l**) 0.15, and (**m**-**o**) 0.3 wt% SDS. The weight ratios of PBTPA:PMMA was 5:5. As-made particles (**a**, **b**, **d**, **e**, **g**, **h**, **j**, **k**, **m**, **n**) and those after soaking in acetone (**c**, **f**, **i**, **l**, **o**) were shown. The values of M_n (g mol^{-1}) of PBTPA and PMMA were 4,800 (PDI = 1.7) and 9,200 (PDI = 1.4), respectively. All scale bars represent 4 μm.

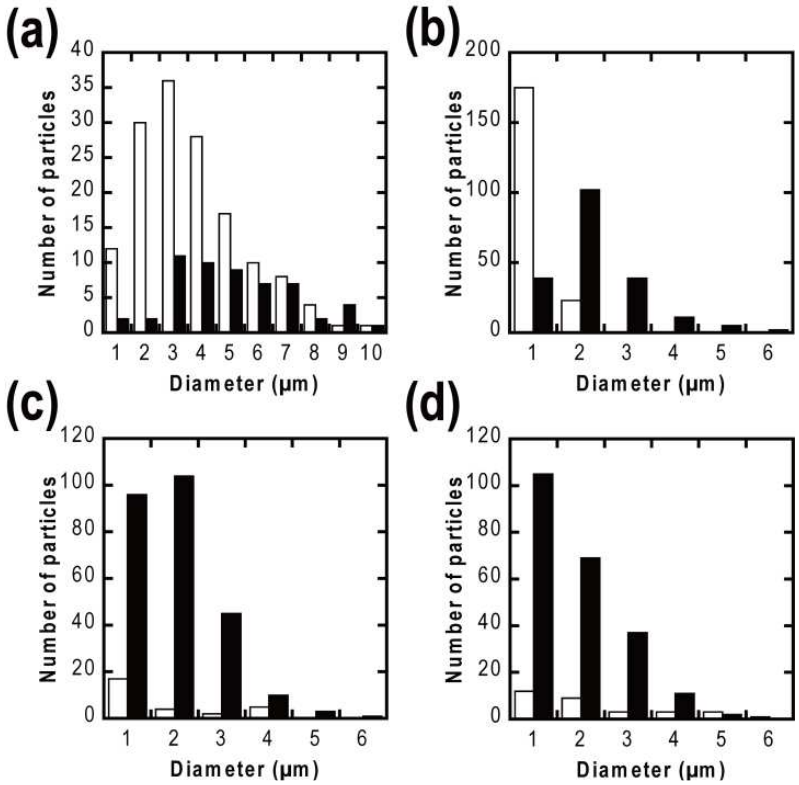

Figure 2-7. Size distributions of spherical (filled bar) - and hemispherical (open bar) particles obtained after soaking in acetone. (**a**); 0.03 wt%, (**b**); 0.06 wt%, (**c**); 0.15 wt% and (**d**); 0.3 wt% of SDS. The other fabrication conditions are the same as those described in Figure 2-6.

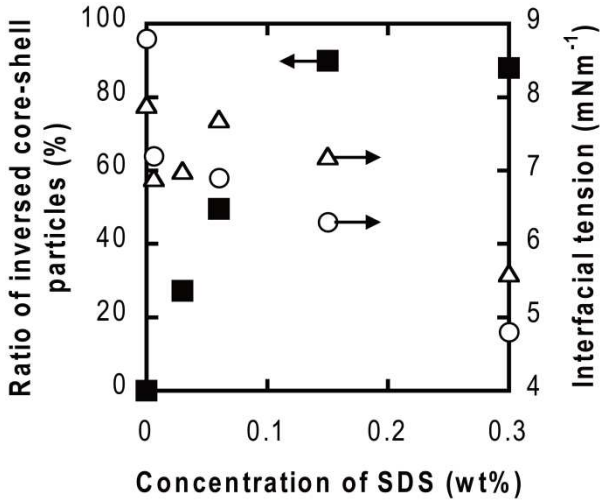

Figure 2-8. Dependences of the concentration of SDS on the ratio of inversed core-shell particles to Janus ones (filled square), and the interfacial tension of the 10 wt% toluene solution of (open triangle) PMMA and (open circle) PBTPA to aqueous solution (0.6 wt% PVA with various concentration of SDS). The other fabrication conditions are the same as those described in Figure 2-6.

For the multi layered particle consisting of PS-*b*-poly(2-vinylpyridine) (P2VP), using SDS as the surfactant affords the particles with the surface layer consisting of PS, whereas SDS-OH, surfactant in which a hydroxyl group is attached to the end of the dodecyl chain, as the surfactant provides the particles with the surface layer consisting of P2VP.[18] This is because the polymer composition at the surface of the particle is determined by the affinity between polymer and the inner surface of the droplet in the analogy with the selective wetting and associated self-assembly of block copolymers in thin films on the substrate.[19,20] Since the surfactants are absorbed at the surface of the solution droplet with directing hydrophobic portion to the inside of the droplets, the affinity of the inner surface can be controled can be controlled by modifying the hydrophobic part of surfactants. According to the values of the contact angles, PBTPA is more hydrophobic than PMMA. Therefore, PBTPA should have higher affinity to hydrocarbon chain of SDS than PMMA. The lower interfacial tension of PBTPA solution to SDS aqueous solution than that of PMMA suggests the higher affinity between PBTPA and SDS. The strong interaction between hydrophobic tail of SDS and PBTPA moiety near the surface of the solution droplet promotes the formation of PBTPA shell. As shown in Figures 2-5 and 2-7, there is a tendency that smaller particles exhibited Janus typed morphology. This can be explained by the kinetic consideration as follows. At the beginning of liquid-liquid phase separation in solution droplets, it is considered that the interfacial tensions between aqueous phase and each polymer are nearly equal due to the low concentration of the polymer. Therefore, the phase separated morphology thermodynamically favors Janus structure at the initial stage. Since the specific surface area is inversely proportional to the diameter, the decrease of the diameter accelerates the diffusion of the solvent from the droplet to the aqueous medium. The concentration of polymer and viscosity of the solution increased more rapidly by accelerated diffusion for the droplets with smaller droplets. Resulting high viscosity limits the motion of separated phases to retain the Janus

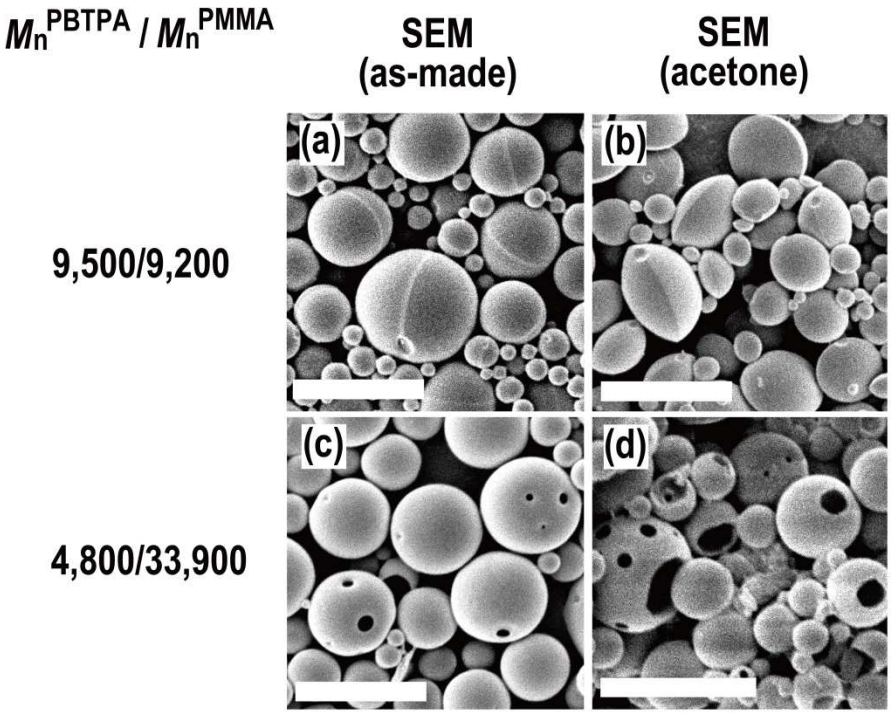

Figure 2-9. SEM images of polymer blend particles fabricated from toluene solution droplets dissolving 10 wt% of polymer dispersed in 0.6 wt% PVA and 0.3 wt% SDS aqueous solution. The weight ratio of PBTPA:PMMA was 5:5. As-made particles (**a**, **c**) and those after soaking in acetone (**b**, **d**) were shown. M_n^{PBTPA}/M_n^{PMMA} were (**a**, **b**) 9,500/9,200 and (**c**, **d**) 4,800/33,900, respectively. All scale bars represent 4 μm.

morphology formed at the initial state of the phase separation even though the inversed core-shell one is favored thermodynamically. Increasing the molecular weight of the polymers has same effect as shown in Figure 2-9. High viscosity due to the high molecular weight suppresses the motion of domains, resulting in the the incomplete structure on the way to inverse core-shell (Figure 2-10).

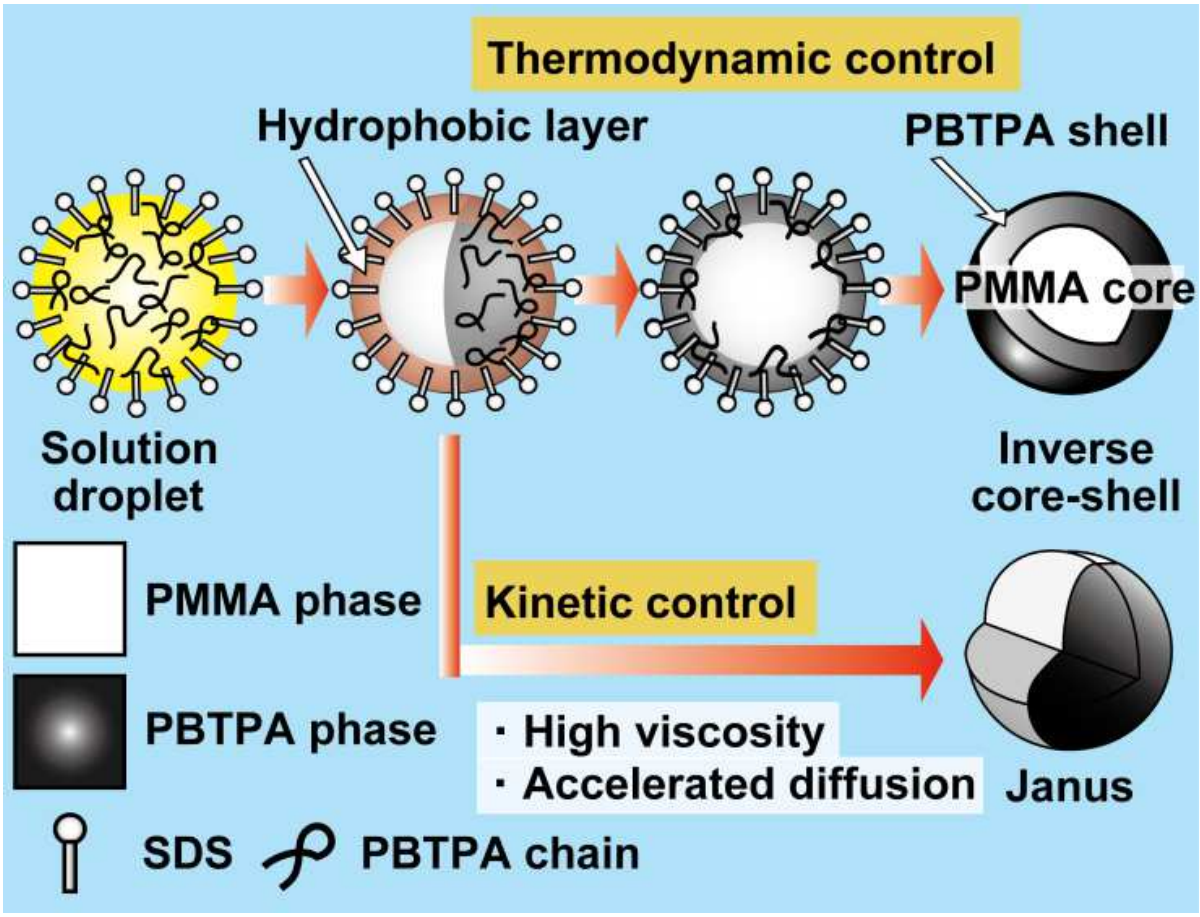

Figure 2-10. Schematic models of the formation of the Janus and the inverse core-shell particles.

2-4. Conclusions

Micron-sized polymer blend particles comprising PBTPA and PMMA were fabricated by a solvent evaporation method. Effects of SDS as a surfactant on the morphology were investigated. When only PVA was used as a suspension stabilizer, Janus particles in which PBTPA domain is partially covered by PMMA domain were obtained from toluene solution droplets. The addition of SDS as the surfactant caused the formation of Janus and inverse core-shell particles with PMMA core and PBTPA shell. The ratio of the inverse core-shell particles was controllable by the composition of polymers and the concentration of SDS. As the content of PBTPA increased, inverse core-shell became favored structure, and PBTPA shell became thicker. The increase of the SDS concentration enhanced the formation of inversed core-shell particles as well. The ratio of the inverse core-shell reached to 90% at

SDS 0.3 wt%. According to the relationship between size and morphology determined by SEM observation, small particles tend to exhibit Janus morphology. Increasing the molecular weight of the polymers suppressed the formation of inverse core-shell. It is noteworthy that concentric nature observed in inverse core-shell particles has been rarely reported for the particles prepared via a solvent evaporation method. The particles with symmetric core-shell structure can be expected as promising candidates in optical applications.

2-5. References

(1) Yamashita, N.; Yamagami, T.; Okubo, M. Preparation of hemispherical particles by cleavage of micrometer-sized, spherical poly(methyl methacrylate)/polystyrene composite particle with Janus structure: effect of molecular weight. *Colloid Polym. Sci.* **2014**, *292*, 733–738.

(2) Saito, N.; Kagari, Y.; Okubo, M. Effect of colloidal stabilizer on the shape of polystyrene/poly(methyl methacrylate) composite particles prepared in aqueous medium by the solvent evaporation method. *Langmuir* **2006**, *22*, 9397–4902.

(3) Ge, X.; Wang, M.; Ji, X.; Ge, X.; Liu, H. Effects of concentration of nonionic surfactant and molecular weight of polymers on the morphology of anisotropic polystyrene/poly(methyl methacrylate) composite particles prepared by solvent evaporation method. *Colloid Polym. Sci.* **2009**, *287*, 819–827.

(4) Sanders, J.V. Diffraction of light by opals. *Acta. Crystall. A-Crys. A.* **1968**, *24*, 427–434.

(5) Fudouzi, H. Optical properties caused by periodical array structure with colloidal particles and their applications. *Adv. Powder Technol.* **2009**, *20*, 502–508.

(6) Gallei, M. Functional polymer opals and porous materials by shear-induced assembly of tailor-made particles. *Macromol. Rapid Commun.* **2017**, *39*, 1700648.

(7) Moroz, A.; Sommers, C. Photonic band gaps of three-dimensional face-centred cubic lattices. *J. Phys: Condens. Matter.* **1999**, *11*, 997–1008.

(8) Breen, M.L.; Dinsmore, A.D.; Pink, R.H.; Qadri, S.B.; Ratna, B.R. Sonochemically produced ZnS-coated polystyrene core-shell particles for use in photonic crystals. *Langmuir* **2001**, *17*, 903–907.

(9) Velikov, K.P.; Moroz, A.; van Blaaderen, A. Photonic crystals of core-shell colloidal particles. *Appl. Phys. Lett.* **2002**, *80*, 49–51.

(10) Zulian, L.; Emilitri, E.; Scavia, G.; Botta, C.; Colombo, M.; Destri, S. Structural iridescent tuned colors from self-assembled polymer opal surfaces. *ACS Appl. Mater. Interfaces* **2012**, *4*, 6071–6079.

(11) Spahn, P.; Finlayson, C.E.; Etah, W.M.; Snoswell, D.R.E.; Baumberg, J.J.; Hellmann, G.P. Modification of the refractive-index contrast in polymer opal films. *J. Mater. Chem.* **2011**, *21*, 8893–8897.

(12) Stubbs, J.; Karlsson, O.; Jönsson, J.E.; Sundberg, E.; Durant, Y.; Sundberg, D. Non-equilibrium particle morphology development in seeded emulsion polymerization. 1: penetration of monomer and radicals as a function of monomer feed rate during second stage polymerization. *Colloids Surf. A: Physicochem. Eng. Asp.* **1999**, *153*, 255–270.

(13) Karlsson, L.E.; Karlsson, O.J.; Sundberg, D.C. Nonequilibrium particle morphology development in seeded emulsion polymerization. II. Influence of seed polymer Tg. *J. Appl. Polym. Sci.* **2003**, *90*, 905–915.

(14) Young, T. An essay on the cohesion of fluids. *Philos. Trans. Royal Soc. London* **1805**, *95*, 65–87.

(15) Owens, D.K.; Wendt, R.C. Estimation of the surface free energy of polymers. *J. Appl. Polym. Sci.* **1969**, *13*, 1741–1747.

(16) Kaelble, D.H.; Uy, K.C. A reinterpretation of organic liquid-polytetrafluoroethylene surface interactions. *J. Adhes.* **1970**, 2, 50–60.

(17) Fowkes, F.M. Attractive forces at interfaces. *Ind. Eng. Chem.* **1964**, *56*, 40–52.

(18) Klinger, D.; Wang, C.X.; Connal, L.A.; Audus, D.J.; Jang, S.G.; Kraemer, S.; Killops, K.L.; Fredrickson, G.H.; Kramer, E.J.; Hawker, C.J. A facile synthesis of dynamic, shape-changing polymer particles. *Angew. Chem. Int. Ed.* **2014**, *53*, 7018–7022.

(19) Mansky, P.; Liu, Y.; Huang, E.; Russell, T.P.; Hawker, C. Controlling polymer-surface interactions with random copolymer brushes. *Science* **1997**, *275*,1458–1460.

(20) Ryu, D.Y.; Ham, S.; Kim, E.; Jeong, U.; Hawker, C.J.; Russell, T.P. Cylindrical microdomain orientation of PS-b-PMMA on the balanced interfacial interactions: composition effect of block copolymers. *Macromolecules* **2009**, *42*, 4902–4906.

Chapter 3

Fabrication of core-shell, Janus, dumbbell, snowman-like and confetti-like structured microspheres of blends of poly(4-butyltriphenylamine) and poly(methyl methacrylate)

3-1. Introduction

In this chapter, the effects of the kind of the solvent, the molecular weight of the polymers and the evaporation rate of the solvent on the morphology of the particles were investigated. During the phase separation, solvents are distributed to each phase unequally depending on the affinity to each polymer. As the result, the polymer which has less affinity to the solvent loses its mobility earlier than the other one. For instance, the core-shell structured particles with the PMMA-shell and the PS-core fabricated from toluene solution has a dent.[1] This is because toluene is favored to distribute to the PS-core rather than the PMMA-shell. After the solidification of the PMMA-shell, the release of the residual toluene causes shrinkage of the PS-core and the formation of cave in. On the other hand, when chloroform, which has higher affinity to PMMA than that of PS, is used as the solvent, spherical particles without a dent are obtained. A molecular weight plays plural roles to determine the phase separated structure. First, the increase of the molecular weight lowers the critical concentration for phase separation. This means that blends of polymers with high molecular weight start phase separation earlier than one with low molecular weight. Second, the interfacial tension between polymers increases with an increase of the molecular weight of polymers.[2,3] The enhanced interfacial tension work to shrink the interfacial area between polymers and promote the formation of a Janus or dumbbell-like structure. Third, a high viscosity originated from a high molecular weight limits the motion of separated phases. High evaporation rate also induces rapid rise of the viscosity and freeze the phase separation before reaching to thermodynamically equilibrium.

This chapter demonstrates the preparation of the polymeric blend particle consisting of PBTPA and PMMA with various morphologies including core-shell, Janus, dumbbell-like, snowman-like and confetti-like structures. The mechanisms of the structure formation are explained based on the thermodynamic and kinetic balance. In particular, confetti-like

particle have been generally developed via seeded emulsion polymerization,[4,5] dispersion polymerization,[6] and seeded dispersion polymerization.[7,8] Few reports are available on the preparation of confetti like particle by solvent evaporation method.

3-2. Experimental section

3-2-1. Materials

PBTPA and PMMA were polymerized by the palladium catalyzed C-N coupling and atom transfer radical polymerization (ATRP), respectively.[9] The molecular weights and polydispersity indices (PDI) of obtained polymers were estimated by a gel permeation chromatography, and the results are summarized in Table 1. Poly(vinyl alcohol) (PVA224, Kuraray Co. Ltd., Japan, degree of polymerization; 2,400, degree of saponification; 87-89%) as a dispersion stabilizer, toluene and chloroform were purchased from Wako Pure Chemical Industries, Ltd, and used as received. Deionized water with specific resistance of 15 MΩ was distilled. The density (ρ) of polymers (PBTPA; ρ = 1.09 g cm^{-1}, PMMA; ρ = 1.20 g mL^{-1}) was evaluated by using an electronic balance AUX220 (Shimadzu Co., Kyoto, Japan).

Table 3-1. Molecular Weight of PBTPA and PMMA Used for Preparing Polymer Blend Particles

Polymer	M_n (g mol^{-1})	M_w (g mol^{--1})	PDI
PBTPA	10,000	23,000	2.3
PMMA-1	2,000	3,200	1.6
PMMA-2	25,000	46,000	1.8
PMMA-3	40,000	107,000	2.7

3-2-2. Measurement of interfacial tension

Interfacial tension between polymer- and aqueous solutions was measured by a pendant drop method with a contact angle gauge (DM-501, Kyowa Interface Science Co., Ltd., Japan)

at room temperature (ca. 20 °C). A drop of the polymer solution in toluene (1-10 wt%) with a volume of 15-30 μL was formed at the tip of the stainless steel needle in a glass cell filled with the aqueous solution containing 0.6 wt% of PVA, and allowed to stand for 30 minutes to stabilize.

3-2-3. Preparation of PBTPA and PMMA polymer blend particles

The mixture of PBTPA and PMMA at weight ratio of 9:1, 5:5, 3:7 or 1:9 (totally 0.05 g) was dissolved into 4.95 g of toluene or chloroform. 5.7 or 3.4 mL of the toluene or chloroform solution was dispersed to 15 or 20 mL of the aqueous solution containing 0.6 wt% of PVA using a homogenizer (X520 CAT, As One Co., Japan) at 25,000 rpm for 2 s in a test-tube (115 mL. opening diameter; 2.7 cm). The obtained dispersion was stirred using a mechanical stirrer (Shinto Scientific Co., Ltd., Japan) at 100 rpm in the uncovered glass vial (50 mL. opening diameter; 2.0 cm) or 300-mL beaker (opening diameter; 8.0 cm) to evaporate the solvent at room temperature. The particles were collected by centrifugation, and washed with distilled water three times.

3-2-4. Observation of polymer blend particles

PBTPA and PMMA blend particles were observed by optical microscope (OM), scanning electron microscope (SEM) (JSM-6510, JEOL Ltd., Japan) and transmission electron microscope (TEM) (JEM-2100, JEOL Ltd., Japan). Samples for SEM were prepared by putting one drop of the dispersion of particles in water on a sample stage and then drying in air. The samples were coated by gold (Au) with an ion coater (IB-3, EIKO Engineering Co., Ltd., Japan) to avoid the charging. Samples for TEM were prepared as follows; dried particles were dispersed to epoxy resin, cured at 60 °C for three days, and microtomed (UC7, Leica, Germany). The ultrathin cross sections were put on the copper grid and stained with ruthenium tetraoxide (RuO_4) vapor at room temperature for 5 min in the capped vial containing 1% RuO_4 aqueous solution.

3-3. Results and discussion

3-3-1. Effect of molecular weight of PMMA

Fig. 3-1 shows OM and SEM images of polymer blend particles fabricated from toluene solution containing PBTPA (M_n = 10,000) and PMMA with various molecular weight. The morphologies of particles changed from the core-shell type consisting of the PBTPA core and the PMMA shell, to the Janus one with the increase of the molecular weight of PMMA (Fig. 3-1 (a-f)). The shape of the PBTPA phase can be identified by soaking particles in acetone since acetone can only dissolve PMMA. The shape of the residues remained after soaking in acetone was changed from spherical to hemispherical as the molecular weight increased (Fig. 3-1 (g-i)).

From the contact angles of the aqueous solutions on the polymer thin films, the interfacial tensions of PBTPA and PMMA to 0.6 wt% PVA aqueous solution were determined to be 38.2 and 30.9 mN m^{-1}, respectively.[10] The lower value for PMMA demonstrates that PMMA is more hydrophilic than PBTPA. Therefore, the core-shell structure with PMMA shell is thermodynamically stable. However, the particle consisted of polymer with high molecular weight exhibited Janus structure. It is considered that the kinetic limitation caused the formation of the Janus structure. The composite particles consisting of PS and PMMA have shown similar dependency on the molecular weight.[11, 12] Just after the phase separation in the solution droplets, the interfacial tensions between aqueous phase and each polymer solution should be nearly equal because of the low concentration of the polymer. Therefore, it is reasonable that the phase separated morphology is Janus-typed at the thermodynamic equilibrium in the early stage of phase separation. In the case that the high molecular weight of PMMA was applied, it is suggested that highly viscous nature in the PMMA fragment in the droplets suppressed the transformation of the domain to form the

thermodynamically stable morphology in the evaporation process. That is why Janus structure was observed for the particles involving PMMA with high molecular weight.

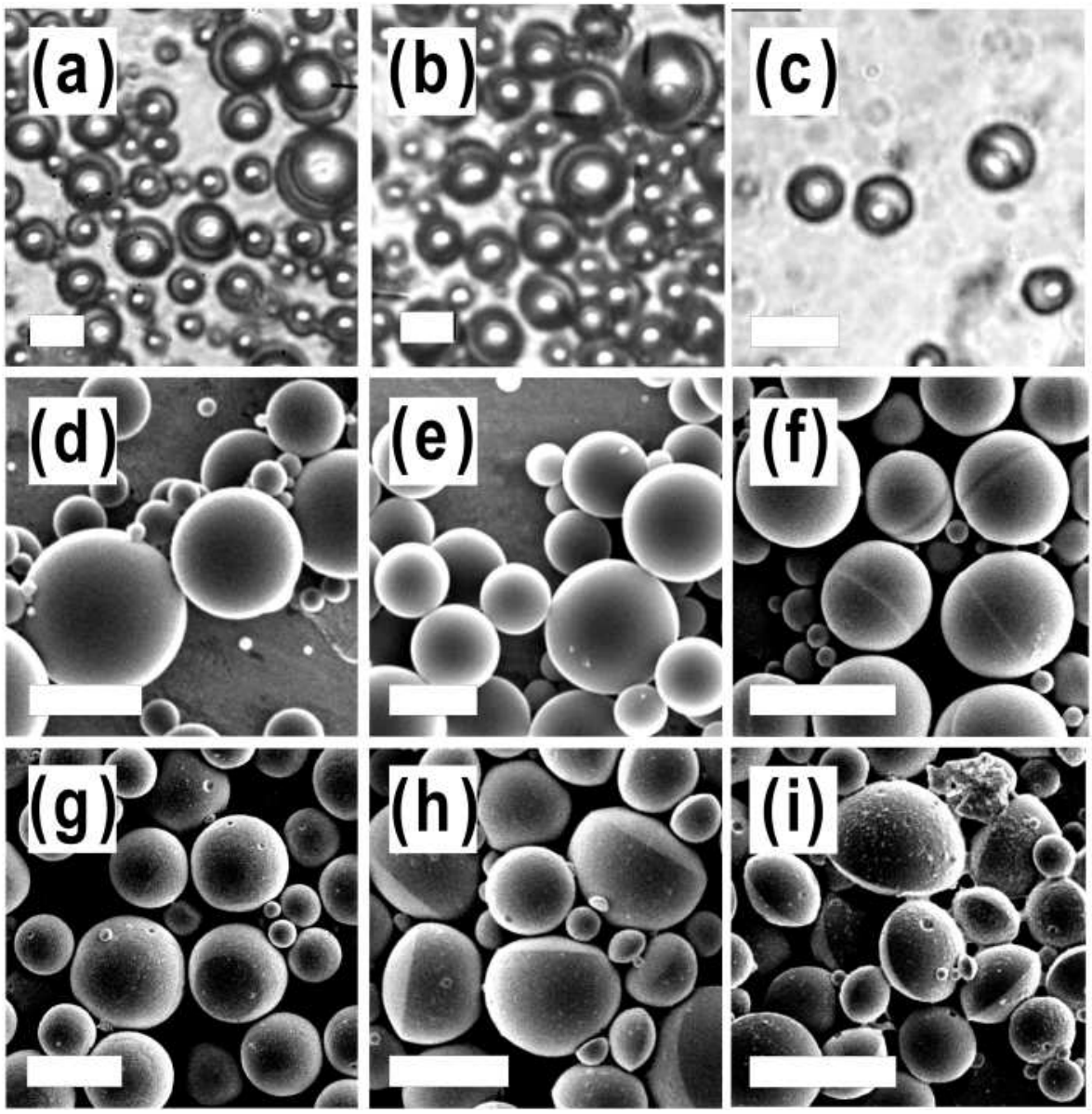

Figure 3-1. OM (**a-c**) and SEM (**d-i**) images of polymer blend particles fabricated from toluene solution droplets. The images show the particles observed before (a-f) and after soaking in acetone (**g-i**). Weight ratio of PMMA was 50 wt%. The values of M_n (g mol^{-1}) of PMMA were 2,000 (PDI = 1.6) (**a**, **d**, **g**), 25,000 (PDI =1.8) (**b**, **e**, **h**), and 40,000 (PDI = 2.7) (**c**, **f**, **i**), respectively. M_n (g mol^{-1}) of PBTPA was 10,000 (PDI = 2.3). All scale bars represent 5 μm.

Fig. 3-2 shows OM and SEM images of polymer blend particles fabricated from chloroform solution droplets. Contrary to the case of toluene, the particles had dumbbell-like structure, in which PBTPA and PMMA particles are interconnected each other (Fig. 3-2 (a-f)). Spherical residues remained after soaking in acetone (Fig. 3-2 (g-i)). When the molecular weight of PMMA was low, triple particles in which three domains were interconnected each other were observed in addition to dumbbell-like one (Fig. 3-2 (d)).

It is recognized that the interfacial tension plays an important role to determine the morphology of the particles. To elucidate the solvent dependency on the final morphology, the interfacial tensions between 0.6 wt% aqueous solution and organic solutions with various concentrations of the polymers were determined by a pendant drop method. Fig. 3-3 showed that the interfacial tensions of the solutions were in the range of 6-9 (toluene) and 2-4 (chloroform) mN m^{-1}, respectively. The interfacial tensions of toluene and chloroform to distilled water without PVA were 33.1 and 25.6 mN m^{-1}, respectively. These results demonstrated that the addition of PVA to water significantly lowered the interfacial tension. This reduction originates from the adsorption of PVA chains at the interface between organic and aqueous solution.[13, 14] In particular, the interfacial tension between the chloroform solutions and PVA solution was lower than compared with the toluene solutions. The solubility parameters (SPs) of 100% hydrolyzed PVA, chloroform and toluene are 25.78, 19.0 and 18.2 $(MPa)^{1/2}$, respectively.[15] The SP value of chloroform is closer to that of PVA compared with toluene. It is reasonable that the SP value of 87-89% hydrolyzed PVA is lower than 100% hydrolyzed PVA, and the difference between partially hydrolyzed PVA and chloroform decreases.

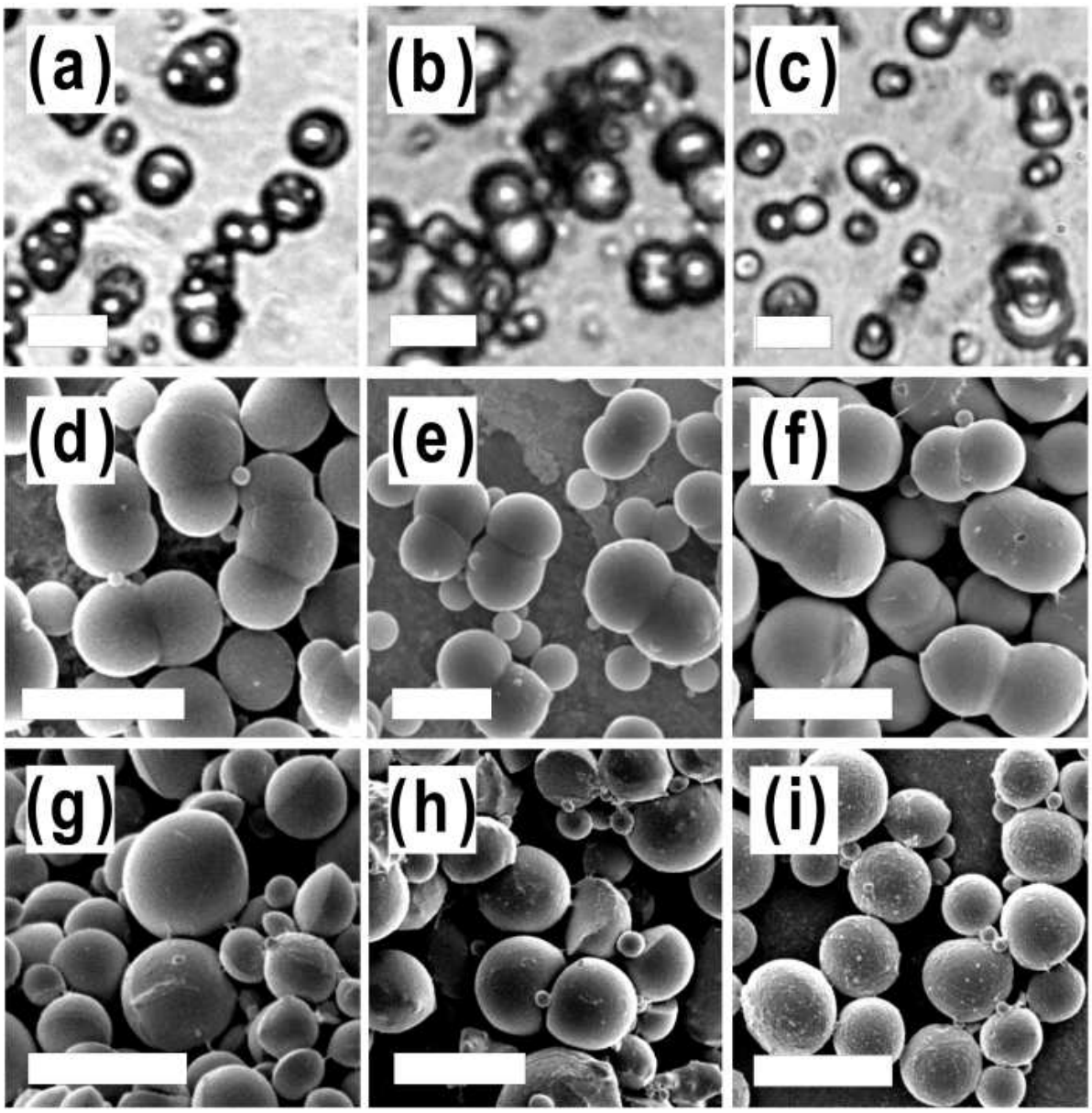

Figure 3-2. OM (**a**-**c**) and SEM (**d**-**i**) images of polymer blend particles fabricated from chloroform solution droplets. The images show the particles observed (**a**-**f**) before and (**g**-**i**) after the soaking in acetone. Weight ratio of PMMA was 50 wt%. M_n (g mol^{-1}) of PBTPA was 10,000 (PDI = 2.3), and M_n (g mol^{-1}) of PMMA were 2,000 (PDI = 1.6) (**a**, **d**, **g**), 25,000 (PDI =1.8) (**b**, **e**, **h**), and 40,000 (PDI = 2.7) (**c**, **f**, **i**), respectively. All scale bars represent 5 μm.

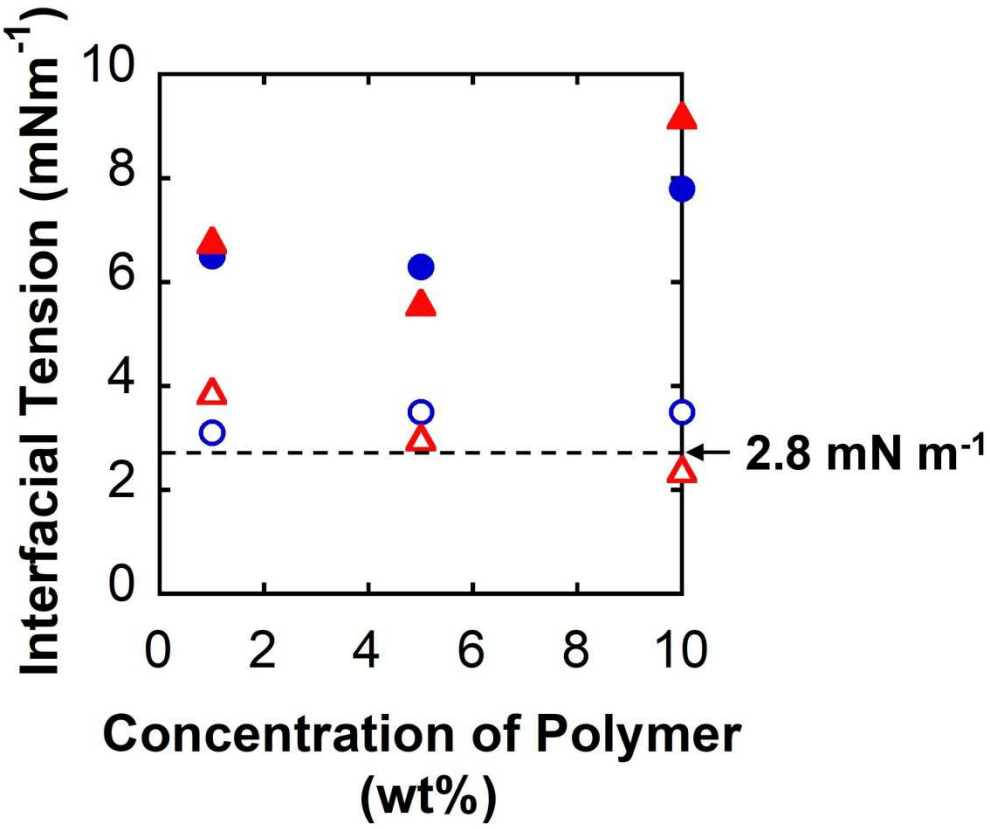

Figure 3-3. Interfacial tensions between the polymer solution and 0.6 wt% PVA aqueous solution as a function of the concentration of the polymers; (filled circle): PBTPA-toluene; (filled triangle): PMMA-toluene; (opened circle): PBTPA-chloroform; (opened triangle): PMMA-chloroform. M_n (g mol^{-1}) of PBTPA was 10,000 (PDI = 2.3), and M_n (g mol^{-1}) of PMMA was 25,000 (PDI =1.8).

The interfacial tension between PBTPA and PMMA were calculated as follows. The work of adhesion W_{12} is calculated as the following Equation (3-1) expressed by Dupré:[16]

$$W_{12} = \gamma_1 + \gamma_2 - \gamma_{12} \quad (3\text{-}1)$$

where γ_1 and γ_2 are the surface tension of the materials 1 and 2 adhering to each other. γ_{12} is the interfacial tension between the materials 1 and 2. Owens and Wendt described W_{12} as following Equation (3-2) using γ^d and γ^h: "d" and "h" mean dispersion and polar component of surface tension:[17]

$$W_{12} = 2(\gamma_1^d \gamma_2^d)^{1/2} + 2(\gamma_1^h \gamma_2^h)^{1/2}. \quad (3\text{-}2)$$

From equations (3-1) and (3-2), the interfacial tension γ_{12} is calculated by Equation (3-3):

$$\gamma_{12} = \{(\gamma_1^d)^{1/2} - (\gamma_2^d)^{1/2}\}^2 + \{(\gamma_1^d)^{1/2} - (\gamma_2^d)^{1/2}\}^2. \quad (3\text{-}3)$$

The values of γ^d and γ^h for PMMA were 38.8 and 3.9 mN m^{-1}, and those of γ^d and γ^h for PBTPA were 42.7 and 0.1 mN m^{-1}. The interfacial tension between PBTPA and PMMA calculated from Equation (3-3) is 2.8 mN m^{-1}, which is close to the interfacial tension between the chloroform solution and the 0.6 wt% PVA aqueous solution.

The interfacial energy between polymers is the driving force to form dumbbell like structure. The interfacial tension of polymer/polymer interface is generally small enough to be ignorable compared with that of polymer/water interface. However, when surfactants such as sodium dodecyl sulfate (SDS) lower the interfacial tension of polymer/water interface to the comparable value to that of polymer/polymer interface, the interfacial area between polymers becomes smaller to keep the thermodynamic equilibrium. The reduction of the interfacial tension caused by the addition of PVA makes the tension between the chloroform and the aqueous solution comparable to that of the PBTPA/PMMA interface. Therefore, the particles fabricated from the chloroform solution formed dumbbell-like structure to decrease the interfacial area between PBTPA and PMMA. In the case of toluene, since the interfacial tension to PVA aqueous solution remained enough higher than that of the interface between the polymers, the particles formed core-shell structure based on the comparison of the interfacial tensions of the polymer/aqueous solution interface (Fig. 3-4).

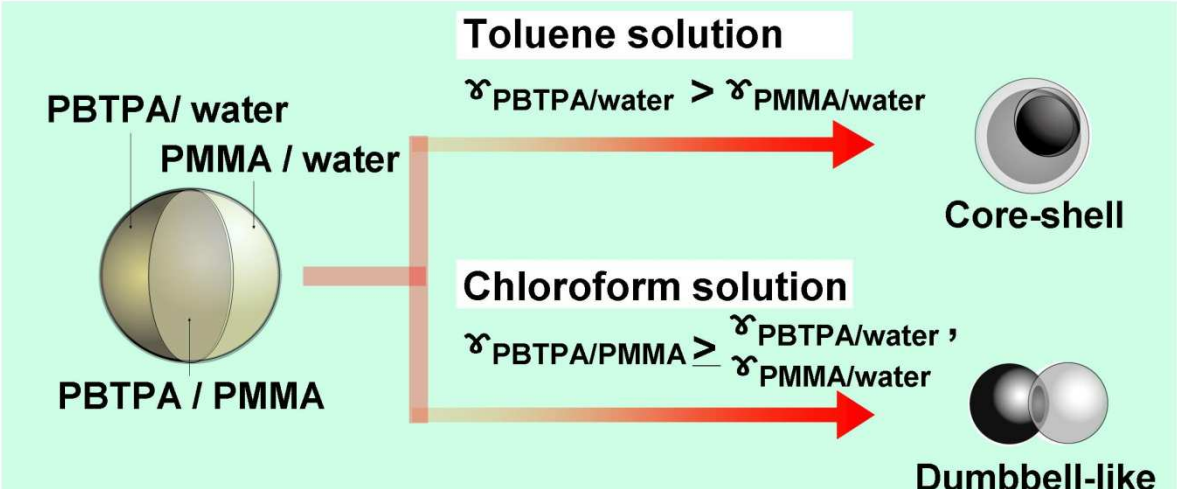

Figure 3-4. Schematic models of the formation of the core-shell and the dumbbell-like particles.

3-3-2. Effect of the polymer composition

Fig. 3-5 shows OM and SEM images of polymer blend particles fabricated from toluene solution droplets. The particles consisted of 90 wt% of PMMA exhibited the core-shell structure. Some of the particles had more than two PBTPA cores (Fig. 3-5 (a)). The particles containing less than 70 wt% of PMMA exhibited the Janus structure (also see Fig. 3-1 (c, f, i)) In the case of 10 wt% of PMMA, some of the particles had a number of spots of the PMMA phase on the surface (Fig. 3-5 (f)).

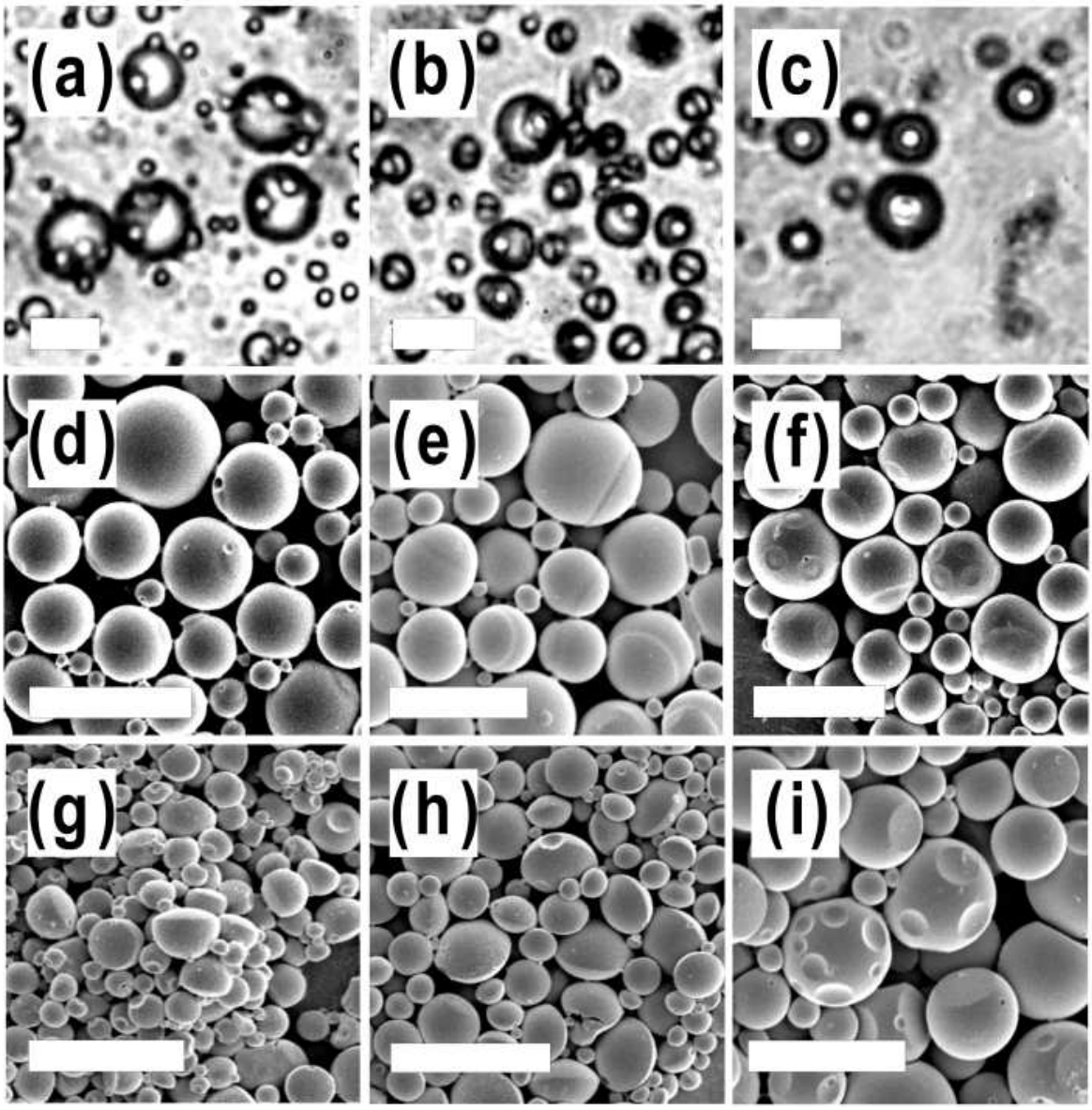

Figure 3-5. OM (**a**-**c**) and SEM (**d**-**i**) images of polymer blend particles fabricated from toluene solution droplets. The images show the particles observed before (**a**-**f**) and after (**g**-**i**) soaking in acetone. Weight ratios of PMMA were 90 (**a**, **d**, **g**), 70 (**b**, **e**, **h**) and 10 (**c**, **f**, **i**) wt%, respectively. Number-average molecular weights (M_n) (g mol^{-1}) of PBTPA was 10,000 (PDI = 2.3), and M_n (g mol^{-1}) of PMMA was 40,000 (PDI = 2.7). All scale bars represent 5 μm.

The multiple cores of PBTPA observed in particles with 90 wt% of PMMA can be interpreted as follows. It is considered that the dispersed phases consisting of minor

component of the polymer mixture are formed in the continuous phase with major component at the early stage of the phase separation. The coalescence of these dispersed phases occurred to minimize the interfacial energy.[18] The biased volume ratio of the polymer reduces the interfacial area resulting in the weakened driving force of the coalescence. As a result, multiple cores remain at the later stage of the phase separation. It is also considered that the spotted structure of the particles consisting of 10 wt% of PMMA is due to the similar mechanism.

The effect of solvent was also investigated for the composition dependence. Fig. 3-6 shows OM and SEM images of polymer blend particles fabricated from chloroform solution droplets. The particles showed similar dependency on the weight ratio with the particles fabricated from toluene. However, PBTPA cores extruded due to the low tension of chloroform solution/aqueous solution interface even at the biased volume fractions. Therefore, the particles containing 90% of PMMA had snowman-like structure, consisted of PBTPA head and PMMA body. Some of the particles had more than two PBTPA heads (Fig. 3-6 (d)). The particles consisted of 70 wt% of PMMA exhibited snowman-like structure as well. The particles consisted of 10 wt% of PMMA had a number of spots of PMMA phases on the surface (Fig. 3-6 (f)).

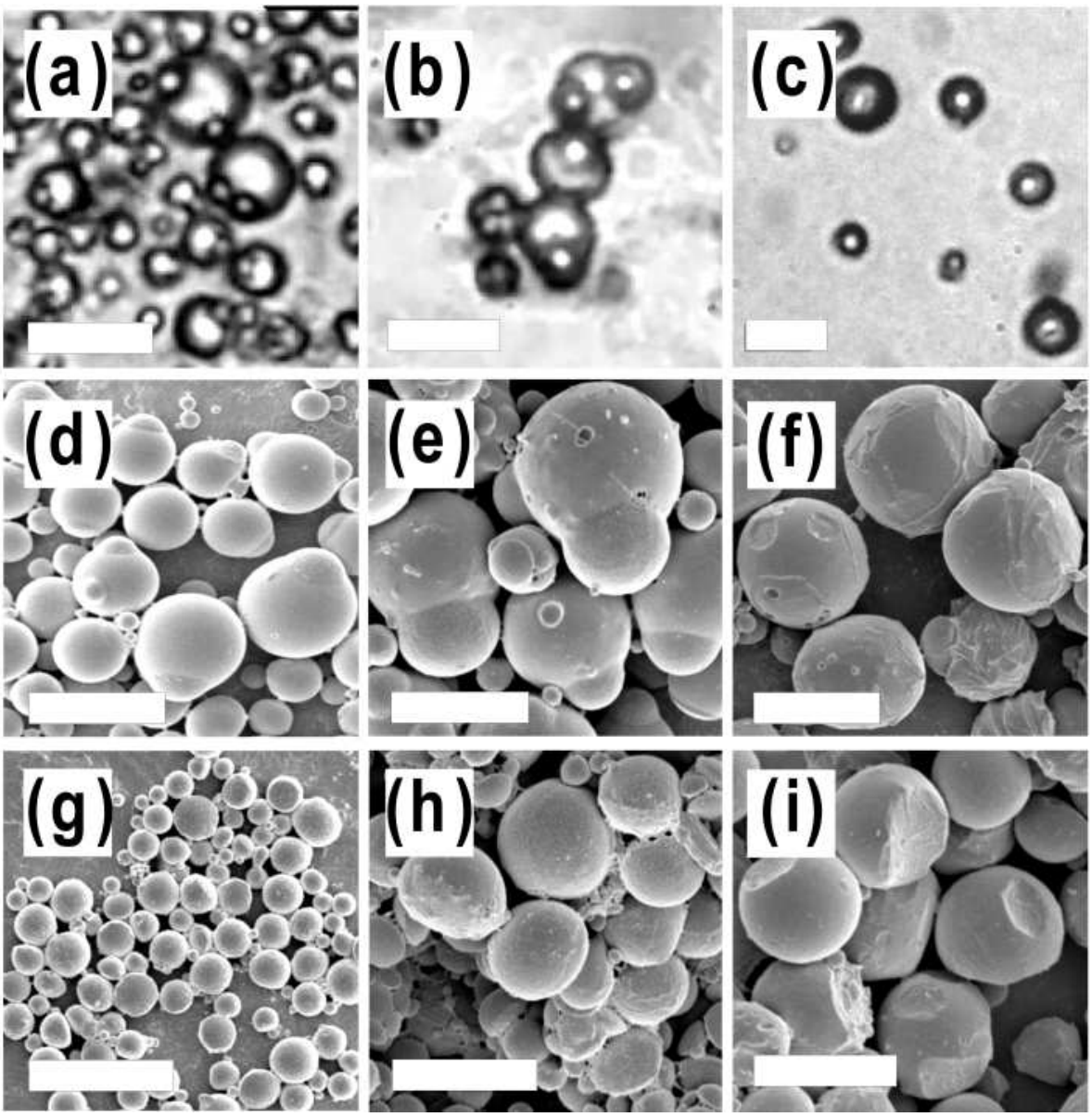

Figure 3-6. OM (**a**-**c**) and SEM (**d**-**i**) images of polymer blend particles fabricated from chloroform solution droplets. The images show the particles observed before (**a**-**f**) and after (**g**-**i**) soaking in acetone. Weight ratios of PMMA were 90 (**a**, **d**, **g**), 70 (b, e, h) and 10 (**c**, **f**, **i**) wt%, respectively. Number-average molecular weights (M_n) (g mol^{-1}) of PBTPA was 10,000 (PDI = 2.3), and M_n (g mol^{-1}) of PMMA was 40,000 (PDI = 2.7). All scale bars represent 5 μm.

3-3-3. Effect of the evaporation rate

Fig. 3-7 shows OM, SEM and TEM images of polymer blend particles fabricated from chloroform solution droplets. All the conditions were the same as described in Fig. 3-6 (a, d, g) except the evaporation speed. In this case, the dispersion of solution droplets was stirred in a 300-mL beaker (opening diameter; 8.0 cm) to accelerate solvent evaporation. The particles had the confetti-like structure, where smaller PBTPA particles existed near the surface of PMMA main particles. Fig. 3-7 (d) shows the size distribution for 112 particles (N) determined from SEM images. Filled bars represent the numbers of confetti-like particles in which extruded individual PBTPA particles are discernible. Open bars represent the numbers of non-confetti-like particles. Number averaged diameter was 3.0 μm. The ratio of confetti-like particles increased with the increase of the diameter. All particles of more than 5 μm in diameter exhibited the confetti-like structure. The size of the PBTPA particles in confetti-like particle was less than 1 μm in diameter.

It is considered that the rapid evaporation accelerates the increase of viscosity accompanied with the solvent evaporation. High viscosity limits the motion of polymer chains and retains the morphology generated at the early stage resulting in the formation of the confetti-like particles. Furthermore, the large diameter of the droplets suppresses the coalescence due to the requirement of the transport of the phase separated minor domain in longer distance. It is suggested that the confetti-like structure in the larger particles is due to this limitation of mass transfer (Fig. 3-8).

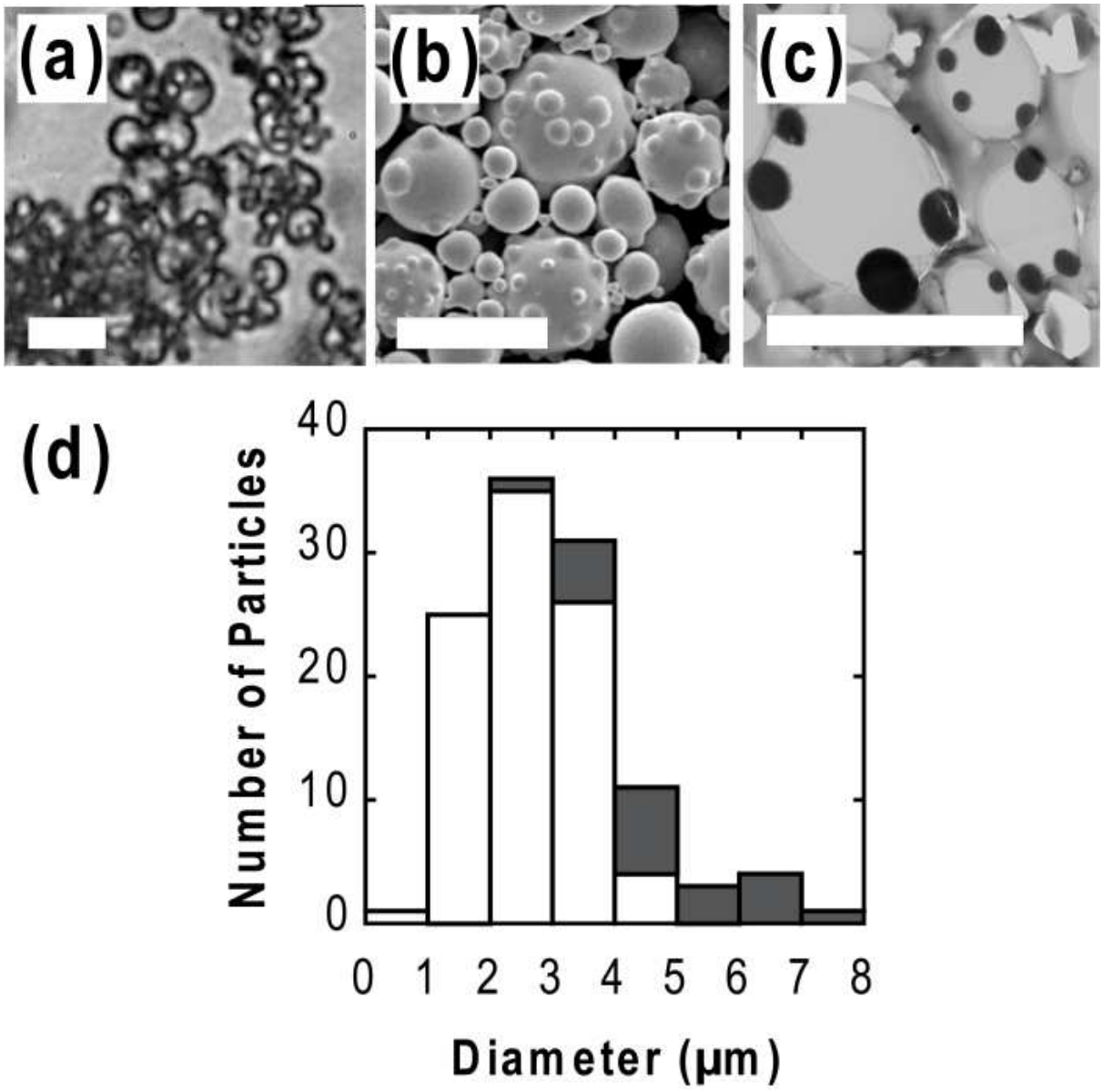

Figure 3-7. OM (**a**), SEM (**b**) and TEM (**c**) images of polymer blend particles fabricated from chloroform solution droplets. Dark and white regions in TEM image represent PBTPA and PMMA phase, respectively. (**d**) Size distributions of (filled bar) confetti like and (open bar) non-confetti like particles (N = 112). The dispersion was stirred at 100 rpm in the 300-mL beaker (opening diameter; 8.0 cm). Weight ratio of PMMA was 90 wt%. Mn (g mol^{-1}) of PBTPA was 10,000 (PDI = 2.3), and Mn (g mol-1) of PMMA was 40,000 (PDI = 2.7). All scale bars represent 5 μm.

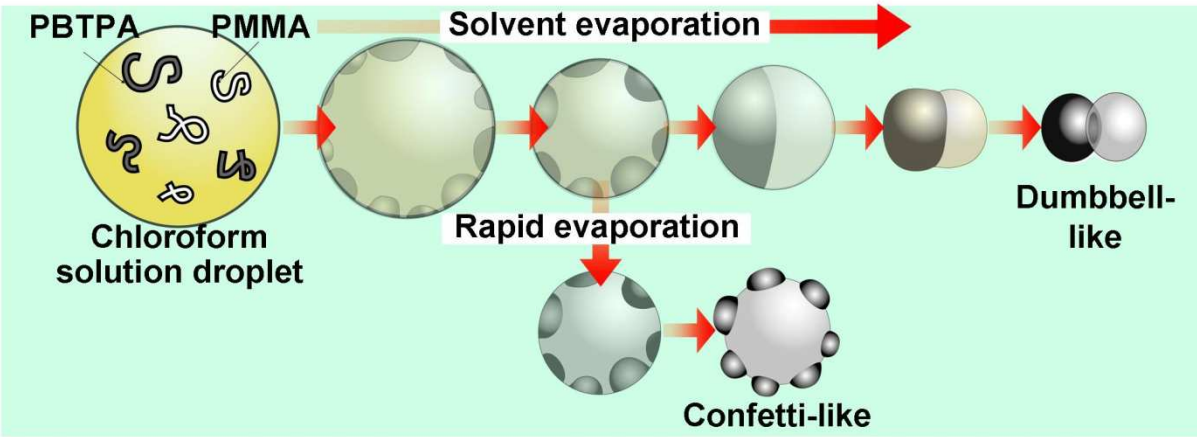

Figure 3-8. Schematic models of the formation of the confetti-like particles.

3-4. Conclusions

The effect of the solvent, molecular weight, compounding ratio and evaporation speed on the morphology of polymeric blend particles consisting of PBTPA and PMMA fabricated by solvent evaporation method was studied. For the particle fabricated from toluene solution droplets, the increase of the molecular weight of PMMA transformed the morphology from core-shell to Janus. Chloroform solution droplets gave dumbbell like particles independently on the molecular weight. According to the measurement of interfacial tension, PVA decreased the interfacial tension between chloroform solution and aqueous phase to the level comparable with that of polymer/polymer interface. Confetti like particles with PMMA core coated by PBTPA particles was obtained by rapid evaporation of chloroform.

3-5. References

(1) Okubo, M.; Saito, N.; Fujibayashi, T. Preparation of polystyrene/poly(methyl methacrylate) composite particles having a dent. *Colloid Polym. Sci.* **2005**, *283*, 691–698.

(2) Anastasiadis, S. H. In *Polymer Thermodynamics Liquid Polymer-Containing Mixtures*; Wolf, B. A., Enders, S., Eds.; Springer Berlin Heidelberg: Berlin, 2011; p 179–269.

(3) Anastasiadis, S.H.; Gancarz, I.; Koberstein, J. T. Interfacial tension of immiscible polymer blends: temperature and molecular weight dependence. *Macromolecules* **1988**, *21*, 2980–2987.

(4) Matsumoto, T.; Okubo, M.; Shibao, S. Studies on suspensions and emulsions. XXVIII. Formation mechanism of heterogeneous structure in particles produced by seed-emulsion polymerization. *Kobunshi Ronbunshu* **1976**, *33*, 575–583.

(5) Shi, S.; Kuroda, S.; Kubota, H. Anomalous particles formed in two-stage soap-free emulsion polymerization of styrene on poly(2-acetoxyethyl methacrylate). *Colloid Polym. Sci.* **2003**, *281*, 331–336

(6) Chen, M. Q.; Kaneko, T.; Chen, C. H.; Akashi, M. Preparation of “confetti” particles by dispersion copolymerization of acrylonitrile/styrene with poly(ethylene glycol) macromonomer. *Chem. Lett.* **2001**,*30* , 1306–1307.

(7) Okubo, M.; Fujibayashi, T.; Yamada, M.; Minami, H. Micron-sized, monodisperse, snowman/confetti-shaped polymer particles by seeded dispersion polymerization. *Colloid Polym. Sci.* **2005**, *283*, 1041–1045.

(8) Ostovar, M.; Eslami, H. Synthesis of nanostructured confetti-like and mace-like particles via dispersion polymerization of alkyl methacrylates on polystyrene seeds. *Colloid. Polym. Sci.* **2016**, *294*, 1633–1642.

(9) Kikuchi, S.; Kanehashi, S.; Ogino, K. Transition of phase-separated PBTPA/PMMA solution droplets from core–shell to Janus morphology under UV light irradiation. *Polym. J.* **2018**, *50*, 1089–1092.

(10) S. Kikuchi, S. Kanehashi, G. Ma and K. Ogino, manuscript in preparation (2019).

(11) Tanaka, T.; Nakatsuru, R.; Kagari, Y.; Saito, N.; Okubo, M. Effect of molecular weight on the morphology of polystyrene/poly(methyl methacrylate) composite particles prepared by the solvent evaporation method. *Langmuir* **2008**, *24*, 12267–12271.

(12) Ge, X.; Wang, M.; Ji, X.; Ge, X.; Liu, H. Effects of concentration of nonionic surfactant and molecular weight of polymers on the morphology of anisotropic polystyrene/poly(methyl methacrylate) composite particles prepared by solvent evaporation method. *Colloid Polym. Sci.* **2009**, *287*, 819–827.

(13) Matsumoto, T.; Nakamae, K.; Nonaka, K.; Uehara, T. *Kobunshi Ronbunshu*, **1974**, *31*, 508–514.

(14) Glass, J. E. Adsorption characteristics of water-soluble polymers at aqueous-organic liquid interfaces. *J. Polym. Sci., Part C: Polym. Symp.* **1971**, *34*, 141–157.

(15) E. A. Grulke, “Polymer handbook, 4th ed”. Wiley-Interscience, New York (1999).

(16)Chibowski, E.; Perea-Carpio, R. Problems of contact angle and solid surface free energy determination. *Adv. Colloid Interface Sci.* **2002**, *98*, 245–264.

(17) Kloubek, J. Development of methods for surface free energy determination using contact angles of liquids on solids. *Adv. Colloid Interface Sci.* **1992**, *38*, 99–142.

(18) Jang, B. Z.; Uhlmann, D. R.; van der Sande, J. B. The Postdispersion Coalescence Phenomenon in Polymer-Polymer Blends. *Rubber Chem. Technol.* **1984**, *57*, 291–306.

Chapter 4

Morphology control of poly(4-butyl triphenylamine)/poly(methyl methacrylate) blend particle based on the block copolymer

4-1. Introduction

This chapter is focused on the morphology control of the polymer particles consisting of PBTPA, PMMA and PBTPA-*b*-PMMA. As mentioned in Chapter 1, the particles fabricated from block copolymers exhibit periodical morphologies including lamella or cylindrical structures. [1,2,3,4,5,6] Unfortunately, such ordered structures of the phase separation has not been observed in the particles consisting of PBTPA-*b*-PMMA in this study. However, when the block copolymers were added to the homopolymer blend of PBTPA and PMMA, the particles with unique morphology including "watermelon-like" structure, in which microphase separation of block copolymer coexist with the inversed core-shell typed macro phase separation, were obtained. According to the literatures, for the particles consisting of the blend of homopolymer and block copolymer, the homopolymers with lower molecular weight than that of corresponding segment in block copolymer dissolve into block copolymer and expands the lamella spacing. On the other hand, the homopolymers with higher molecular weight causes macrophase separation against block copolymers.[3] However, not much is available on the study of the morphology control of the phase separated structure in the composite particles consisting of homopolymers and block copolymers. Although our research group has reported that the addition of PBTPA-*b*-PMMA to the homopolymer blend particles transformed the morphology from core-shell to inversed core-shell,[7] the mechanism of the morphological transformation has not been clarified. In the present study, the effects of the molecular weight and segment ratio of block copolymer were investigated in detail. Furthermore, the measurement of interfacial tension by pendant drop method revealed the thermodynamic effect of the block copolymers on the interfacial tension between polymer solution and aqueous phase. The results will help to understand the mechanism of the phase separation in the blend particles consisting of homopolymers and block copolymers.

4-2. Experimental section

4-2-1. Materials

PBTPA and PMMA homopolymers were synthesized by the palladium catalyzed C-N coupling[8] and atom transfer radical polymerization (ATRP), respectively. Weight-average molecular weights (M_w) and M_n were estimated by gel permeation chromatography. PVA (PVA224, Kuraray Co. Ltd., Japan, degree of polymerization; 2,400, degree of saponification; 87-89%) as a dispersion stabilizer, toluene and chlorobenzene were purchased from Wako Pure Chemical Industries, Ltd, and used as received. Deionized water with specific resistance of 15 MΩ was distilled.

4-2-2. Synthesis of 2-(4-bromophenoxy)ethanol

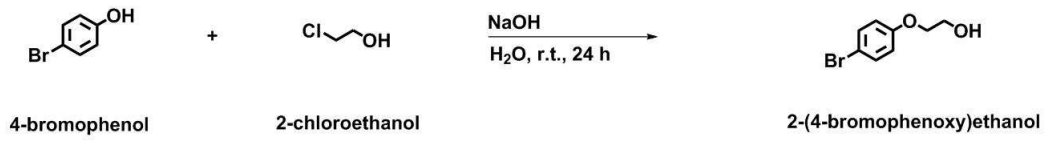

4-bromophenol 2-chloroethanol 2-(4-bromophenoxy)ethanol

<Materials>

Sodium hydroxide (NaOH): Wako, Tokyo, Japan

4-bromophenol: TCI, Tokyo, Japan

2-chloroethanol: Aldrich, St. Louis, MO, USA; SAJ Special Grade

<Operations>

To a 50-mL flask equipped with a magnetic stirrer bar were NaOH (7 g, 0.17 mol), distilled water (28 mL), 4-bromophenol (14 g, 0.081 mol), and 2-chloroethanol (46.5 g, 0.18 mol). The mixture was stirred at room temperature for 24 h. The mixture was extracted with CH_2Cl_2, washed with distilled water and dried over anhydrous $MgSO_4$. The extracted solution was filtered and evaporated. White solid (15.7 g, 89%) was obtained. ^{1}H NMR [300 MHz, $CDCl_3$, δ(ppm)] δ7.39 (*d*, 2H), 6.79 (*d*, 2H), 4.05 (*t*, 2H), 3.97 (*dt*, 2H,), 2.07 (*t*, 1H)

4-2-3. Synthesis of 2-(4-bromophenoxy)ethoxy-tert-butyldimethylsilane

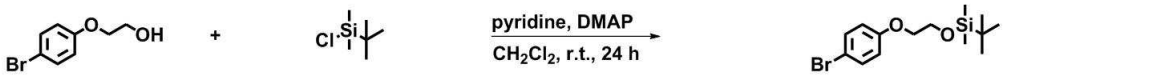

2-(4-bromophenoxy)ethanol *tert*-butyldimethylchlorosilane 2-(4-bromophenoxy)ethoxy-*tert*-butyldimethylsilane

<Materials>

Tert-butyldimethylchlorosilane: TCI, Tokyo, Japan

4-dimethylaminopyridine (DMAP): Wako, Tokyo, Japan; Wako Special Grade

Pyridine: Wako, Tokyo, Japan; Wako 1st Grade

Dichloromethane (CH_2Cl_2): Wako, Tokyo, Japan; Wako 1st Grade

<Operations>

To a 300-mL flask equipped with a magnetic stirrer bar were added 2-(4-bromophenoxy)ethanol (15.0 g, 0.069 mol), *Tert*-butyldimethylchlorosilane (12.9 g, 0.085 mol), DMAP (0.15 g, 0.0012 mol) and CH_2Cl_2 (56 mL). Pyridine (6.7 mL, 0.087 mol) was added to the mixture at 0 °C. The mixture was stirred at room temperature for 24 h under. The mixture was extracted with CH_2Cl_2, washed with distilled water and dried over anhydrous $MgSO_4$. The product was purified by column chromatography on silica gel (eluent: dichloromethane). The colorless liquid (19.51 g, 85%) was obtained. ^{1}H NMR [300 MHz, $CDCl_3$, δ (ppm)] δ7.36 (*sextet*, 2H), 6.79 (*sextet*, 2H), 4.00 (*m*, 2H), 3.95 (*m*, 2H), 0.90 (*s*, 9H,), 0.09(s, 6H)

4-2-4. Synthesis of PBTPA--*tert*-butyldimethylsilane (PBTPA-TBDS)

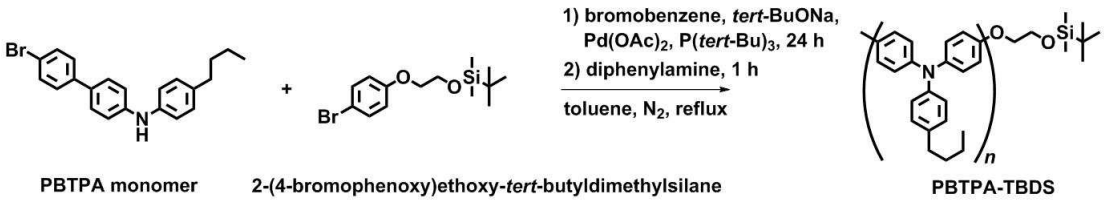

<Materials>

Palladium acetate(II) ($Pd(OAc)_2$): Wako, Tokyo, Japan

Sodium *tert*-butoxide (*tert*-BuONa): TCI, Tokyo, Japan

Tri-*tert*-butylphosphine (P(*tert*-Bu)$_3$): Wako, Tokyo, Japan

Diphenylamine: TCI, Tokyo, Japan

Toluene, deoxidized: Wako, Tokyo, Japan; for Organic Synthesis

<Operations>

To a 20-mL glass vial equipped with a magnetic stirrer bar and a nitrogen inlet was added $Pd(OAc)_2$ (36 mg, 0.16 mmol). Toluene (1 mL), 2-(4-bromophenoxy)ethoxy-*tert*-butyldimethylsilane (0.52 g, 1.6 mmol) and P(*tert*-Bu)$_3$ solution in toluene (0.13, 0.63 mmol) were added via a syringe. The mixture was stirred at room temperature for 1 h under a nitrogen atmosphere. Separately, to a 50-mL flask equipped with a magnetic stirrer bar and a condenser were added PBTPA monomer (3.0 g, 7.9 mmol) and *tert*-BuONa (0.83 g, 8.7 mmol). Toluene (29 mL) and the solution of initiator were added via a syringe. The mixture was stirred at 120 °C for 24 h under a nitrogen atmosphere followed by the addition of toluene solution of diphenylamine (0.54 g, 3.2 mmol) and additional stirring at 120 °C for 1 h. After cooling down to ambient temperature, the reaction mixture was filtered and poured into methanol. The precipitation was purified by a Soxhlet extraction using 2-butanone for 2 days. Finally, the product was reprecipitated from acetone. The pale yellow solid of PBTPA-TBDS (1.6 g, 59%) was obtained. ^{1}H NMR [300 MHz, $CDCl_3$, δ(ppm)] δ: 7.44 (*d*), 7.17~7.01 (*m*), 4.02 (*t*), 3.96 (*t*), 2.58 (*t*), 1.61(*tt*), 1.38 (*quat*), 0.94 (*t*), 0.15 (*s*)

4-2-5. Synthesis of PBTPA-OH

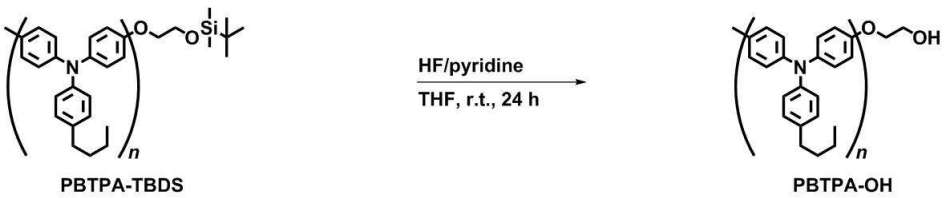

PBTPA-TBDS　　PBTPA-OH

<Materials>

Hydrogen fluoride pyridine (pyridine ~30%, hydrogen fluoride ~70%): Aldrich, St. Louis, MO, USA

Tetrahydrofuran (THF): Wako, Tokyo, Japan; Wako 1st grade

<Operations>

To a 200-mL flask equipped with a magnetic stirrer bar were added PBTPA-TBDS (1.6 g, 1.1 mmol), THF (80 mL) and hydrogen fluoride pyridine (4 mL). The mixture was stirred at room temperature for 24 h. The reaction mixture was filtered and concentrated by evaporation. The concentrated residue was poured into methanol. The pale yellow solid of PBTPA-OH (1.4 g, 95%) was obtained. ^{1}H NMR [300 MHz, $CDCl_3$, δ(ppm)] δ: 7.44 (d), 7.09 (m), 6.87 (m), 4.07 (m), 3.96 (m) , 2.59 (t), 1.61 (t), 1.38 (quartet), 0.94 (m)

4-2-6. Synthesis of PBTPA-macroinitiator (PBTPA-MI).

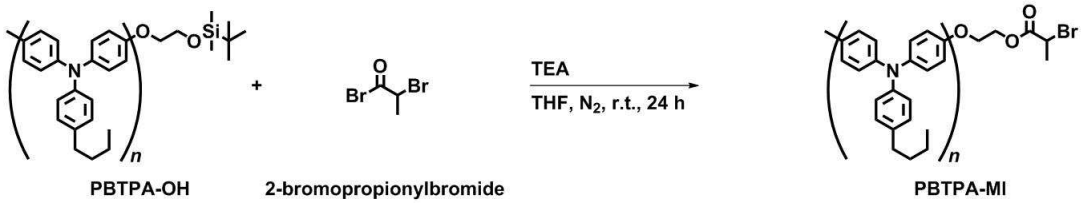

PBTPA-OH 2-bromopropionylbromide PBTPA-MI

<Materials>

Triethylamine (TEA): Wako, Tokyo, Japan; Wako Special Grade

2-bromopropionylbromide: TCI, Tokyo, Japan

Tetrahydrofuran (THF): Wako, Tokyo, Japan; Wako 1st grade

<Operations>

To a 100-mL flask equipped with a magnetic stirrer bar were added PBTPA-OH (1.4 g, 0.67 mmol), THF (60 mL) and TEA (5 g, 45 mmol). 2-bromopropionylbromide (9 g, 42 mmol) was added slowly to the mixture at 0 °C. The mixture was stirred at room temperature for 24 h. The reaction mixture was filtered and concentrated by evaporation. The concentrated residue was poured into methanol. The pale yellow solid of PBTPA-MI (1.4 g, 83%) was obtained. ^{1}H NMR [300 MHz, $CDCl_3$, δ(ppm)] δ: 7.43 (*d*), 7.13 (*d*), 7.08 (*s*), 4.51 (*t*), 4.42 (qua), 4.18 (*t*), 2.58 (*t*), 1.84 (*d*), 1.60 (*tt*), 1.38 (*tqua*), 0.94(*t*)

4-2-7. Synthesis of PBTPA-*b*-PMMA block copolymer

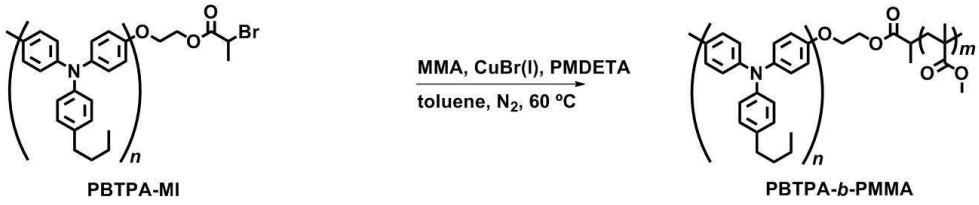

PBTPA-MI　　PBTPA-*b*-PMMA

<Materials>

Methyl methacrylate (MMA): Wako, Tokyo, Japan; distilled over CaH_2 under reduced pressure before use

Copper(I) bromide (CuBr(I)): TCI, Tokyo, Japan; washed with acetic acid and dried in vacuo before use

N, N, N', N', N"-pentamethyldiethylenetriamine (PMDETA): Wako, Tokyo, Japan; Wako 1st Grade

Toluene, deoxidized: Wako, Tokyo, Japan; for Organic Synthesis

<Operations>

To a 10-mL flask equipped with a magnetic stirrer bar were added CuBr(I) (33 mg, 0.23 mmol) and PBTPA-MI (0.2 g, 0.05 mmol). The flask was evacuated for an hour. Separately, to a 10-mL flask equipped with a magnetic stirrer bar were added MMA (1.7 mL, 17 mmol), toluene (1.7 mL), and PMDETA (46 mg, 0.27 mmol). After three freeze-pump-thaw cycles, the mixture of MMA monomer was added to the mixture of PBTPA-MI via a syringe. The mixture was stirred at 60 °C under a nitrogen atmosphere for 30 minutes. After cooling down to ambient temperature, THF (10 mL) was added to the reaction mixture. The THF solution of reaction mixture was filtered through alumina chromatographic column and concentrated by evaporation. The reaction mixture was poured into methanol. The pale yellow solid of PBTPA-*b*-PMMA (0.47 g) was obtained; GPC: M_n of PBTPA-*b*-PMMA was 3,900-*b*-7,400, PDI=4.9.

4-2-8. Characterization

^{1}H-NMR spectra were recorded at 25 °C on a JEOL ECX300 instrument at 300 MHz, respectively. Deutrated chloroform was used as a solvent with tetramethylsilane as an internal standard. Number- and weight-average molecular weights (M_n and M_w) were determined by gel permeation chromatography (GPC) analysis with a JASCO RI-2031 detector eluted with chloroform at a flow rate of 1.0 mL min^{-1} and calibrated by standard polystyrene samples.

4-2-9. Measurement of density

The density (ρ) of the polymers (PBTPA; ρ = 1.09 g cm^{-1}, PMMA; ρ = 1.20 g mL^{-1}) was evaluated by taking weight of the specimen in air (W_a) and water (W_l) using an electronic balance AUX220 (Shimadzu Co., Kyoto, Japan). The bulk samples were prepared by evaporation of chlorobenzene from 5 wt% polymer solution of chlorobenzene. The density is calculated as

$$\rho = \rho_l \cdot W_a / (W_a - W_l) \quad (4\text{-}1)$$

ρ_l is the density of water at 25 ºC; 0.9971 g cm^{-1}

4-2-10. Measurement of refractive index

The refractive index (n) of the polymer was evaluated using a Metricon prism coupler Model 2010/M (Metricon Co., Pennington, USA) equipped with a YAG laser (wavelength: 532 nm), a He-Ne laser (632.8 nm), and a diode laser (780 nm). The bulk samples were prepared by evaporation of chlorobenzene from 5 wt% polymer solution of chlorobenzene.

4-2-11. Measurement of interfacial tension

Interfacial tension between the polymer-solvent solution and PVA aqueous solution was measured by pendant drop method with contact angle gauge (DM-501, Kyowa interface science Co., Ltd., Japan). A drop of the toluene or chloroform solution dissolving of the polymer was formed at the tip of the stainless steel needle in the PVA aqueous solution.

4-2-12. Measurement of differential scanning calorimetry (DSC)

Glass transition temperatures (T_g) were determined using a differential scanning calorimetry (DSC) (Thermoplus DSC 823, Rigaku, Japan). The measurements were carried out under N_2 at a heating rate of 10 °C/min. The sample size was about 5-10 mg. Two heating scans, a first scan and a rescan, of each sample were performed from 40 to 240 °C. The T_g's were taken as the onset points of the specific heat jumps.

4-2-13. Preparation of PBTPA/PBTPA-*b*-PMMA/PMMA blend particles

Polymer blend particles were fabricated by following method. The 0.05 g of the mixture of polymers was dissolved into 0.95 g of toluene or chlorobenzene. 1 mL of the toluene or chloroform solution was dispersed to 7 mL of aqueous solution containing 0.6 wt% of PVA using a homogenizer (X520 CAT, As One Co., Japan) at 25,000 rpm for 10 s in a test-tube (115-mL. i.d.= 2.7 cm). The obtained dispersion was stirred using a mechanical stirrer (Shinto Scientific Co., Ltd., Japan) at 100 rpm to evaporate the solvent at room temperature. The particles were collected by centrifugation, and washed with distilled water three times. The molecular weights of the polymers used for preparing the blend particles are listed in Table 4-1.

4-2-14. Observation of polymer blend particles

Polymer particles were observed by scanning electron microscope (SEM) (JSM-6510, JEOL Ltd., Japan) and transmission electron microscope (TEM) (JEM-2100, JEOL Ltd., Japan). Samples for SEM were prepared by putting one drop of the dispersion of particles in water on sample stage and then drying in air. The samples were coated by osmium tetraoxide (OsO_4) using ion coater (Neoc-STB, Meiwafosis Co. Ltd., Japan) to avoid the charging. Samples for TEM were prepared as follows; dried particles were dispersed to epoxy resin, cured at 60 °C for three days, and microtomed (UC7, Leica, Germany). The ultrathin cross sections were put on the copper grid and stained with ruthenium tetraoxide (RuO_4) vapor at room temperature for 15 min in the capped vial with the presence of 1% RuO_4 aqueous solution.

Table 4-1. Molecular Weights of PBTPA, PMMA and Block Copolymers Used for the Preparation of Polymer Particles

Polymer	GPC			NMR	
	M_n	M_w	PDI	M_n (PBTPA / PMMA)	PMMA (vol%)
PBTPA-1	4,100	6,400	1.6	-	-
PBTPA-2	14,200	34,900	2.5		
PMMA-1	3,400	6,100	1.8	-	-
PMMA-2	25,000	45,800	1.8	-	-
Block-1	5,100	25,000	4.0	3,800 / 7,200	67.6
Block-2	8,100	13,200	1.8	3,500 / 1,200	26.8
Block-3	16,000	54,600	3.4	6,300 / 5,100	47.1
Block-4	13,000	34,200	2.6	6,300 / 1,300	18.5

4-3. Results and discussion

4-3-1. Synthesis of PBTPA-*b*-PMMA

The conditions of ATRP and molecular weights and dispersions of resulted polymers are listed in table 4-2. The length of the PMMA segment was controllable by reaction time in the same condition (run 1-6). The effect of the kinds of solvent and the initial concentration of MMA monomer were evaluated by monitoring the molecular weight during the reaction as shown in figure 4-1. The resulted molecular weights and PDI values were almost same between the polymers polymerized in toluene or anisole (run 7 and 8). The results strongly depended on initial concentration of MMA monomer $[MMA]_0$. No PMMA segments were observed in NMR spectra even after 4 hours at $[MMA]_0 = 0.42$ M (run 9). When the initial concentration was 1.2 M, the PBTPA-*b*-PMMA block copolymers were obtained (run 8). The

length of the PMMA segment increased at higher initial concentration (run 10). These results indicate that there is lower limit of the concentration. Termination and other side reaction occur with the usual rates, while propagation slows down as the monomer concentration becomes low. Therefore, there is a certain window of concentrations to promote the reaction.[9]

Table 4-2. Conditions and Results of ATRP of PBTPA-*b*-PMMA[a]

Run	PBTPA-MI		[PBTPA-MI]/[Cu]/[ligand]	solvent	$[M]_0$	Time	PBTPA-*b*-PMMA	
	M_n[b]	PDI[c]			(M)	(min)	M_n[b]	PDI[c]
1	3,500	1.8	1/4.57/5.30	toluene	5.0	1.5	3,500-*b*-1,200	1.8
2	3,800	1.9	1/4.57/5.30	toluene	5.0	7.5	3,800-*b*-700	1.9
3	3,800	1.9	1/4.57/5.30	toluene	5.0	30	3,800-*b*-7,200	4.0
4	3,800	1.9	1/4.57/5.30	toluene	5.0	60	3,800-*b*-8,900	5.3
5	6,300	2.0	1/6.86/8.08	toluene	5.0	1.5	6,300-*b*-1,300	2.6
6	6,300	2.0	1/6.86/8.08	toluene	5.0	18	6,300-*b*-5,100	3.4
7	3,200	1.9	1/3.63/4.47	anisole	1.2	240	3,200-*b*-3,000	2.1
8	3,200	1.9	1/3.63/4.47	toluene	1.2	240	3,200-*b*-3,100	2.4
9	3,200	1.9	1/3.63/4.47	toluene	0.42	240	-	-
10	3,200	1.9	1/3.63/4.47	toluene	2.1	240	3,200-*b*-6,400	3.5

[a] All reactions were conducted at 60 °C. [b] M_n was determined by ^{1}H NMR spectroscopy. [c] PDI was determined by GPC.

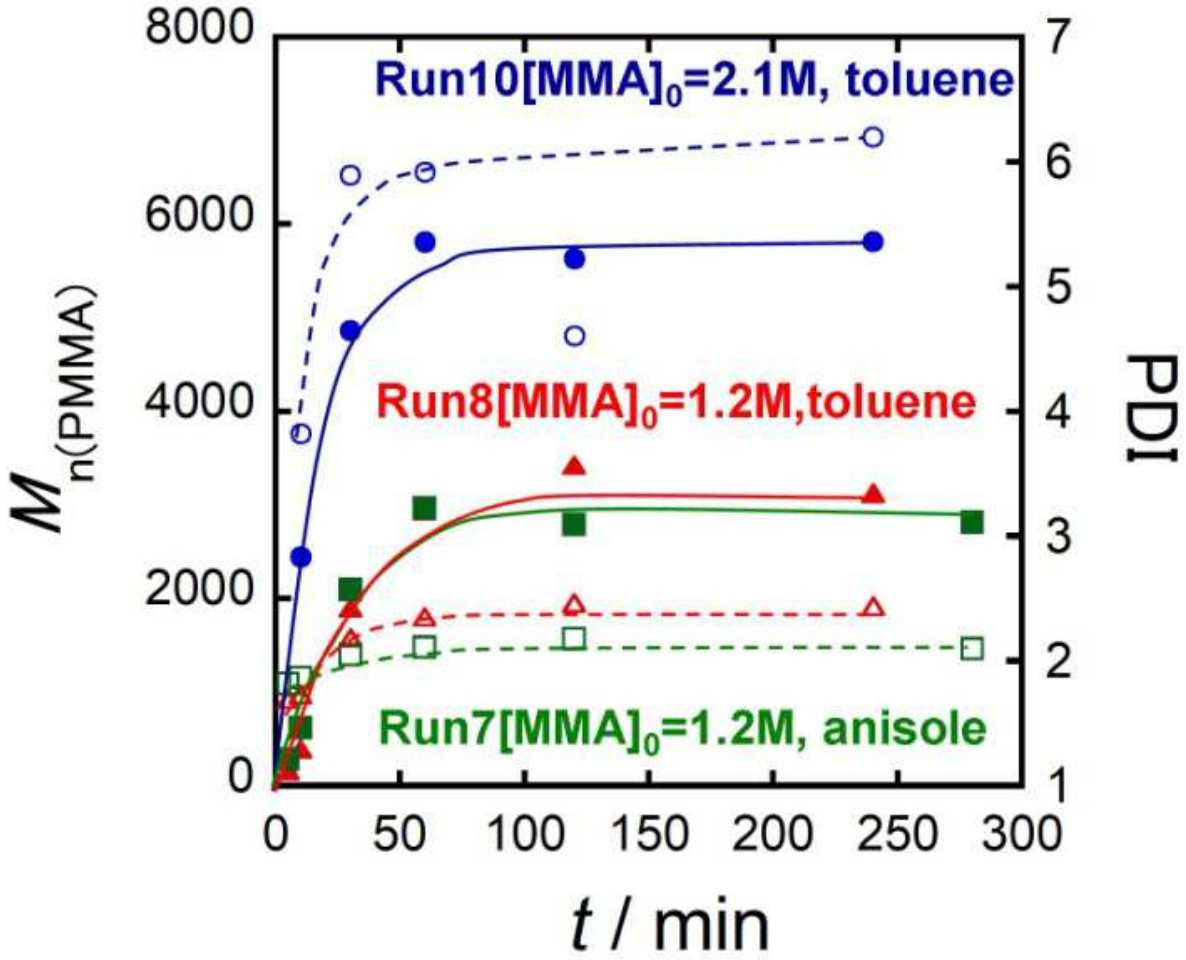

Figure 4-1. Molecular weights of PMMA segments and polydispersities as function of reaction time *t*. M_n and polydispersity index (PDI) were measured by NMR and GPC, respectively.

4-3-2. PBTPA-*b*-PMMA particles

Effect of Molecular Weight and Molar Ratio of PBTPA-b-PMMA.

Figure 4-2 shows TEM images of block copolymer particles fabricated from toluene solution droplets. The particles consisting of block copolymer with M_n(PMMA) of 1,200 showed no contrast attributed to phase separation (Figure 4-2a, b). The particles consisting of block copolymer with M_n(PMMA) of 7,400 showed disordered micro phase separation (Figure 4-2c, d). The particles consisting of copolymer M_n(PBTPA) of 6,300 also showed disordered micro phase separation (Figure 4-2e, f).

The particles consisting of block copolymer with M_n(PMMA) of 1,200 showed homogeneous phase. Driving force to cause microphase separation is the chemical incompatibility between different polymers. The mixing free energy is commonly described as a Flory-Huggins interaction parameter, χ, which describes the free-energy cost per monomer of contacts between A and B monomers. For the polymers with N of degree of polymerization, the free energy of mixing is described as χN. The block copolymer with χN lower than the limit of the phase separation forms homogeneous phase.

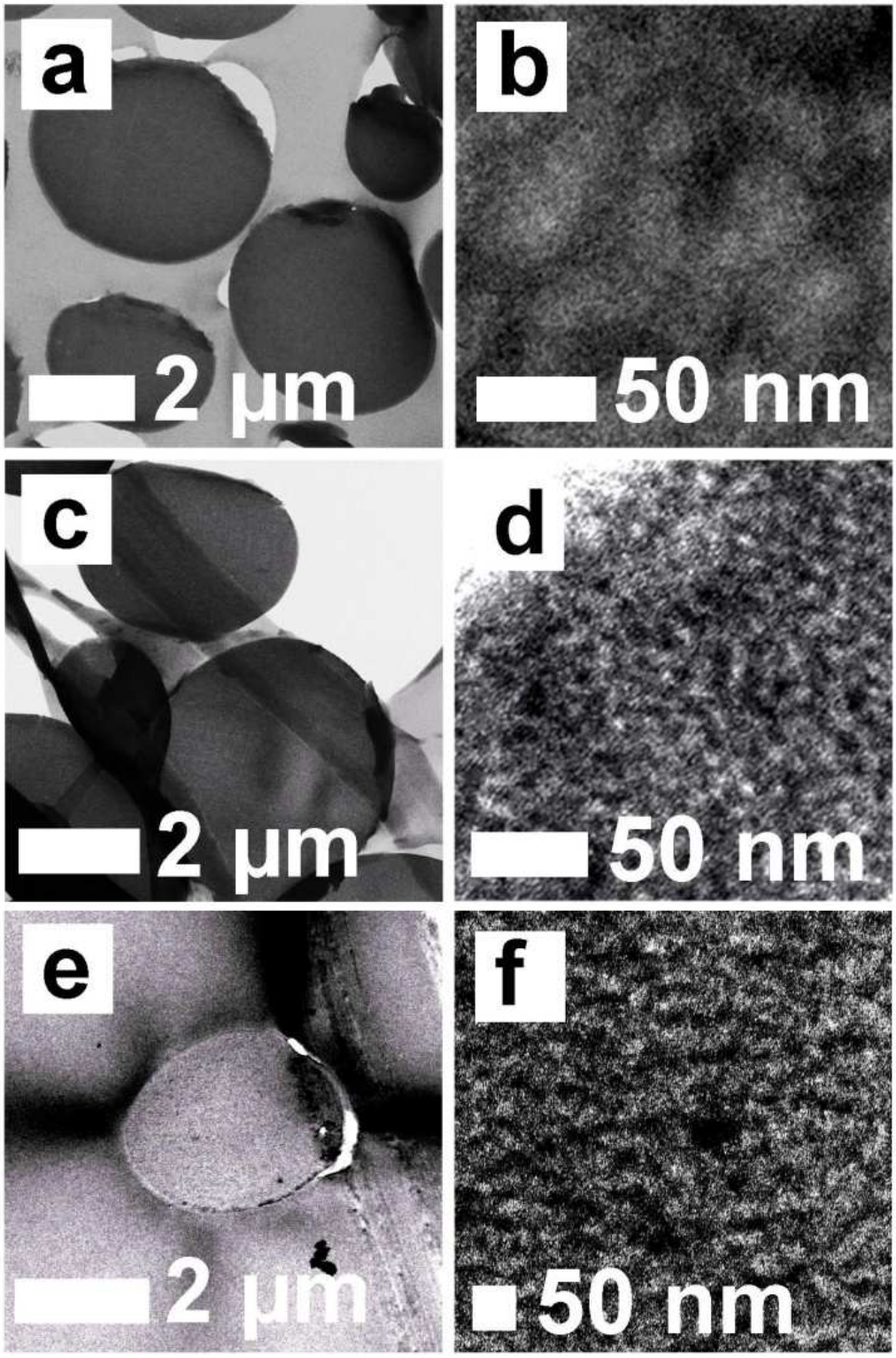

Figure 4-2. TEM images of block copolymer particles fabricated from toluene solution droplets. Number-average molecular weights (M_n) (g mol^{-1}) of PBTPA-*b*-PMMA were (**a**, **b**) 3,500-*b*-1,200 (PDI = 1.8), (**c**, **d**) 3,900-*b*-7,400 (PDI = 4.0), and (**e**, **f**) 6,300-*b*-5,100 (PDI = 3.4).

Effect of the Type of the Solvent.

Figure 4-3 shows TEM images of block copolymer particles fabricated from chlorobenzene solution droplets. Both of the copolymers formed disordered micro phase separation. The contrast became more distinguish rather than that observed in the particles fabricated from toluene solution.

Chlorobenzene has higher affinity to PBTPA than PMMA since chlorobenzene can dissolve high molecular weight of PBTPA which is difficult to dissolve into toluene. Further, boiling point of chlorobenzene and toluene are 131 and 111 °C, respectively. Higher affinity to PBTPA and slow evaporation led the phase separation in chlorobenzene solution reach to more thermodynamically stable state, and provided definite phases.

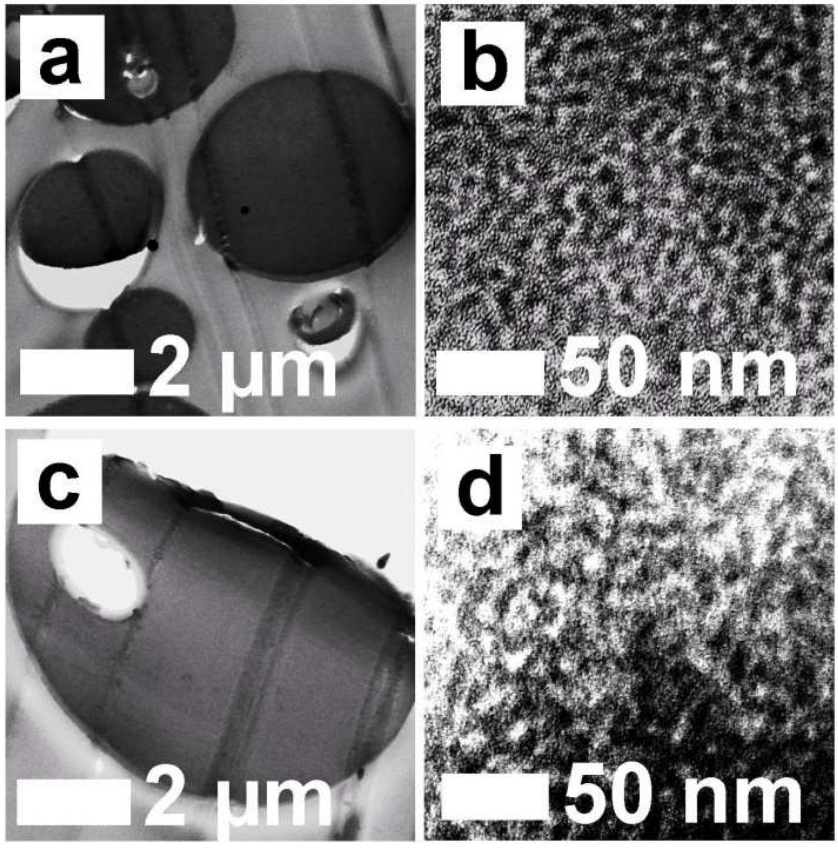

Figure 4-3. TEM images of block copolymer particles fabricated from chlorobenzene solution droplets. M_n (g mol^{-1}) of PBTPA-*b*-PMMA were (**a**, **b**) 3,900-*b*-7,400 (PDI = 4.0), and (**c**, **d**) 6,300-*b*-5,100 (PDI = 3.4).

Effect of the Thermal Annealing.

Figure 4-4 shows TEM images of block copolymer particles fabricated from chlorobenzene solution droplets. The particles were thermally annealed at 160 °C under vacuum for 48 hours before embedded in epoxy resin. After the annealing, the particles lost spherical shape by softening and aggregation at high temperature. Further, the phase separated structure became ambiguous. These results indicate that the solvent annealing is more favored than thermal annealing to obtain ordered structure.

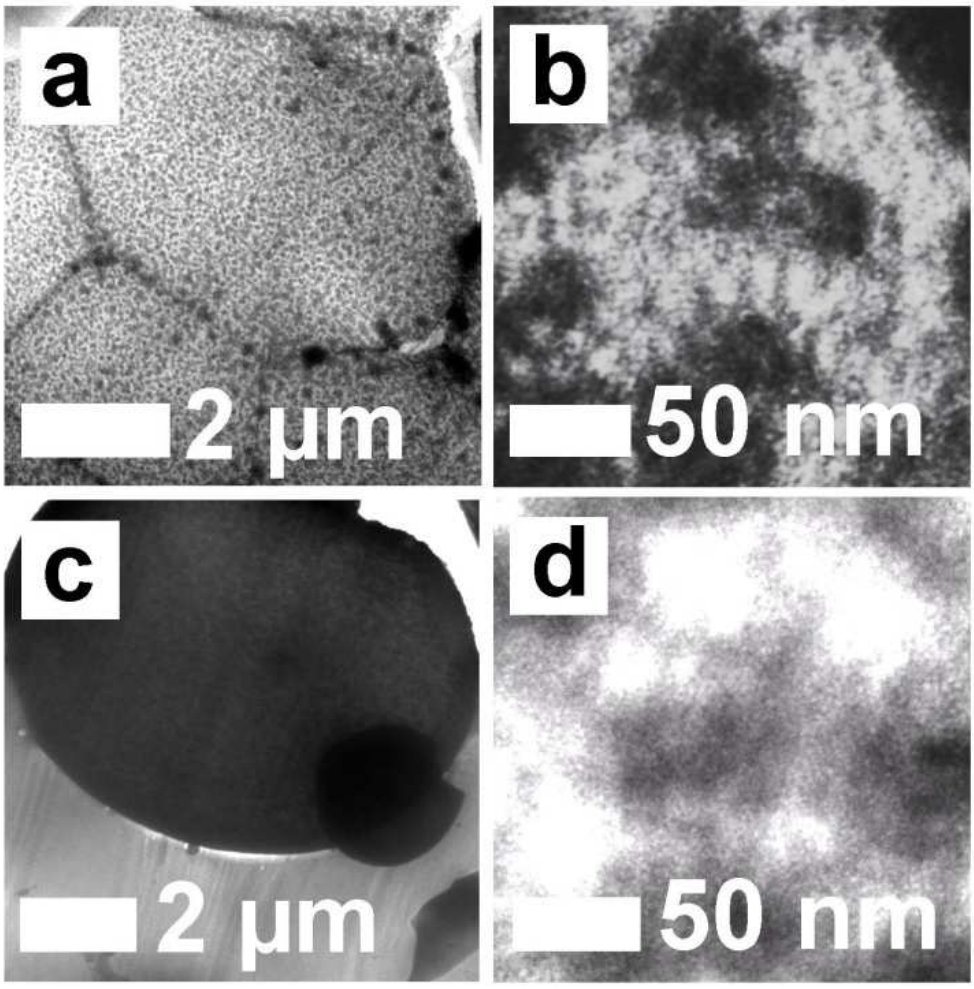

Figure 4-4. TEM images of block copolymer particles fabricated from chlorobenzene solution droplets. The particles were thermally annealed at 160 °C under vacuum for 48 hours. M_n (g mol^{-1}) of PBTPA-*b*-PMMA were (**a**, **b**) 3,800-*b*-7,200 (PDI = 4.0), and (**c**, **d**) 6,300-*b*-5,100 (PDI = 3.4).

4-3-3. PBTPA/PBTPA-*b*-PMMA particles

Effect of Weight Ratio of PBTPA.

Figure 4-5 shows TEM images of the polymer blend particles consisting of PBTPA-*b*-PMMA and PBTPA homopolymer fabricated from toluene solution droplets with various weight ratio of PBTPA homopolymers. The particles consisting of 7 wt% of PBTPA homopolymer showed no contrast attributing to phase separation. The particles consisting of 22 and 34 wt% of PBTPA homopolymer formed a sea-islands structure consisting of islands of PBTPA domains. The diameter of the PBTPA phase increased as the content of the PBTPA homopolymer increased.

For the polymer blend of block copolymer and homopolymer, homopolymers with lower molecular weight than those of the corresponding segments of the block copolymer intrude into the block copolymer chains and increase the domain size of the separated microphase[10]. Homopolymers with higher molecular weight than those of the corresponding segments of the block copolymer cause phase separation from the block copolymer phase. Since the molecular weight of the PBTPA homopolymer used to prepare the particle was too close to that of the PBTPA-*b*-PMMA, the phase separation between PBTPA and PBTPA-*b*-PMMA occurred. Microphase separation of PBTPA-*b*-PMMA which was observed in block copolymer particles was not seen in the blend particles with PBTPA homopolymer. This result indicates the addition of PBTPA homopolymer suppressed the microphase separation.

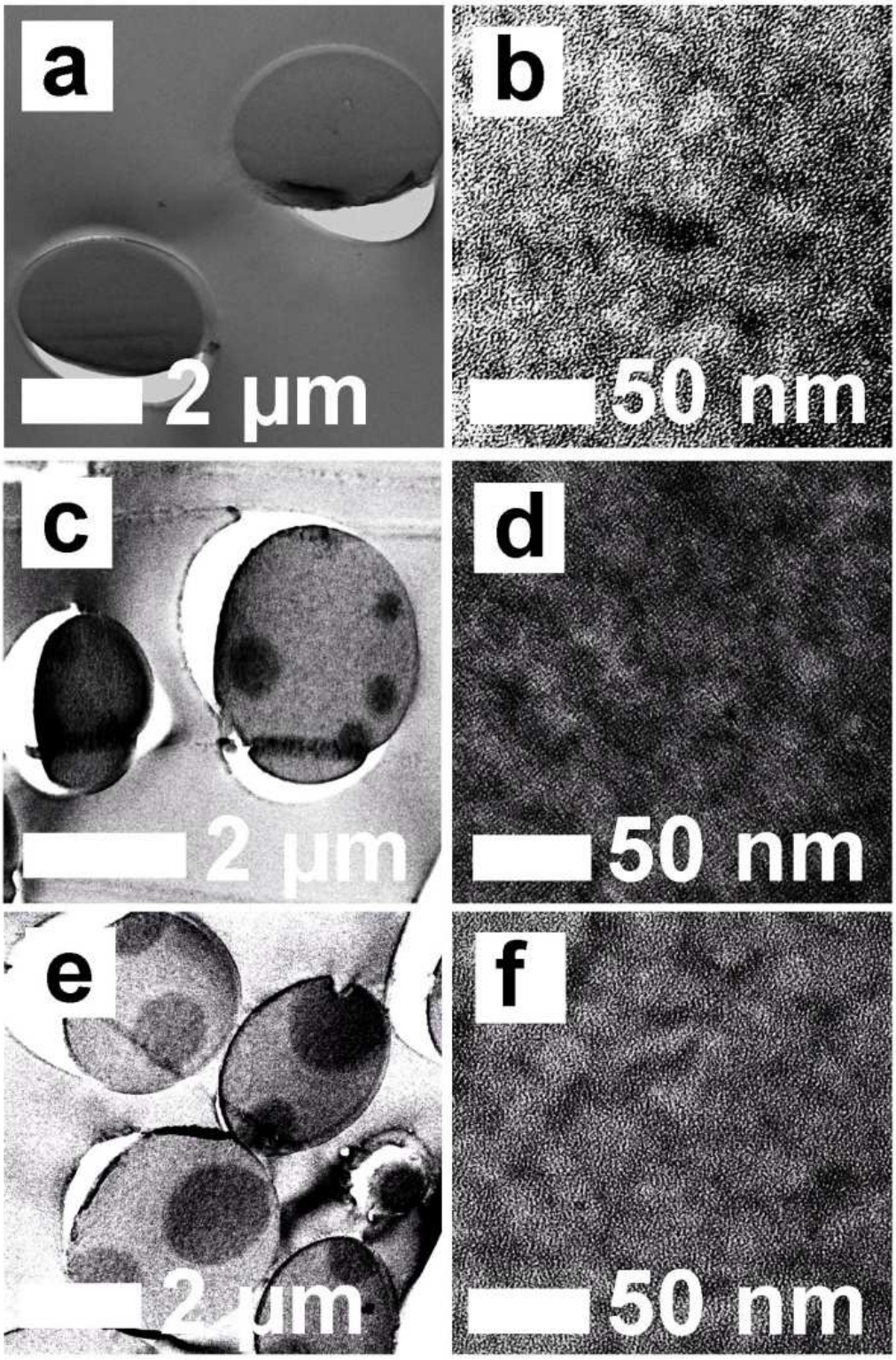

Figure 4-5. TEM images of polymer blend particles consisting of PBTPA-*b*-PMMA and PBTPA homopolymer fabricated from toluene solution droplets. M_n (g mol^{-1}) of PBTPA-*b*-PMMA was 3,800-*b*-7,200 (PDI = 4.0), and *M*n (g mol^{-1}) of PBTPA was 4,100 (PDI = 1.6). Weight ratio of PBTPA homopolymer was (**a**, **b**) 7, (**c**, **d**) 22 and (**e**, **f**) 34 wt%, respectively.

4-3-4. PBTPA/PBTPA-*b*-PMMA/PMMA particles

Effect of the Molecular Weight of Homopolymers.

Figure 4-7 shows TEM and SEM images of polymer blend particles consisting of PBTPA, PMMA, and PBTPA-*b*-PMMA fabricated from toluene solution droplets with various molecular weight of homopolymers. The particles containing PMMA with M_n of 25,000 formed inversed core-shell structure with PMMA core and PBTPA shell. Furthermore, in spite of the existence of the block copolymer, microphase separations were not observed in both of the PBTPA and the PMMA phases. On the other hand, the particles containing PBTPA with M_n of 14,200 formed core-shell structure with PBTPA core and PMMA shell. Dark spots of PBTPA microdomains of 10 nm in diameter were observed in PMMA shell phase.

The block copolymers are localized at the interface between different polymer phases, and suppress macrophase separation by reducing the interfacial tension.[11,12] Whereas the block copolymer can also dissolve into the bulk phases with forming micelles[13,14] or meso-phases depending on the molecular weight and segment ratio.[15,16] The dark spots observed in the particle composed of high molecular weight PBTPA (M_n = 14,200) demonstrate that PBTPA-*b*-PMMA block copolymer are distributed into PMMA macrophase with forming micelles (Figure 4-7c'). This is because PBTPA-*b*-PMMA (M_n = 3,800-*b*-7,200) can dissolve into PMMA macrophase due to high affinity originated from high content of PMMA segment (Figure 4-8a). On the contrary, for the particle composed of high molecular weight PMMA (M_n = 25,000), no micelles were observed, and the macrophase separated structure changed to inversed core-shell structure. This morphological transition is because block copolymer worked as a surfactant in PBTPA macrophase. Since the increment of χN induces the strong segregation between polymers,[17] block copolymers were repelled from the PMMA

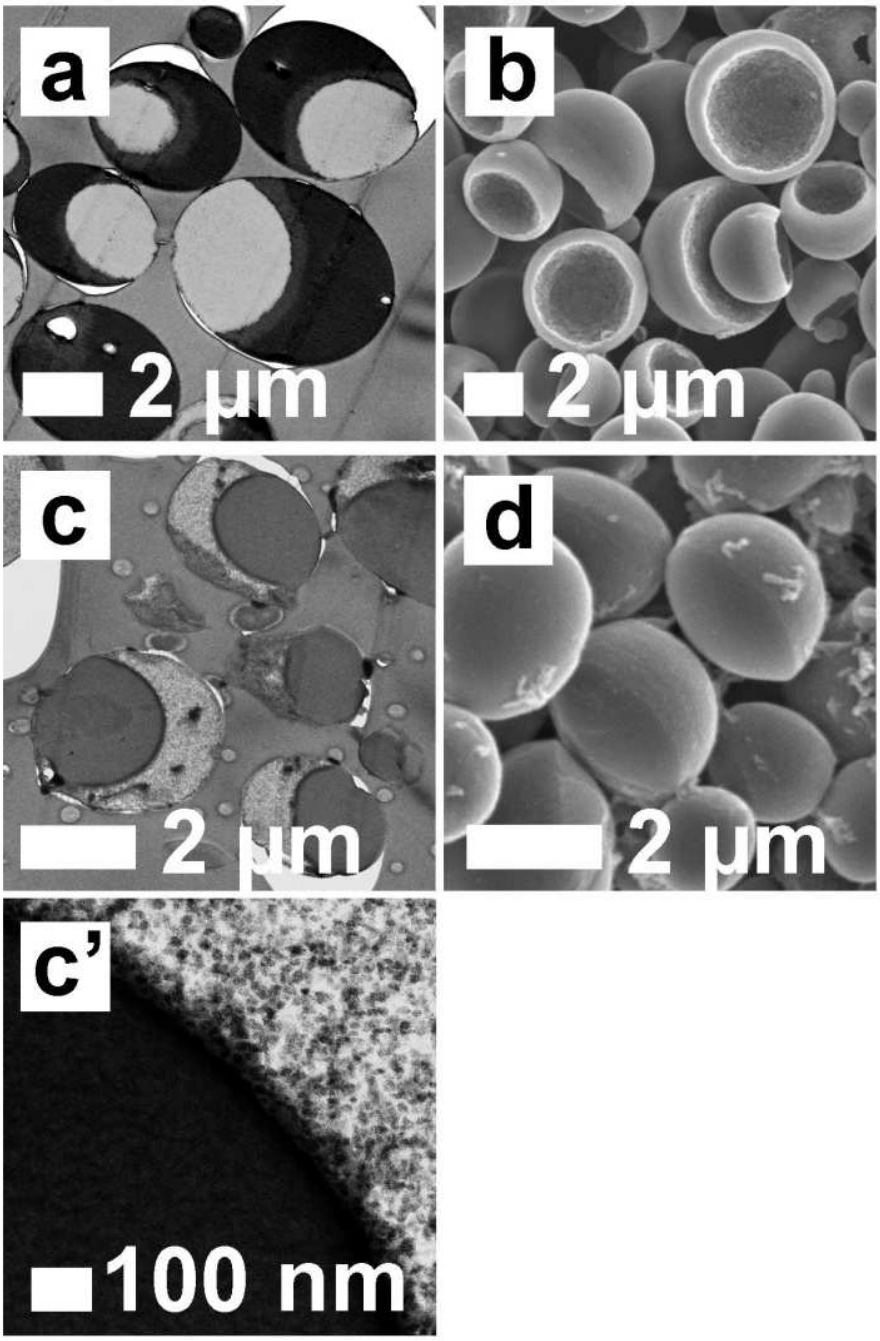

Figure 4-7. (**a**, **c**, **c'**) TEM and (**b**, **d**) SEM images of polymer blend particles fabricated from toluene solution droplets. The SEM images show the particles observed after the soaking in acetone. M_n (g mol^{-1}) of PBTPA/PBTPA-*b*-PMMA/PMMA was (**a**, **b**) 4,100/3,800-*b*-7,200/25,000 and (**c**, **c'**, **b**) 14,200/3,800-*b*-7,200/3,400, respectively. Weight ratio of PBTPA/PBTPA-*b*-PMMA/PMMA was 45/10/45 (w/w/w).

macrophase and moved to PBTPA phase due to the strong repulsive forces between the PBTPA segment and high molecular weight PMMA homopolymer. PBTPA-*b*-PMMAs repelled from the PMMA phase are expected to be located at near to the interface between PBTPA- and PMMA macrophase, or the surface of the droplet with PMMA segment in contact with the aqueous phase due to the hydrophilic nature. These PBTPA-*b*-PMMAs form PMMA layer on the droplet surface, and make the interfacial tension between the PBTPA solution phase and aqueous phase close to that of the PMMA solution (Figure 4-8b). As the result, PBTPA phase came to face aqueous phase and formed inversed core-shell structure.

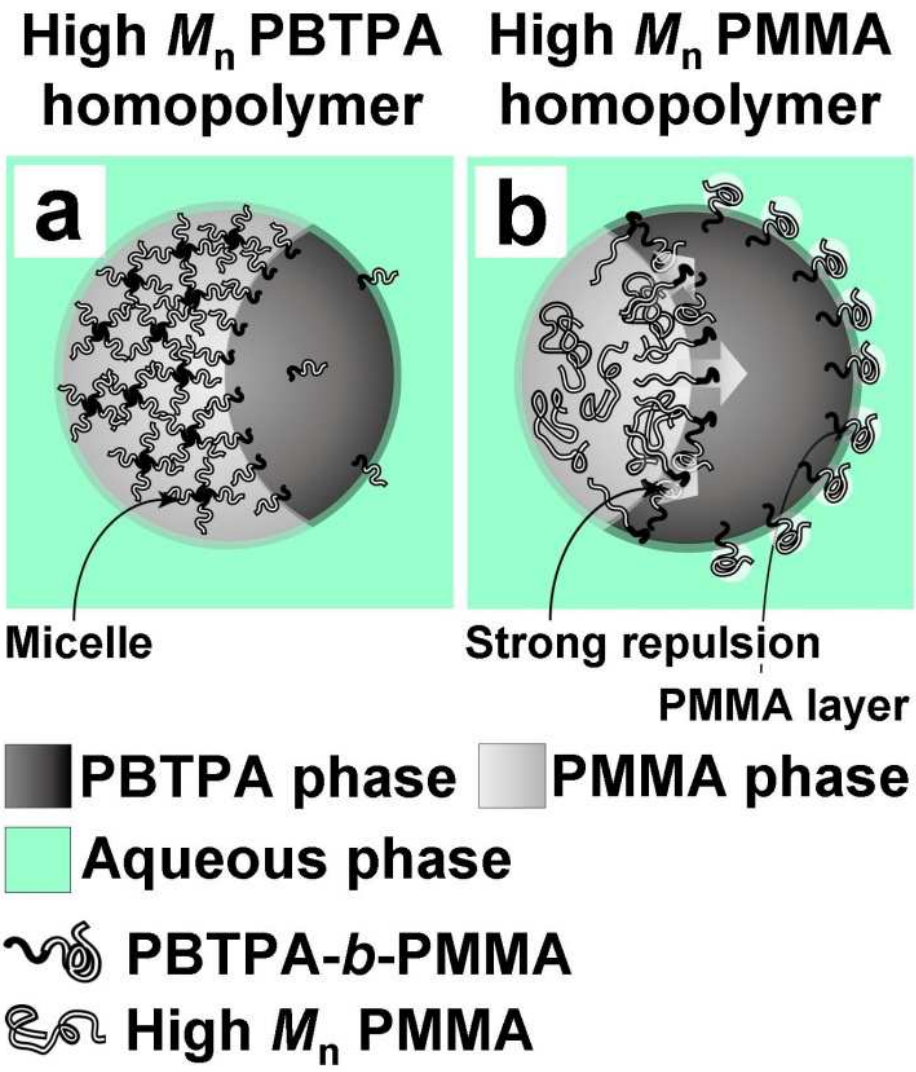

Figure 4-8. Schematic graphs of PBTPA/PBTPA-*b*-PMMA/PMMA polymer blend particle with high M_n of (**a**) PBTPA- and (**b**) PMMA homopolymers.

Figure 4-9 shows the interfacial tension between polymer solution and distilled water (DW) or 0.6 wt% PVA aqueous solution as the function of the concentration of PBTPA-*b*-PMMA. PBTPA showed higher interfacial tension to DW and PVA solution than that of PMMA at 0 wt% of PBTPA-*b*-PMMA. The interfacial tension of PBTPA dropped down to the close value to that of PMMA at 10 wt% of PBTPA-*b*-PMMA. Block copolymer reduced the interfacial tension of the 20 wt% PBTPA solution as well. These results are showing the PBTPA-*b*-PMMA is working as the surfactant in PBTPA macrophase.

Figure 4-10 shows the DSC curves of polymer blend particles and polymers contained in the particles. For the 1st scan of the blend particles with high molecular weight of PBTPA homopolymer (M_n = 14,200), three different T_gs were detected at 114, 167 and 200 °C as marked by arrows (Figure 4-10, green line). As shown in the TEM images (Figure 4-7c, c', d), the PBTPA- and PMMA homopolymers were separated into macrophase, and PBTPA-*b*-PMMA formed microdomains as micelles in the PMMA macrophase. Since the glass transition of phase separated polymer blend occurs at the temperature corresponding to that of each homopolymer component, these three T_gs can be assigned to PMMA macrophase, PBTPA segment in the micelles, and PBTPA macrophase in ascending order. On the other hand, the blend particles with high molecular weight of PMMA (M_n = 25,000) also exhibited three different T_gs (Figure 4-10, red line). For the 1st scan, the heat jumps at 112 and 165 °C can be assigned to the glass transition of PMMA and PBTPA macrophases. However, the heat jump detected at 140 °C was not agreed with that of neither PBTPA nor PMMA homopolymers. This intermediary heat jump can be assigned to PBTPA segment of PBTPA-*b*-PMMA located at near to the PBTPA/PMMA interface. In phase separated block copolymer, it has been reported that the increment of the interfacial layer at the domain boundary lowers the T_g of the harder segment of block copolymer.[18] In the blend particles, PBTPA-*b*-PMMA located at the boundary area are expected to have high content of the

interfacial region. This intermediate layer lowered the glass transition temperature of PBTPA segment to 140 °C.

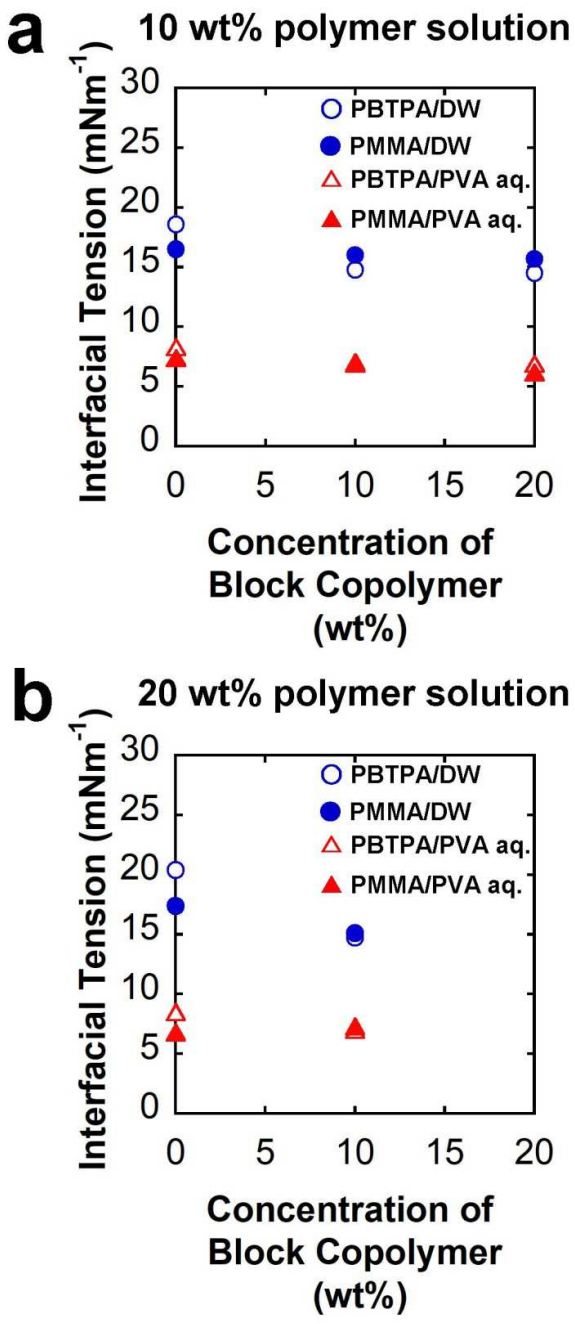

Figure 4-9. Interfacial tensions between (**a**) 10 or (**b**) 20 wt% of polymer solution and distilled water (DW) or 0.6 wt% PVA aqueous solution as a function of weight ratio of block copolymer measured by pendant drop method. M_n (g mol^{-1}) of PBTPA, PMMA, and PBTPA-*b*-PMMA were 4,100, 3,400, and 4,000-*b*-2,800, respectively.

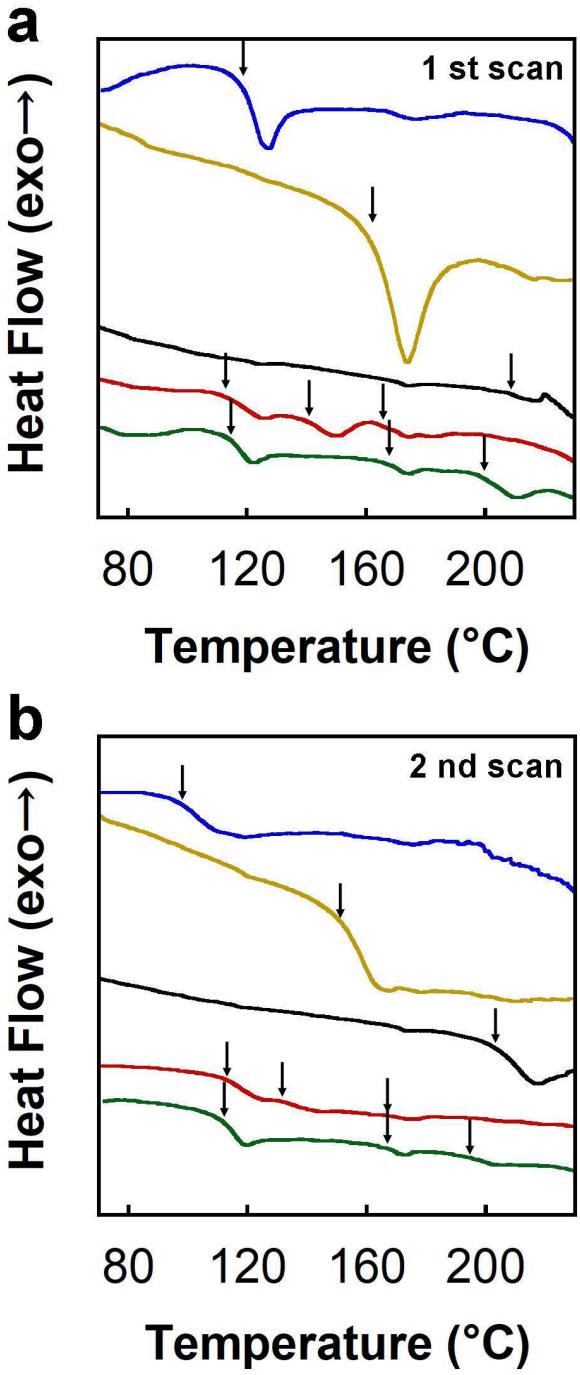

Figure 4-10. DSC curves blue: PMMA- (M_n = 3,400), yellow: high M_n PBTPA- (M_n = 4,100), black: low M_n PBTPA homopolymer (M_n = 13,000), and polymer blend particles, in which M_n of PBTPA/PBTPA-*b*-PMMA/PMMA were red: 4,100/3,800-*b*-7,200/25,000 and green: 13,000/3,800-*b*-7,200/3,400. Weight ratio of PBTPA/PBTPA-*b*-PMMA/PMMA in polymer blend particle was 45/10/45 (w/w/w). T_gs are marked by allows.

Effect of the Molecular Weight and Segment Ratio of PBTPA-b-PMMA.

Figure 4-11 shows TEM and SEM images of polymer blend particles consisting of PBTPA, PMMA, and PBTPA-*b*-PMMA fabricated from toluene solution droplets with various molecular weight of PBTPA-*b*-PMMA. The particles consisting of PBTPA-*b*-PMMA with M_n of 6,300-*b*-5,100 formed core-shell like structure with PBTPA shell and PMMA core. PBTPA microdomeins of smaller than 80 nm in diameter were dispersed in PMMA core (Figure 4-11a, b). PBTPA shell with porous inner surface remained after removing PMMA core by soaking in acetone (Figure 4-11c).

The morphologies of blend particles depended on the content of the PMMA segment in PBTPA-*b*-PMMA, and the molecular weight of PBTPA segment. When the content of PMMA segment was relatively high (6,300-*b*-5,100 and 3,800-*b*-7,200), PBTPA micelles were observed in PMMA macrophase. This is because PBTPA-*b*-PMMA was distributed into PMMA phase due to high solubility of block copolymer with PMMA phase originated from high content of PMMA segment (Figure 4-12a, c). Whereas the macrophase separated structure depended on the molecular weight of PBTPA segment. When the molecular weight of PBTPA segment was relatively high (6,300-*b*-5,100 and 6,300-*b*-1,300), inversed core-shell structure was obtained because PBTPA-*b*-PMMA in PBTPA macrophase worked as surfactant (Figure 4-12a, b). On the other hand, when the molecular weight of PBTPA segment was relatively low (3,800-*b*-7,200 and 3,500-*b*-1,200), the structure remained as core-shell with PBTPA core and PMMA shell. For the PBTPA-*b*-PMMA with M_n of 3,800-*b*-7,200, since the block copolymer has high affinity with PMMA homopolymer due to the high content of the PMMA segment and low molecular weight of PBTPA segment, PBTPA-*b*-PMMAs are mainly located in PMMA macrophase with forming micelles. This makes the reduction of interfacial tension by block copolymer less effective to tuning the morphology to inversed core-shell (Figure 4-12c). For the PBTPA-*b*-PMMA with M_n of 3,500-*b*-1,200, the

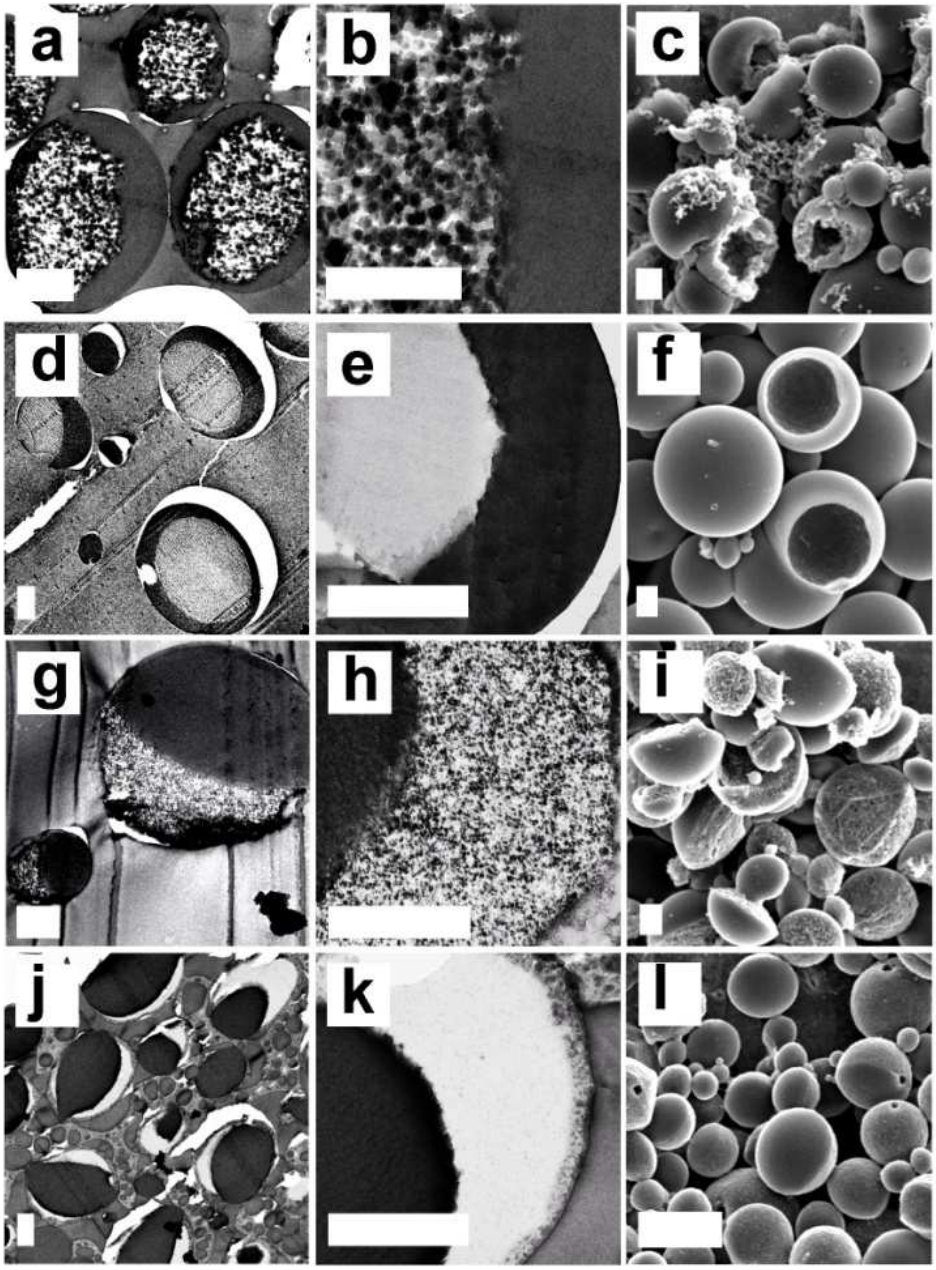

Figure 4-11. (**a**, **b**, **d**, **e**, **g**, **h**, **j**, **k**) TEM and (**c**, **f**, **i**, **l**) SEM images of polymer blend particles consisting of PBTPA, PMMA and PBTPA-*b*-PMMA fabricated from toluene solution droplets. The SEM images show the particles observed after the soaking in acetone. Weight ratios of PBTPA/PBTPA-*b*-PMMA/PMMA were 45/10/45 (w/w/w). M_n (g mol^{-1}) of PBTPA and PMMA homopolymer were 4,100 (PDI = 1.6) and 3,400 (PDI = 1.8). M_n (g mol^{-1}) of PBTPA-*b*-PMMA were (**a**-**c**) 6,300-*b*-5,100, (**d**-**f**) 6,300-*b*-1,300, (**g**-**i**) 3,800-*b*-7,200, and (**j**-**l**) 3,500-*b*-1,200. All scale bars represent 1 μm.

repulsive forces between PMMA segments and PBTPA homopolymers is small due to the low molecular weight of PMMA segment. Therefore, block copolymers are not localized at the interface but are uniformly dispersed in the PBTPA macrophase. This makes the interfacial tension of PBTPA phase remained as same as that of pure PBTPA homopolymer, and phase separated structure as core-shell morphology (Figure 4-12d).

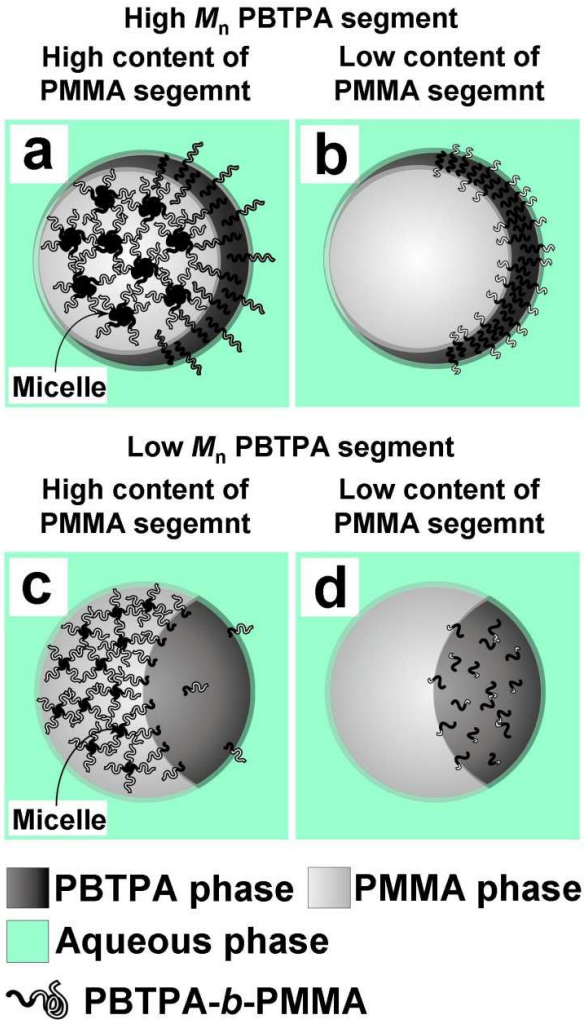

Figure 4-12. Schematic graphs of PBTPA/PBTPA-*b*-PMMA/PMMA polymer blend particles. The PBTPA-*b*-PMMA are classified into fourth groups; high M_n of PBTPA segment with (**a**) high- and (**b**) low content of PMMA segments, and low M_n of PBTPA segments with (**c**) high- and (**d**) low content of PMMA segment.

Effect of the Weight Ratio of PBTPA-b-PMMA.

Figure 4-13 shows TEM and SEM images of polymer blend particles consisting of PBTPA, PMMA, and PBTPA-*b*-PMMA fabricated from toluene solution droplets with various weight ratio of PBTPA-*b*-PMMA. The particles containing 20 wt% of PBTPA-*b*-PMMA formed core-shell like structure with PBTPA shell and PMMA core (Figure 4-13a, b). The interface between PMMA core and PBTPA shell became obscure in the particles containing 30 wt% of PBTPA-*b*-PMMA, and white regions originated from PMMA phase came to be seen in PBTPA shell, (Figure 4-13d, e). The macrophase in the particles became single phase at 50 wt% of PBTPA-*b*-PMMA (Figure 4-13g).

PBTPA-*b*-PMMA form aggregates with incorporating PBTPA homopolymers into the micelle core. Adding block copolymer promotes PBTPA homopolymers dissolve into the PMMA macrophase, which weaken the macrophase separation between PBTPA and PMMA. At the point where the amount of the block copolymer is enough to wrap the PBTPA homopolymers, the internal morphology becomes a single phase.

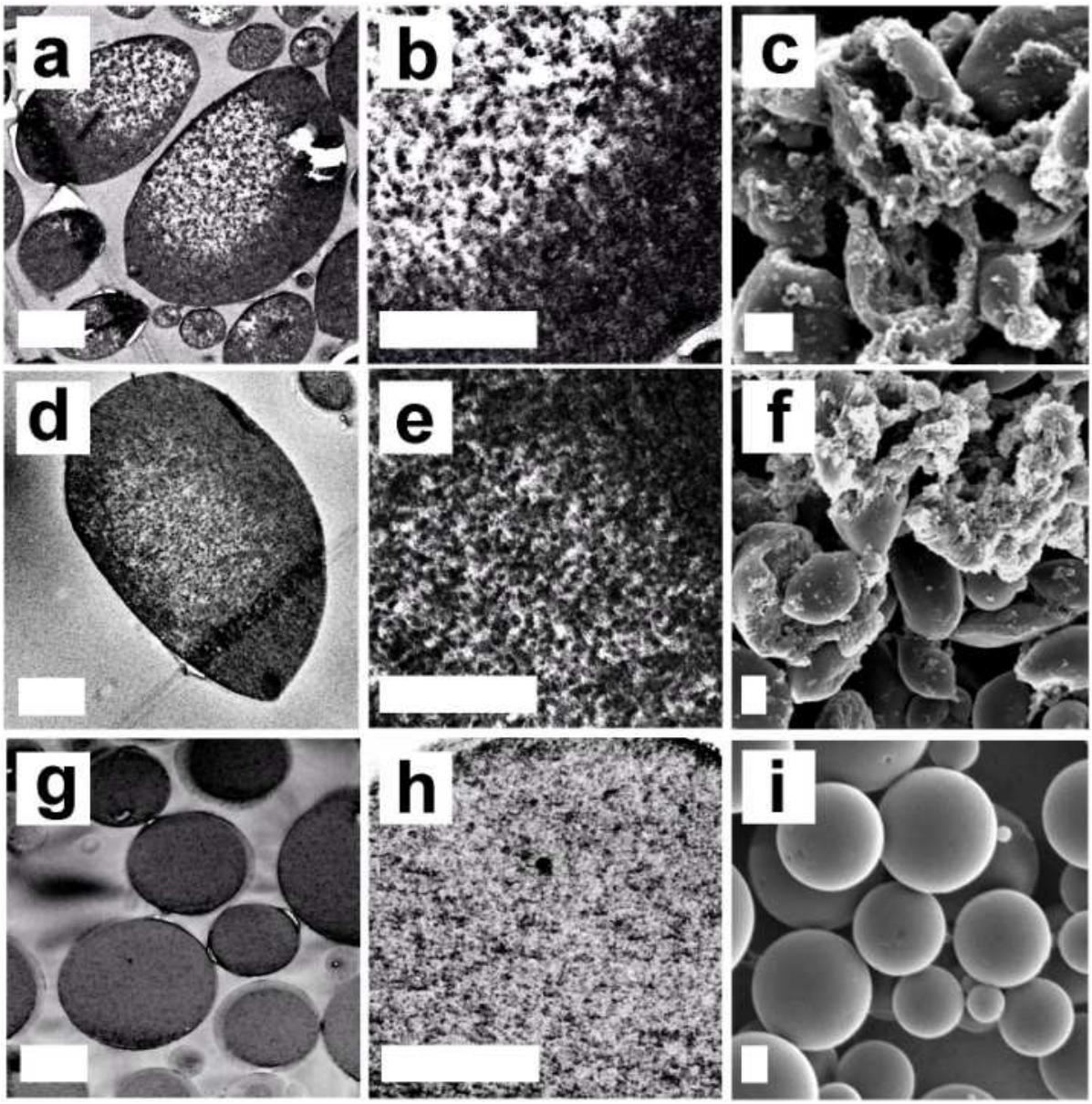

Figure 4-13. (**a**, **b**, **d**, **e**, **g**, **h**) TEM and (**c**, **f**, **i**) SEM images of polymer blend particles consisting of PBTPA, PMMA and PBTPA-*b*-PMMA fabricated from toluene solution droplets. The SEM images show the particles observed after the soaking in acetone. Weight ratios of PBTPA/PBTPA-*b*-PMMA/PMMA were (**a**-**c**) 40/20/40, (**d**-**f**) 35/30/30, and (**g**-**i**) 25/50/25 (w/w/w), respectively. M_n (g mol^{-1}) of PBTPA, PMMA and PBTPA-*b*-PMMA were 4,100 (PDI = 1.6), 3,400 (PDI = 1.8) and 6,300-*b*-5,100 (PDI = 3.4). All scale bars represent 1 μm.

4-4. Conclusions

The polymer blend particles consisting of poly(4-butyltriphenylamine) (PBTPA), poly(methyl methacrylate) (PMMA) and PBTPA-*block*-PMMA were fabricated by solvent evaporation method. The effect of the molecular weight and segment ratio of PBTPA-*b*-PMMA, molecular weight of homopolymers, and composition of the blend on the morphology was investigated. The polymer blend particle consisting of PBTPA and PMMA homopolymers forms thermodynamically preferable core-shell structure in which more hydrophilic PMMA-shell is surrounding PBTPA-core. Addition of 10 wt% of the PBTPA-*b*-PMMA caused transition from core-shell to Janus or inversed core-shell, in which PBTPA-shell is surrounding PMMA-core, depending on the molecular weight of PBTPA segment in PBTPA-*b*-PMMA. When the molecular weight of PMMA segment was higher than that of PMMA homopolymer, “watermelon-like” particles in which PBTPA microphases of smaller than 80 nm dispersed in PMMA macrophase surrounded by PBTPA shell were observed. As the composition of PBTPA-*b*-PMMA increased, the interface of the macrophase separation became obscure. At the 50 wt% of the PBTPA-*b*-PMMA, only microphase separation was observed. The measurement of interfacial tension by pendant drop method demonstrated that PBTPA-*b*-PMMA lower the interfacial tension between PBTPA and aqueous phase to the value similar to that of PMMA and aqueous phase. The reduction of interfacial tension is driving force for the morphological transition of macrophase separated structure caused by block copolymer. This result also indicates PBTPA-*b*-PMMA has similar behavior as surfactant because of the amphiphilic nature. PBTPA microphases in PMMA macrophase is the aggregate of PBTPA-*b*-PMMA like “micelle” which is aggregate of surfactant.

4-5. References

(1) Higuchi, T.; Tajima, A.; Motoyoshi, K.; Yabu, H.; Shimomura, M. Frustrated phases of block copolymers in nanoparticles. *Angew. Chem. Int. Ed.* **2008**, *47*, 8044–8046.

(2) Yabu, H. Creation of functional and structured polymer particles by self-organized precipitation (SORP). *Bull. Chem. Soc. Jpn.* **2012**, *85*, 265–274.

(3) Tanaka, T.; Saito, N.; Okubo, M. Control of layer thickness of onionlike multilayered composite polymer particles prepared by the solvent evaporation method. *Macromolecules* **2009**, *42*, 7423–7429.

(4) Klinger, D.; Wang, C. X.; Connal, L. A.; Audus, D. J.; Jang, S. G.; Kraemer, S.; Killops, K. L.; Fredrickson, G. H.; Kramer, E. J.; Hawker, C. J. A facile synthesis of dynamic, shape-changing polymer particles. *Angew. Chem. Int. Ed.* **2014**, *53*, 7018–7022.

(5) Jeon, S. J.; Yi, G. R.; Yang, S. M. Cooperative assembly of block copolymers with deformable interfaces: Toward nanostructured particles. *Adv. Mater.* **2008**, *20*, 4103–4108.

(6) Jang, S. G.; Audus, D. J.; Klinger, D.; Krogstad, D. V.; Kim, B. J.; Cameron, A.; Kim S. W.; Delaney, K. T.; Hur, S. M.; Killops, K. L.; Fredrickson, G. H.; Kramer, E. J.; Hawker, C. J. striped, ellipsoidal particles by controlled assembly of diblock copolymers *J. Am. Chem. Soc.* **2013**, *135*, 6649–6657.

(7) Taherzadeh, H.; Ogino, K. Fabrication of microspheres based on poly(4-butyltriphenylamine) blends with poly(methyl methacrylate) and block copolymer by solvent evaporation method. *Open J. Org. Polym. Mater.* **2015**, *5*, 37–42.

(8) Tsuchiya, K.; Shimomura, T.; Ogino, K. Preparation of diblock copolymer based on poly(4- *n*-butyltriphenylamine) via palladium coupling polymerization. *Polymer* **2009**, *50*, 95–101.

(9) Matyjaszewski, K.; Xia, J. Atom transfer radical polymerization. *Chem. Rev.* **2001,** *101,* 2921–2990.

(10) Tanaka, T.; Saito N.; Okubo, M. Control of layer thickness of onionlike multilayered composite polymer particles prepared by the solvent evaporation method. *Macromolecules* **2009**, *42*, 7423–7429.

(11) Kang, E. A.; Kim, J. H.; Kim, C. K.; Oh, S. Y.; Rhee, H. W. The effects of PC-PMMA block copolymer on the compatibility and interfacial properties of PC/SAN blends. *Polym. Eng. Sci.* **2000**, *40*, 2374−2384.

(12) Kim, J. H.; Kim, C. K. Changes in the Interfacial Properties of PC/SAN Blends with Compatibilizer. *J. Appl. Polym. Sci.* **2003**, *89*, 2649−2656.

(13) Cavallo, A.; Müller, M.; Binder, K. Formation of micelles in homopolymer-copolymer mixtures: Quantitative comparison between simulations of long chains and self-consistent field calculations. *Macromolecules* **2006**, *39*, 9539−9550.

(14) Klymenko, A.; Colombani, O.; Nicol, E.; Chassenieux,C.; Nicolai, T. Effect of self-assembly on phase separation of di- and triblock copolymers mixed with homopolymers in aqueous solution *Macromolecules* **2016**, *49*, 3427−3432.

(15) Horák, Z.; Hlavatá, D.; Hromádková, J.; Kotek, J.; Hašová, V.; Mikešová, J.; Pleska, A. Effect of selected structural parameters of styrene–butadiene block copolymers on their

compatibilization efficiency in polystyrene/polybutadiene blends. *J Polym Sci Part B: Polym Phys.* **2002**, *40*, 2612−2623.

(16) Adedeji, A.; Lyu, S.; Macosko, C. W. Block copolymers in homopolymer blends: Interface vs micelles. *Macromolecules*, **2001**, *34*, 8663–8668.

(17) Reed, W. F.; Ghosh, S.; Medjahdi, G.; Francois, J. Dependence of polyelectrolyte apparent persistence lengths, viscosity, and diffusion on ionic strength and linear charge density. *Macromolecules*, **1991**, *24*, 6189–6198.

(18) Morèse-Séguéla, B.; St-Jacques, M.; Renaud, J. M.; Prod'homme, J. Microphase separation in low molecular weight styrene-isoprene diblock copolymers studied by DSC and 13C NMR. *Macromolecules*, **1980**, *13*, 100–106.

Chapter 5

Transition from core-shell to Janus morphology for phase-separated PBTPA / PMMA solution droplets by UV light irradiation

5-1. Introduction

The microscopic observation of the phase separated structure in the polymer solution droplets during the solvent evaporation process helps to understand the formation mechanism of the morphology. To identify the component of the each separated phase, the polymer blend solution droplets containing PBTPA and PMMA were observed via a fluorescence microscope. Since PBTPA emits fluorescent light by the excitation of ultraviolet (UV) ray having wavelengths of 270-430 nm, PBTPA and PMMA phase were expected to appear as light and dark region, respectively, in fluorescent micrograph. However, it was accidentally found that the phase separated core-shell structure was converted to Janus type structure, during the fluorescence microscope observations. The fabrication and structural control of polymer particles utilizing UV light irradiation have been studied for the last couple of decades.[1,2] For instance, Wang et al. have been reported the photosensitive polymer particles which can be anisotropically stretched by the *trans–cis* photoisomerization of the azobenzene group. Polymer particles fabricated by a UV curing of monodispersed droplets of a monomer solution fabricated by using microfluidics has been reported as well. When monomer solution droplets contain components which are immiscible to the resulted polymer, photopolymerization causes the phase separation. Furthermore, an irradiation with UV light to the one side of the droplets can produce anisotropic particles because the rate of photopolymerization is different according to which hemisphere of the droplet is exposed to the UV ray. However, to our knowledge, there are few studies about transition of phase separated structure induced by UV light irradiation. In this study, the effects of various factors including the concentration of the polymers, and diameter of droplets on the UV induced morphological transition are investigated.

5-2. Experimental section

5-2-1. Materials

PBTPA (M_n=7200, PDI=2.0) and PMMA (M_n=17400, PDI=2.0) homopolymers were synthesized by the palladium catalyzed C-N coupling [3] and atom transfer radical polymerization (ATRP), respectively. Weight-average (M_w) and number-average (M_n) molecular weights were estimated by gel permeation chromatography. PVA (PVA224, Kuraray Co. Ltd., Japan, degree of polymerization; 2,400, degree of saponification; 87-89%) as a dispersion stabilizer, toluene and chlorobenzene were purchased from Wako Pure Chemical Industries, Ltd, and used as received. Deionized water with specific resistance of 15 MΩ was distilled.

5-2-2. Characterization

^{1}H NMR spectra were recorded on a JMN-300 (300 MHz, JEOL Ltd., Japan) spectrometer in $CDCl_3$, C_6D_6 or D_2O. The molecular weights of polymers were estimated by gel permeation chromatography (GPC) using a 880-PU pump (JASCO Corporation, Japan), a column packed with styrene–divinylbenzene gel beads, and a UV970 detector (JASCO Corporation, Japan). Chloroform was used as an eluent, and the molecular weight was calibrated using polystyrene standards (Shodex, SHOWA DENKO K. K., Japan). The morphology of the PBTPA and PMMA blend solution droplet was investigated by fluorescense microscope (BX53, Olympus corporation, Japan), and UV light was irradiated from the UV lamp (U-HGLGPS, Olympus corporation, Japan) through the objective lens. The rated power of the UV lamp is 130 W, and the irradiation was conducted at 3% of the maximum output. The size of the objective lens is about 0.01 cm^2. The resulting PBTPA and PMMA blend particles were observed by optical microscope, scanning electron microscope (SEM) (JSM-6510, JEOL Ltd., Japan) and transmission electron microscope (TEM) (JEM-2100, JEOL Ltd., Japan). Samples for SEM were prepared by putting one drop of water

dispersion of the particles on a sample stage, and then drying in air. The samples were coated by osmium tetraoxide (OsO_4) using ion coater (Neoc-STB, Meiwafosis Co. Ltd., Japan) to avoid the charging. Samples for TEM were prepared as follows; dried particles were dispersed to epoxy resin, cured at 60 °C for three days and microtomed (UC7, Leica, Germany). The ultrathin cross sections were stained with ruthenium tetraoxide (RuO_4) vapor at room temperature for 5 min in the presence of 1% RuO_4 aqueous solution.

5-2-3. Fabrication of polymer blend solution droplet

PBTPA and PMMA were dissolved into chloroform or toluene at total concentration of 3 wt% (weight ratio = 1 : 1) (totally 1.5 mL). The homogeneous solution was dispersed to poly(vinyl alcohol) (PVA) aqueous solution (10 mL, 0.6 wt%) using a homogenizer at 25,000 rpm for 5 s in a test-tube (115-mL. i.d.= 2.7 cm). Then, the obtained dispersion was stirred at 100 rpm to evaporate the solvent at room temperature. A small portion of dispersion (ca. 0.1 mL) was withdrawn after varying intervals, and placed on the glass slide sandwiched with a cover-glass for optical micrograph (OM) observations, the concentration of the polymer was monitored by ^1H NMR in D_2O. The morphologies of phase separated PBTPA/PMMA droplets were observed by OM with or without UV light (365 nm) irradiation from UV lamp with the band-pass filter attached to the microscope. The resulting particles were collected by centrifugation and washed with distilled water for three times.

5-3. Results and discussion

5-3-1. Effect of UV light irradiation

Figure 5-1 shows OM images of polymer blend solution droplets during the evaporation, TEM and SEM images of particles obtained without UV light irradiation. When toluene was used as a solvent (Figure 5-1a-c), core-shell structure was observed for the droplets during the evaporation of the solvent, and for the resulting particles, which consists of PBTPA-core and PMMA-shell confirmed by TEM image. In the case of chloroform solution (Figure 5-1d-

f), Janus structure was observed at the beginning of the phase separation. The morphology changed to dumbbell-like structure with the evaporation of chloroform.

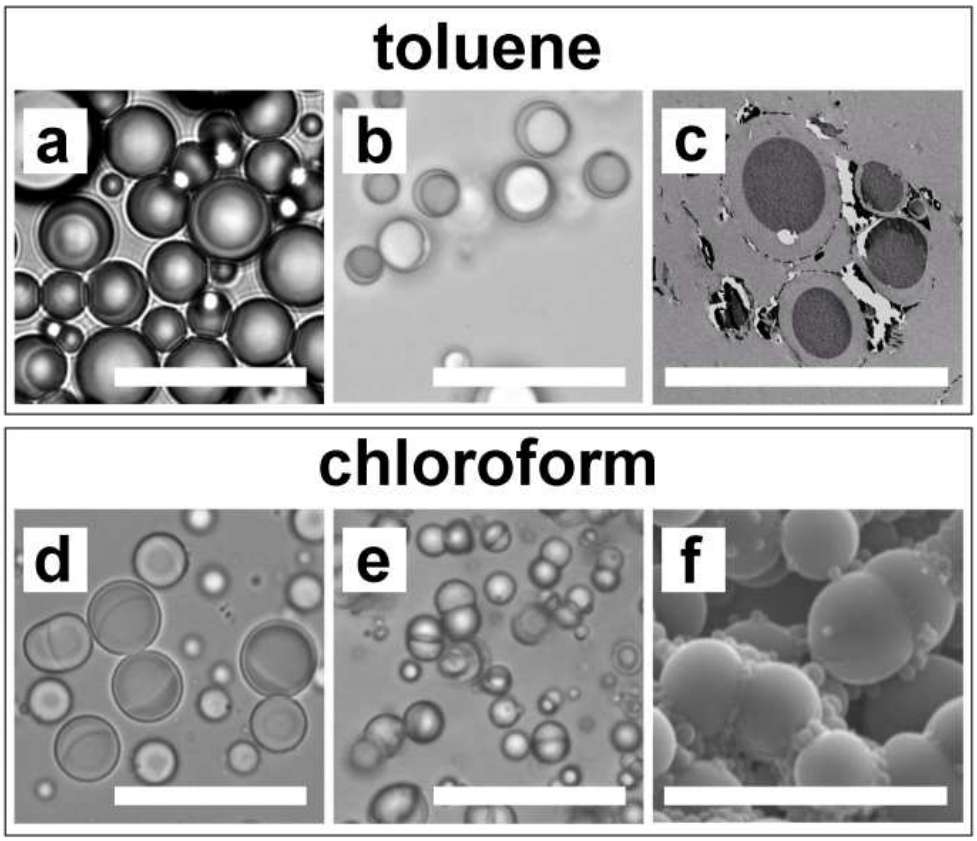

Figure 5-1. OM image of (**a**) toluene and (**d**) chloroform solution droplets dissolving PBTPA and PMMA without UV light irradiation. (**b**, **e**) OM, (**c**) TEM and (**f**) SEM images of resuting particles from (**b**, **c**) toluene and (**e**, **f**) chloroform solution droplets. All scale bars represent 10 μm.

Intriguingly, as shown in the Figure 5-2, the exposure with UV light (365 nm) changed the phase-separated morphology from the core-shell structure formed in toluene to the Janus structure (Figure 5-2a-c). When chloroform was used as solvent (Figure 5-2d-f), the originally formed Janus structure changed to the specific structure, where PBTPA phase surrounded PMMA phase as shown in the schematic representation in Figure 5-2f. The resulting morphologies were sustained at least for 1 h after turning off the UV irradiation.

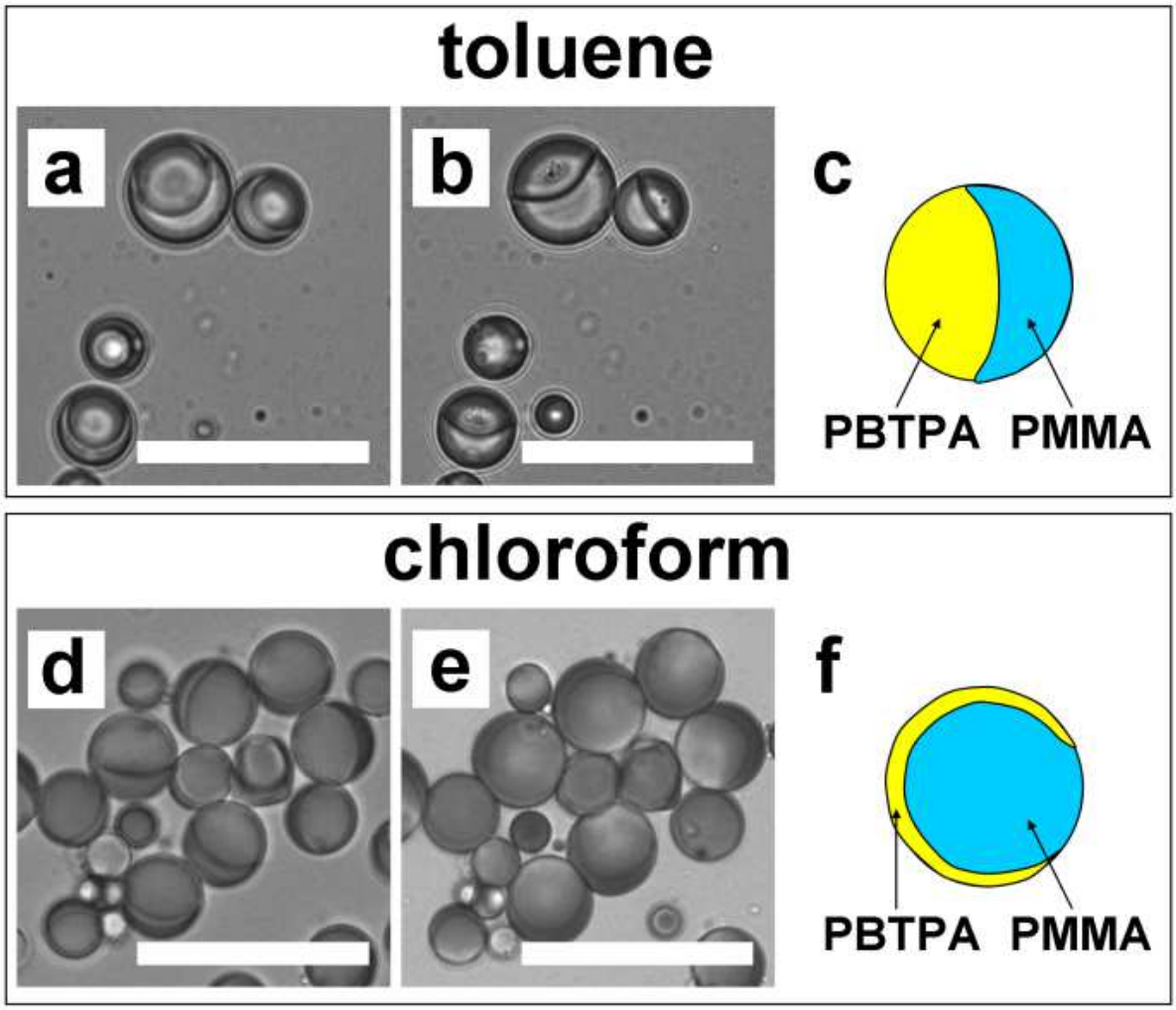

Figure 5-2. OM images of (**a**, **b**) toluene and (**d**, **e**) chloroform solution droplets dissolving PBTPA and PMMA (**a**, **d**) before and (**b**, **e**) after UV light irradiation. Schematic graph of droplets after the transition in (**c**) toluene and (**f**) chloroform solution droplets. Yellow; PBTPA, blue; PMMA. All scale bars represent 10 μm.

5-3-2. Effect of polymer concentration and droplet size

To estimate the time required to complete the structure change, a series of micrographs were shot about 50 droplets. The time when the transition stopped was determined by comparing the each photograph (Figure 5-3). The concentration of the polymer in droplets was determined by ^{1}H NMR spectroscopy. The dispersion in D_2O was measured with a JMN-300 NMR spectrometer at 300 MHz. Each NMR peak was certificated by comparing the

NMR spectra of dispersion and polymer solution in C_6D_6 as shown in Figure 5-4 and 5-5. The weak proton signal (approximately 3 ppm) next to the H_2O signal seems to be the ester group (-OCH_3) of PMMA. Based on the molecular weights of the repeat unit is 100.13 for PMMA, the amount of the toluene $W_{toluene}$ [g] was calculated from following equation (5-1) utilizing the amount of the dissolved PMMA W_{PMMA} [g] and integrated ratio $r_{toluene}$ of the signal at 1.7 ppm assigned to the methyl group (-CH_3) of toluene compared to 3 protons of signal at the 3 ppm (–OCH_3).

$$W_{toluene} = 92.1\ (r_{toluene} / 3)\ (W_{PMMA} / 100.13) \quad (5\text{-}1)$$

Figure 5-7a and b show the UV light irradiation induced transition in toluene solution droplets with the concentration of 7 and 13 wt% determined by ^{1}H NMR, respectively. The resulting droplets had Janus structure regardless of the concentration. The rate of transition was dependent on the concentration. Figure 5-7c shows the time *t* to finish the morphological transition as the function of droplet diameter *r*. There is the trend that the time was increased with the polymer concentration. The limited translational motion of polymer chains in droplets with higher concentration due to the higher viscosity may result in the prolonged time. The time was also increased with the diameter of particle. The transition from core-shell to Janus in the droplet with the larger diameter requires the longer distance of the mass transport polymer chains.

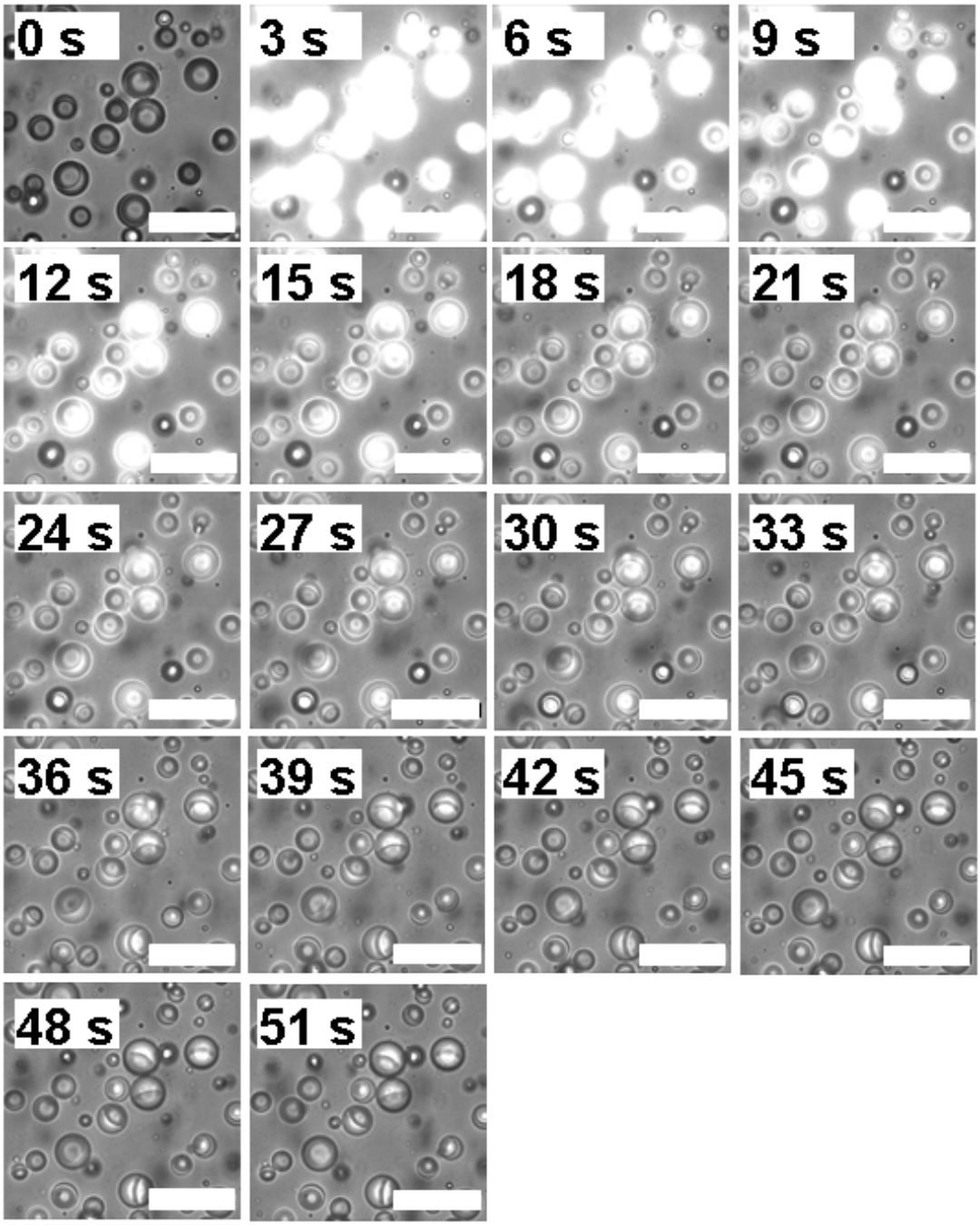

Figure 5-3. Sequence photographs of PBTPA / PMMA / toluene droplets (polymer concentration is 13 wt%,) during the irradiation with the UV light at 365 nm. All scale bars represent 10 μm.

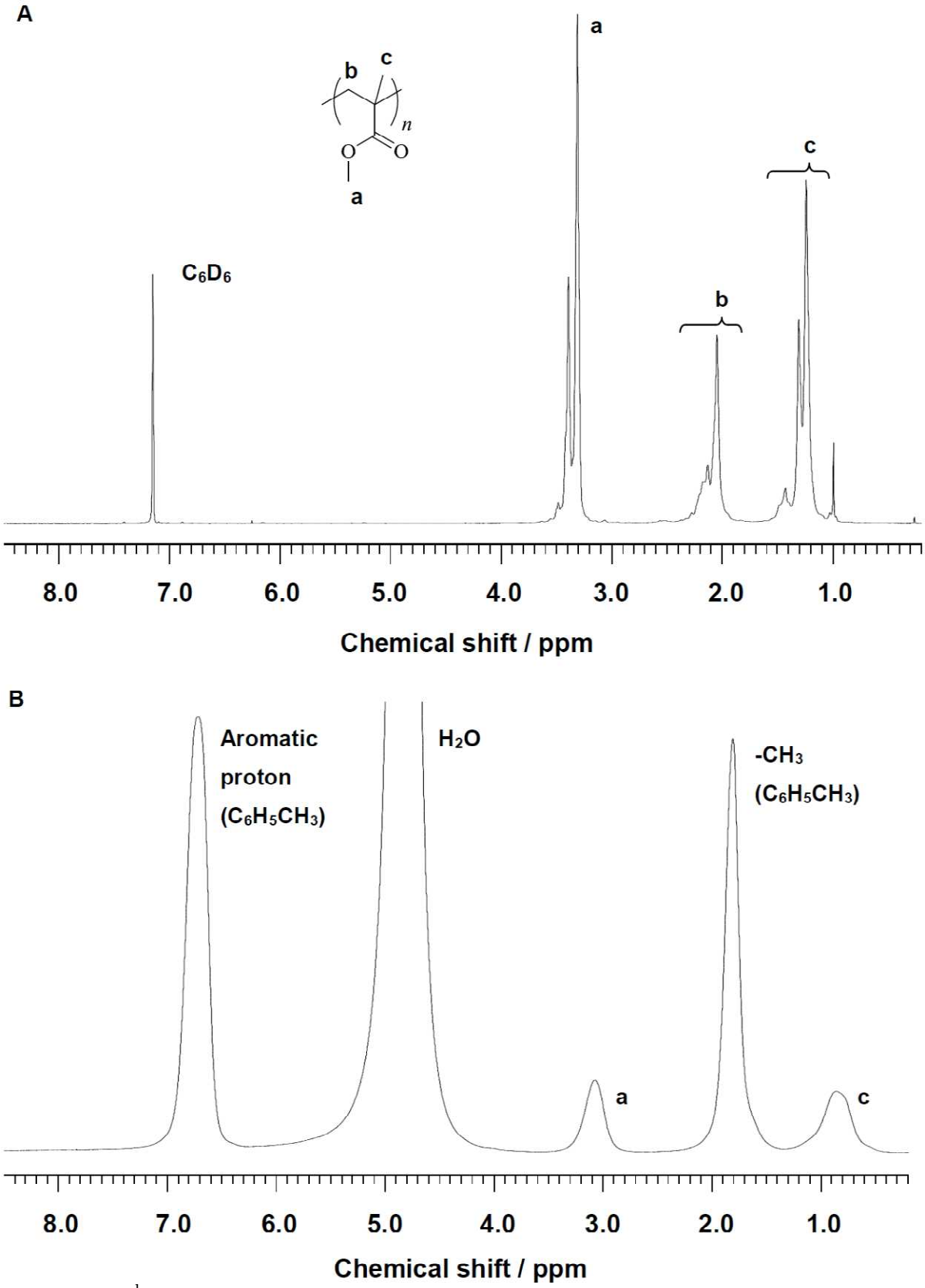

Figure 5-4. ^{1}H NMR spectra of (**A**) PMMA dissolved in C_6D_6 and (**B**) dispersion of the toluene solution containing 24 wt% of PMMA.

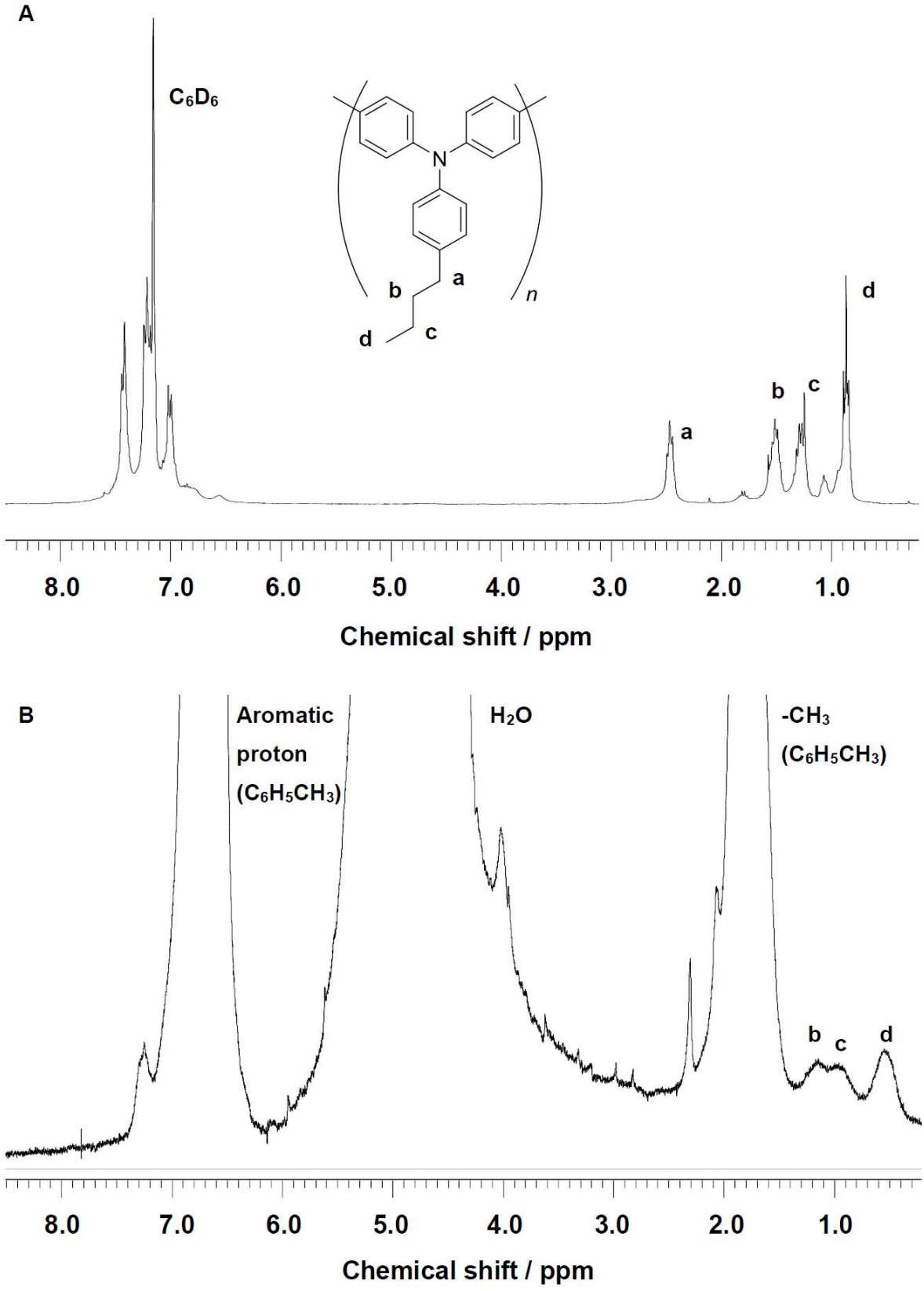

Figure 5-5. ^{1}H NMR spectra of (**A**) dispersion of the toluene solution containing 7 wt% of PBTPA and (**B**) PBTPA dissolved in C_6D_6.

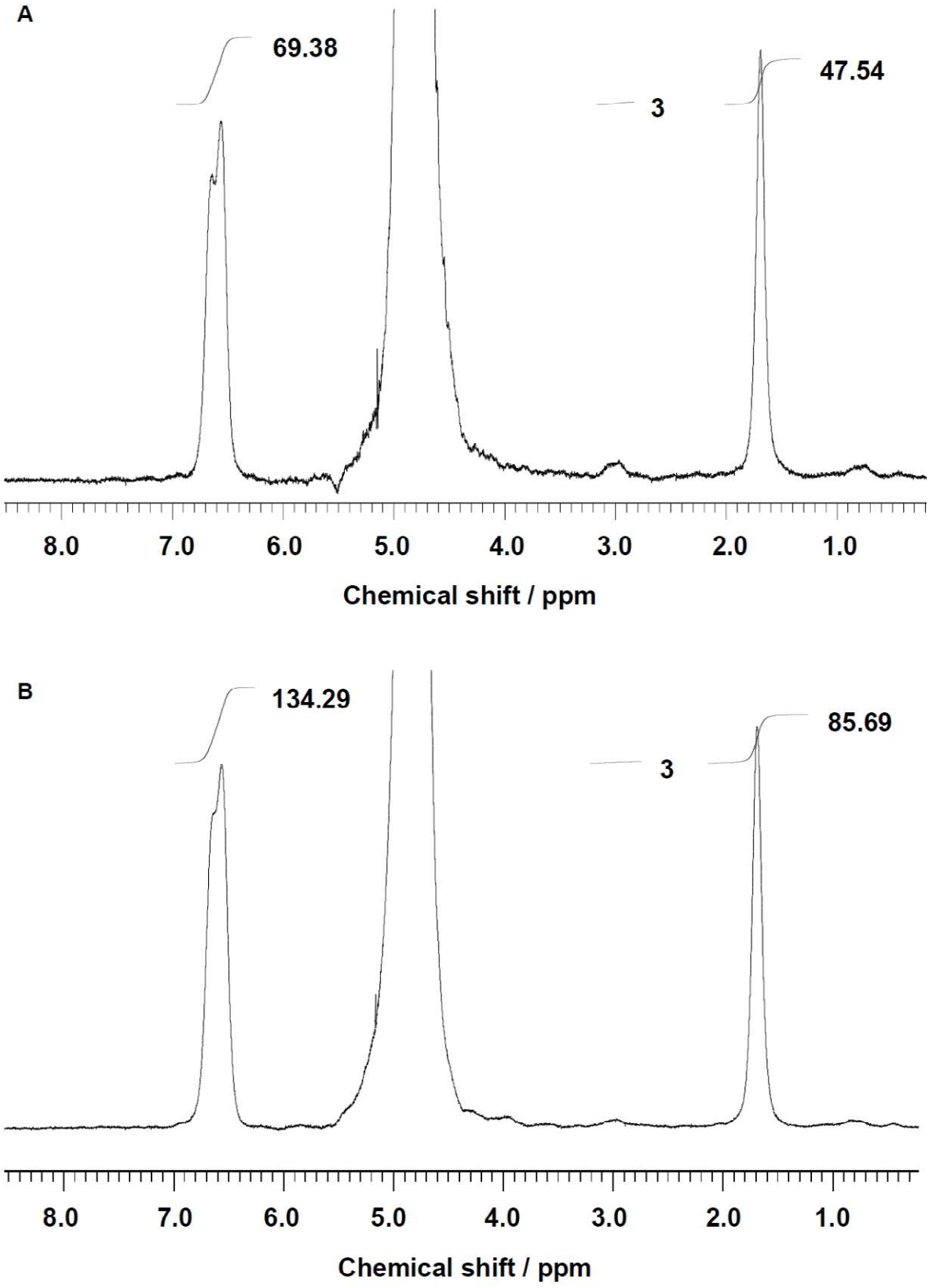

Figure 5-6. ^{1}H NMR spectra of polymer blend solution droplets containing (**A**) 7 wt% and (**B**) 13 wt% of polymers

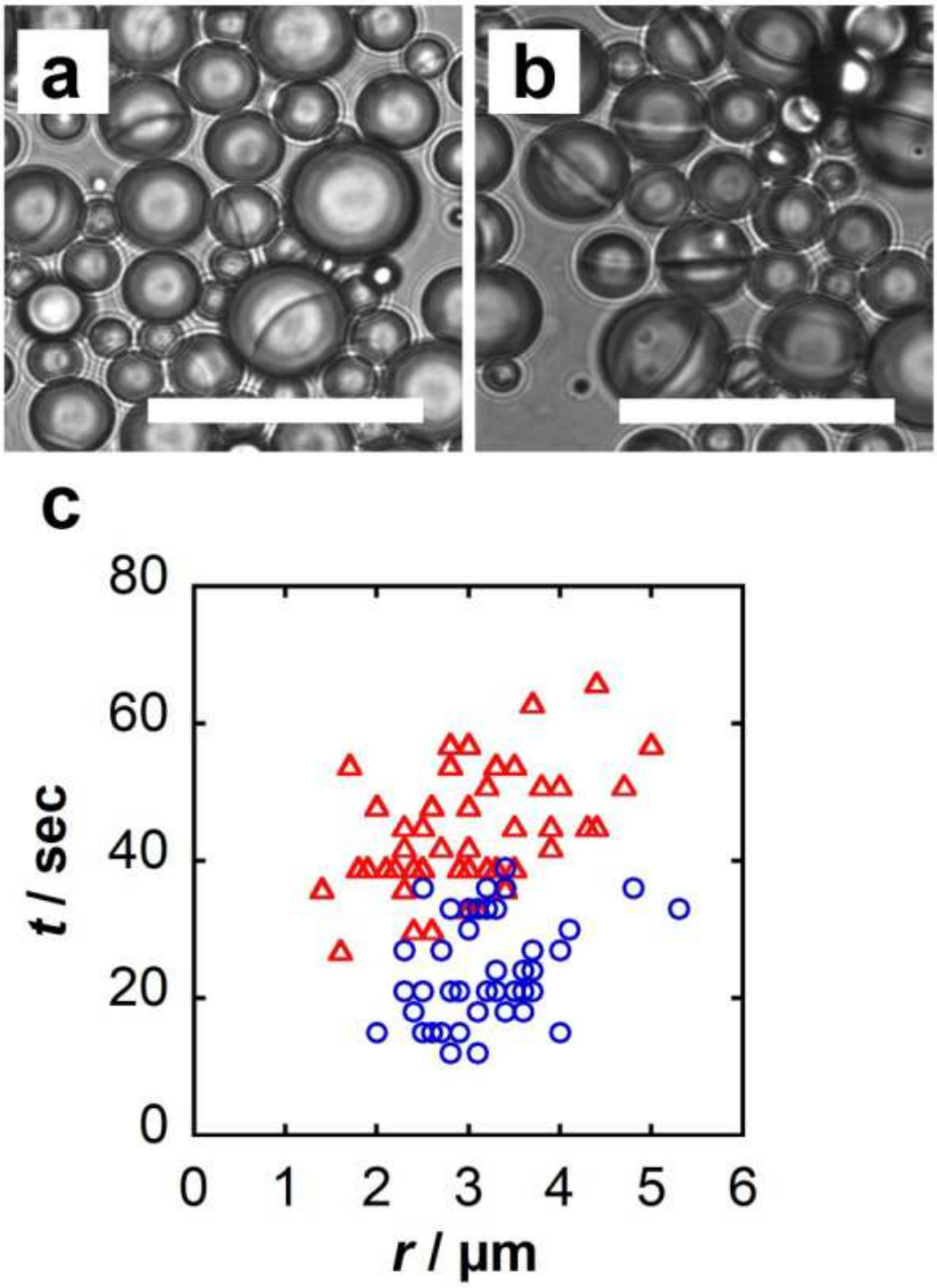

Figure 5-7. OM images of toluene solution droplets dissolving PBTPA and PMMA after the UV irradiation. The concentrations of polymers are (**a**) 7 and (**b**) 13 wt% respectively. (**c**) Times *t* required to finish the structure transition as function of diameter *r*. Circles and triangles represent 7 and 13 wt% respectively. All scale bars represent 10 μm.

5-3-3. Effect of wavelength of UV light

Figure 5-8 shows the wavelength dependence on the structure change of PBTPA / PMMA / toluene droplets after the irradiated with UV light for 4 min, where long (530-550 nm) and short wavelength (365 nm) were utilized. No significant transition was detected after the exposure to the UV light with the longer wavelength band. On the other hand, the obvious change was observed after the exposure to the UV light with shorter wavelength. As shown in Figure 5-8d, PBTPA shows absorption spectrum in the wavelength range of 270-430 nm. This dependence indicates that the formation of the anisotropic structure induced by UV light is originated from PBTPA phase.

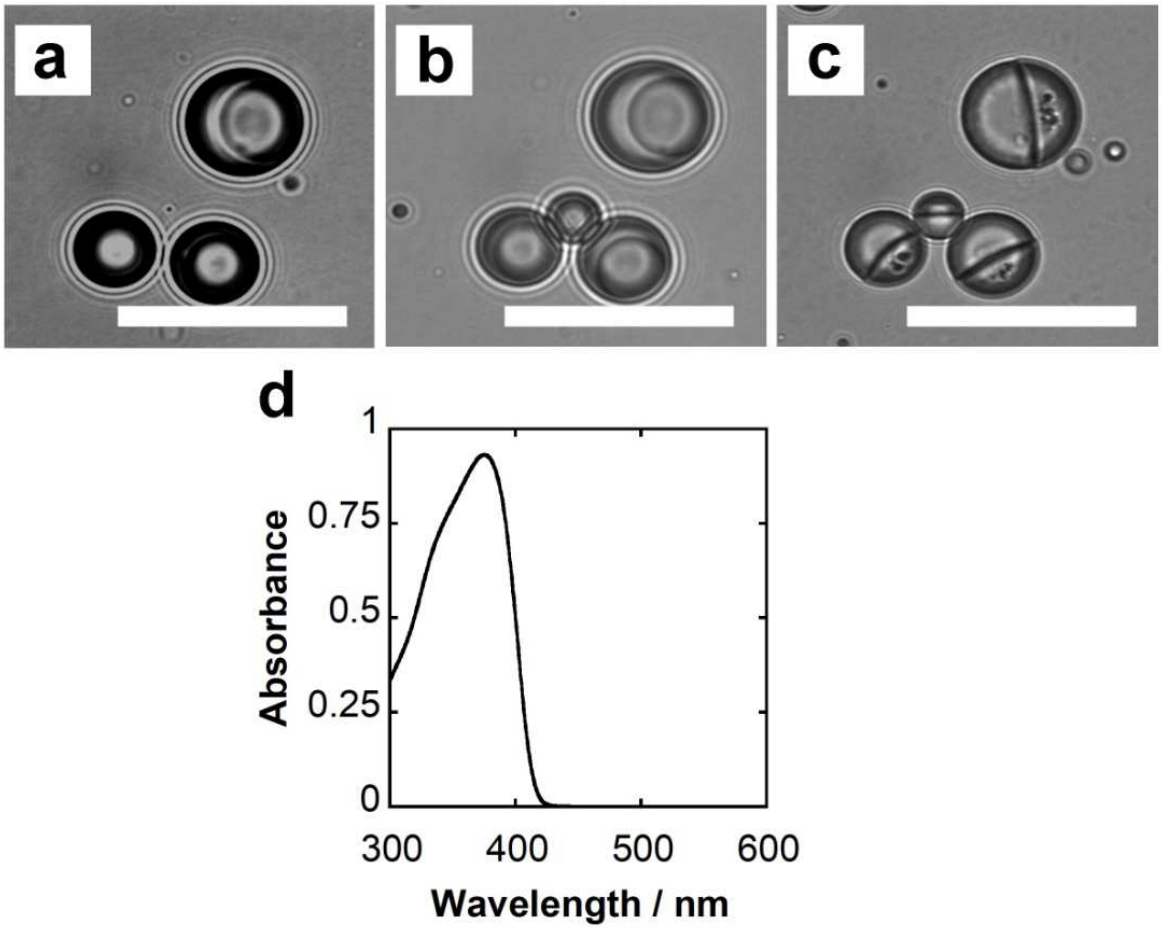

Figure 5-8. OM images of toluene solution droplets dissolving PBTPA and PMMA (**a**) before and after the irradiation with UV lights for 4 min at (**b**) 530-550 nm and (**c**) 365 nm. (**d**) UV-Vis spectrum of PBTPA toluene solution (1 mg L^{-1}). All scale bars represent 10 μm.

5-3-4. Effect of heat

The heat generated by UV lamp was assumed to causes this structural transition. In order to clarify the effect of heat, the dispersion was placed on the hot plate settled at 40 and 75 °C. However, no transition was observed after heating as shown in Figure 5-9. Therefore, UV light at 365 nm causes structural transition from core-shell to Janus in polymer blend solution droplets.

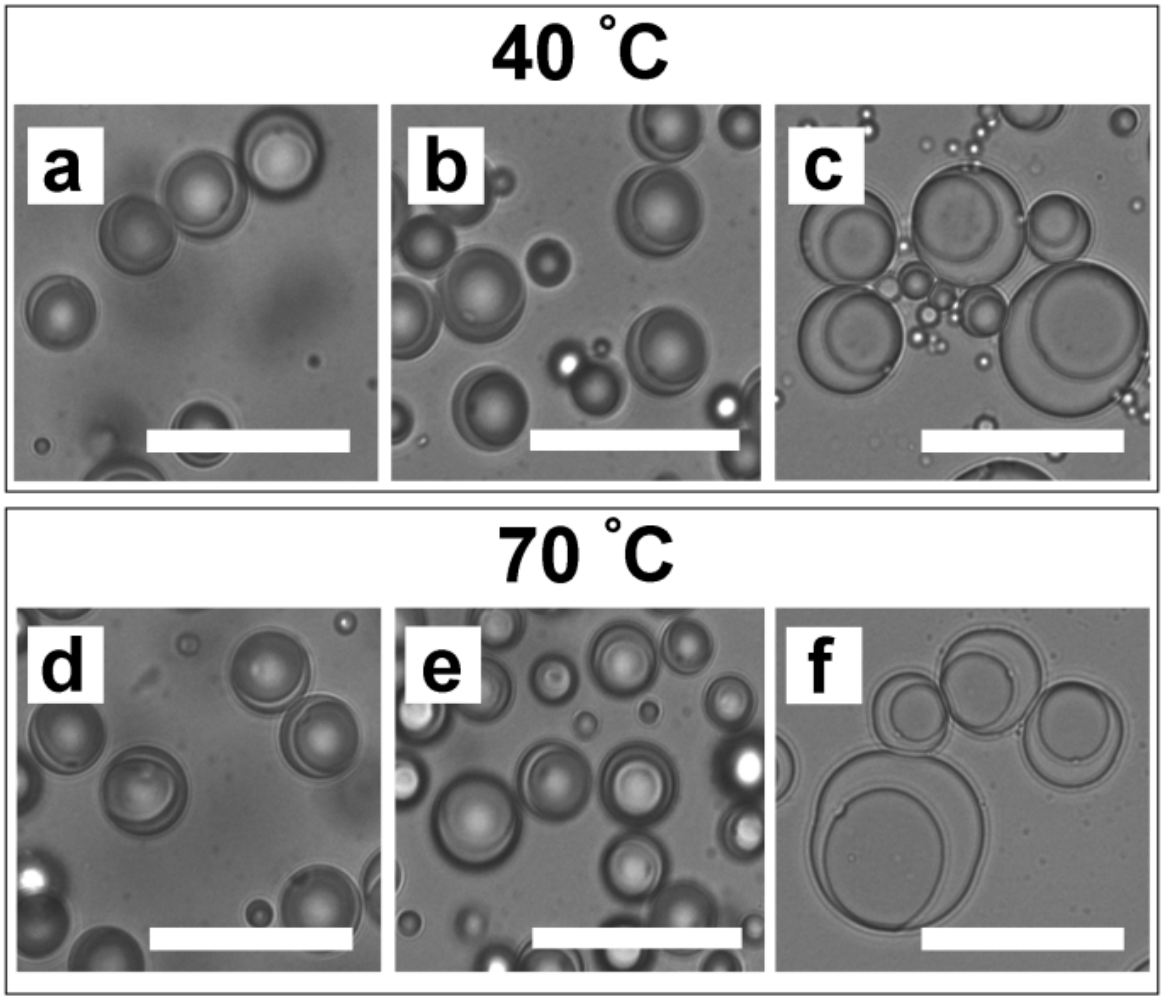

Figure 5-9. OM images of toluene solution droplets dissolving PBTPA and PMMA heated up to (**a**, **b**, **c**) 40 or (**d**, **e**, **f**) 75 °C for (**a**, **d**) 0, (**b**, **e**) 1, (**c**, **f**) 8 min. All scale bars represent 10 μm.

5-3-6. Mechanism of morphological transition

Triphenylamine (TPA) derivatives have been utilized as hole transporters in a variety of applications, and have been known as photoconductors.[4] Photoconductive materials absorb the light to generate the free carriers. Like other TPA derivatives, PBTPA chains absorb UV light to transit to the excited state, and are subsequently oxidized by electron transfer to the surrounding media like toluene and water. The formation of trace amount of radical cations changes the solution characteristics, leading to alter the nature of interface, and reorganize the phase-separated structure. The morphology of polymer blend particle is thermodynamically determined to minimize the total interfacial free energy.[5] As a result, the droplets change its morphology from core-shell to Janus to minimize the total free energy by increasing the interfacial area between the PBTPA-rich phase possessing an ionic or hydrophilic nature and aqueous phase.

5-4. Conclusions

UV light at 365 nm causes the unexpectedly structural transition from core-shell to Janus in PBTPA / PMMA blend solution droplets. The rate of structural transition slowed down with the concentration of polymer and diameter, suggesting that the mass transfer is rate-determining step. No transition was induced by the light at 530-550 nm. This dependency of the wavelength of UV light indicates the transition is originated from the light absorption by PBTPA. Though the droplet was heated up to 75 °C, no transition was observed.

5-5. References

(1) Ikkai, F.; Iwamoto, S.; Adachi, E.; Nakajima, M. New method of producing mono-sized polymer gel particles using microchannel emulsification and UV irradiation. *Colloid Polym. Sci.* **2005**, *283*, 1149–1153.

(2) Kim, J.; Joo, J.; Park, S. Preparation of asymmetric porous Janus particles using microfluidics and directional UV curing. *Part. Part. Syst. Charact.* **2013**, *30*, 981–988.

(3) Tsuchiya, K.; Shimomura, T.; Ogino, K. Preparation of diblock copolymer based on poly(4- *n*-butyltriphenylamine) via palladium coupling polymerization. *Polymer* **2009**, *50*, 95–101.

(4) (a) Tsutsumi, N.; Kinashi, K.; Masumura K.; Kono, K. Photorefractive dynamics in poly(triarylamine)-based polymer composites. *Opt. Express* **2015**, *23*, 25158–25170. (b) Cao, Z.; Yamada, K.; Tsuchiya, K.; Ogino K. Synthesis and characterization of triphenylamine-based organic photorefractive glasses. *J. Photo-polym. Sci. Technol.* **2011**, *24*, 329–335.

(5) Torza, S.; Mason, S. Three-phase interactions in shear and electrical fields. *J. Colloid Interface Sci.* **1970**, *33*, 67–83.

Chapter 6

General conclusions

6-1. Conclusions

In this thesis, the author has presented the morphology control of the phase separated structure in the polymer blend particles consisting of poly(4-butyltriphenylamine) (PBTPA), poly(methyl methacrylate) (PMMA) and PBTPA-*b*-PMMA fabricated by solvent evaporation method.

In chapter 1, the author introduced the use of polymer composite particles in industrial and academic field, and demonstrated that the morphology control can provide novel applications to polymer particles. Solvent evaporation method has advantageous to prepare composite particles. The mechanism of the structure formation in solvent evaporation method was also explained. Although solvent evaporation method can be used for any polymers, the materials of the particles reported so far have been limited to the pair of conventional polymers such as poly(styrene) (PS) and PMMA. To expand the possibility of polymer composite particles, the author started study of morphology control of PBTPA/PMMA blend particles.

In chapter 2, the author presented the facile fabrication of “inversed core-shell” particles with PMMA core surrounded by PBTPA monolayer via solvent evaporation method. While the core-shell particles with PBTPA core surrounded by PMMA shell were obtained from the toluene solution droplets dispersed in poly(vinyl alcohol) (PVA) aqueous solutions, adding sodium dodecyl sulfate (SDS) into aqueous solution as the surfactant gave inversed core-shell particles. The feature of this particle is that the PMMA core is located at the center of the sphere, and the thickness of the PBTPA layer is uniformed in circumferential direction. The symmetric structure and large gap of the refractive index between PBTPA and PMMA make inversed core-shell particle promising material for opal type’s photonic crystal.

In chapter 3, the author presented the PBTPA/PMMA blend particles with the various structures including “core-shell”, “Janus”, “dumbbell like” and “confetti like” fabricated via solvent evaporation method. While conventional methods such as seeded polymerization

require multiple steps to synthesize composite particles, these controlled structures were obtained in a single step by solvent evaporation method. Increment of the molecular weight of polymers induced the formation of Janus structured particles. Chloroform solution droplets provided dumbbell like structure due to low interfacial tension between chloroform solution and PVA aqueous solution. Rapid evaporation suppressed the morphological transition due to high viscosity, and formed confetti like particles which is preceding structure of dumbbell like particles.

In chapter 4, the author presented the morphology control of the PBTPA/PBTPA-*b*-PMMA/PMMA blend particles. PBTPA-*b*-PMMA in polymer blend behaved as surfactant due to its amphiphilic nature. For instance, the block copolymer formed "micelles" of PBTPA microdomains in PMMA macrophase. In addition, adding PBTPA-*b*-PMMA decreased the interfacial tension between PBTPA and aqueous phase, and changed macrophase separated structure from core-shell to Janus or inversed core-shell structure depending on the molecular weight of the PBTPA segment in the block copolymer. The concurrence of the formation of the inversed core-shell structure and PBTPA micelles resulted in the formation of the "watermelon like" particles.

In chapter 5, the author presented the morphological transition from core-shell to Janus for phase-separated PBTPA/PMMA solution droplets by UV light irradiation. To our knowledge, there are few studies about transition of phase separated structure induced by UV light irradiation. The wave length dependence demonstrated that the formation of the anisotropic structure induced by UV light is originated from PBTPA phase. The mechanism of the transition is still under the investigation. However, the UV responsive transition is representing special nature of PBTPA as conjugated polymer.

Through the 5 chapters, the author has achieved to prepare the PBATP/PMMA blend particles with various morphologies. However, the linkage between morphology and

application is still missing. To apply the particles to the material in optical field such as resonator or photonic crystal, repeated structures with the size of around 100 nm are required. The driving force to form periodical structure is the chemical incompatibility between different polymers described as χN. In addition, the distribution of segment ratio affects the temperature of order-disorder transition. Although some promising structures in PBTPA/PBTPA-*b*-PMMA/PMMA blend particles have been observed, polymer with higher molecular weight and narrow distribution will be required to introduce ordered structure.